Journal of Medicinal Chemistry

Article

Discovery of Potent, Selective, and Brain-Penetrant 1#-Pyrazol-5-yl-1#-pyrrolo[2,3-*b*]pyridines as Anaplastic Lymphoma Kinase (ALK) Inhibitors

Makoto Fushimi, Ikuo Fujimori, Takeshi Wakabayashi, Tomoaki Hasui, Youichi Kawakita, keisuke imamura, Tomoko Kato, Morio Murakami, Tsuyoshi Ishii, Yorifumi Kikko, Maki Kasahara, Atsushi Nakatani, Yuto Hiura, Maki Miyamoto, Kumar Singh Saikatendu, Hua Zou, Scott Weston Lane, J. David Lawson, and Hiroshi Imoto

J. Med. Chem., **Just Accepted Manuscript** • DOI: 10.1021/acs.jmedchem.8b01630 • Publication Date (Web): 22 Apr 2019

Just Accepted

ACS Publications

is published by the American Chemical Society. 1155 Sixteenth Street N.W., Washington, DC 20036

Discovery of Potent, Selective, and Brain-Penetrant 1*H*-Pyrazol-5-yl-1*H*-pyrrolo[2,3-*b*]pyridines as Anaplastic Lymphoma Kinase (ALK) Inhibitors

Makoto Fushimi,[†] *Ikuo Fujimori,**[†] *Takeshi Wakabayashi,*[†] *Tomoaki Hasui,*[†] *Youichi Kawakita,*[†] *Keisuke Imamura,*[†] *Tomoko Kato,*[†] *Morio Murakami,*[†] *Tsuyoshi Ishii,*[†] *Yorifumi Kikko,*[†] *Maki Kasahara,*[†] *Atsushi Nakatani,*[†] *Yuto Hiura,*[†] *Maki Miyamoto,*[†] *Kumar Saikatendu,*[‡] *Hua Zou,*[‡] *Scott Weston Lane,*[‡] *J. David Lawson,*[‡] *and Hiroshi Imoto*[†]

AUTHOR ADDRESSES

[†]Neuroscience Drug Discovery Unit, Research, Takeda Pharmaceutical Company Limited, 26-1, Muraoka-Higashi 2-chome, Fujisawa, Kanagawa 251-8555, Japan

[‡]Takeda California, Inc., 10410 Science Center Drive, San Diego, California 92121, United States

KEYWORDS. ALK, structure-based drug design (SBDD), tropomyosin receptor kinases (Trks), brain penetration, phosphorylated-ALK, cognitive improvement

ABSTRACT

Anaplastic lymphoma kinase (ALK), a member of the receptor tyrosine kinase family, is predominantly expressed in the brain and implicated in neuronal development and cognition. However, the detailed function of ALK in the central nervous system (CNS) is still unclear. To elucidate the role of ALK in the CNS, it was necessary to discover a potent, selective, and brain-penetrant ALK inhibitor. Scaffold hopping and lead optimization of *N*-(2,4-difluorobenzyl)-3-(1*H*-pyrazol-5-yl)imidazo[1,2-*b*]pyridazin-6-amine **1** guided by a cocrystal structure of compound **1** bound to ALK resulted in the identification of (6-(1-(5-fluoropyridin-2-yl)ethoxy)-1-(5-methyl-1*H*-pyrazol-3-yl)-1*H*-pyrrolo[2,3-*b*]pyridin-3-yl)((2*S*)-2-methylmorpholin-4-yl)methanone **13** as a highly potent, selective, and brain-penetrable compound. Intraperitoneal administration of compound **13** significantly decreased the phosphorylated-ALK (p-ALK) levels in the hippocampus and prefrontal cortex in the mouse brain. These results suggest that compound **13** could serve as a useful chemical probe to elucidate the mechanism of ALK-mediated brain functions and the therapeutic potential of ALK inhibition.

INTRODUCTION

Protein tyrosine kinases are enzymes that phosphorylate protein substrates on the tyrosine residues. They can be classified into receptor tyrosine kinases (RTKs) and non-RTKs. RTKs are

membrane-spanning cell surface proteins that mediate the transduction of extracellular signals to the cytoplasm.[1-2] They play an important role in the activation of intracellular signaling systems that regulate various cellular events, including cell proliferation, migration, metabolism, differentiation, and survival.[2-3] Therefore, when chemically probing the specific roles of an individual RTK, it is important for the tool compound to be selective for the targeted kinase.

Anaplastic lymphoma kinase (ALK) is a member of the insulin receptor (IR) class of RTKs. The ALK gene is highly expressed in the central nervous system (CNS), and the knock-out (KO) of the ALK gene in mice leads to various interesting phenotypes: enhancement of cognitive functions in spatial memory and reduction of anxiety- and depression-like behaviors without any apparent morphological deficits.[4-6] The endogenous ligand of ALK has yet to be established and the detailed mechanism of the ALK signaling pathway for these phenotypes is still unclear. In the meantime, fusion proteins of the ALK kinase domain with other genes produced by translocations[7] or other chromosomal rearrangements[8] have been discovered in several malignant cells. Unlike endogenous ALK that is expressed in the brain, the fusion proteins show dysregulated expression and activation leading to oncogenesis.[8-10] In 2011, a small molecule inhibitor of ALK, crizotinib (Figure 1), was approved by the U.S. Food and Drug Administration (FDA) for the treatment of echinoderm microtubule-associated protein-like 4 fused ALK (EML4–ALK) positive non-small cell lung cancer (NSCLC).[11-13] Several ALK inhibitors such as

ceritinib (Novartis)[14], brigatinib (Ariad, currently Takeda)[15], and alectinib (Roche/Chugai)[16] were also studied for their potential as an anti-cancer drug during our research period. Interestingly, Pfizer reported a brain-penetrant ALK inhibitor, lorlatinib, to target brain metastases in 2014.[17] However, there is no report supporting the development of ALK inhibitors to elucidate the mechanism of ALK-mediated brain functions. Herein, we report the discovery of a highly selective and brain-penetrant ALK inhibitor that demonstrated a decrease in phosphorylated-ALK levels in mouse brain. Furthermore, we describe our structure-based drug design (SBDD) driven lead generation and optimization efforts resulting in the identification of 1*H*-pyrazol-5-yl-1*H*-pyrrolo[2,3-*b*]pyridine derivatives as a new class of ALK inhibitor.

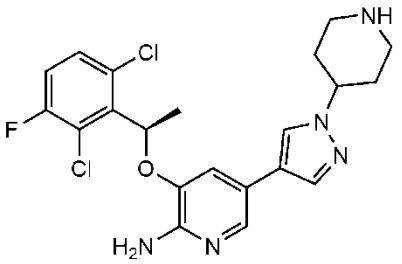

Crizotinib

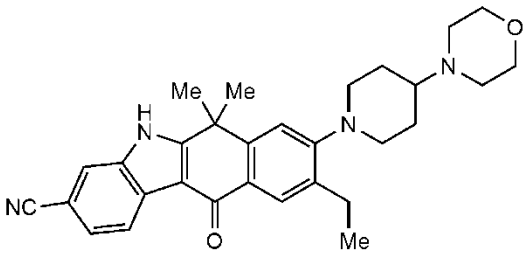

Alectinib

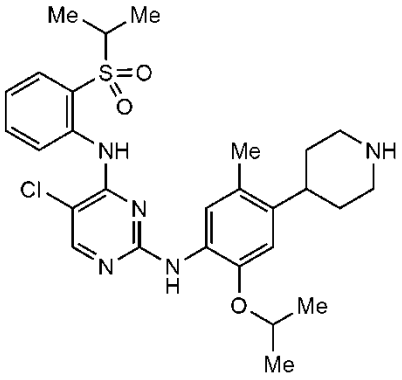

Ceritinib

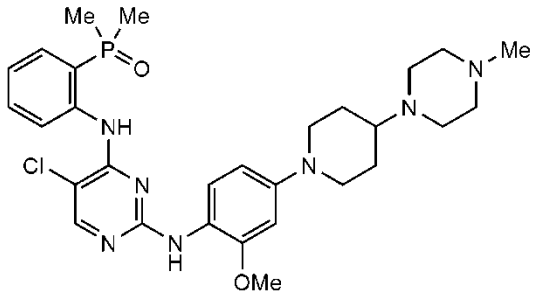

Brigatinib

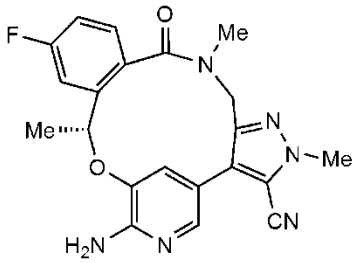

Lorlatinib

Figure 1. Structures of some reported ALK inhibitors.

RESULTS AND DISCUSSION

Lead Generation. To identify a potent, selective, and brain-penetrable ALK inhibitor, we initiated our efforts with a high-throughput screening of our corporate compound library. An

N-benzyl-3-(1*H*-pyrazol-5-yl)imidazo[1,2-*b*]pyridazin-6-amine derivative was identified as a hit with moderate ALK inhibitory activity. The initial structure-activity relationship (SAR) studies around the hit compound led to a highly potent ALK inhibitor **1** in enzymatic and cellular assays with IC_{50} values of 2 nM and 6 nM, respectively (Table 1). This is comparable to crizotinib that showed IC_{50} values of 1.8 nM and 37 nM in our enzymatic and cellular assays, respectively. However, compound **1** also exhibited extremely potent TrkA inhibitory activity (IC_{50} = 0.1 nM) and moderate kinase selectivity in an enzymatic kinase panel that consisted of 39 different kinases (see supporting information). Compound **1** is a chiral compound and its absolute configuration was determined as *S*-form. An *R*-isomer of compound **1** showed lower ALK inhibitory activity with IC_{50} value of 1000 nM.

Table 1. *In vitro* Profiles of Compound **1** Derived from Hit Compound

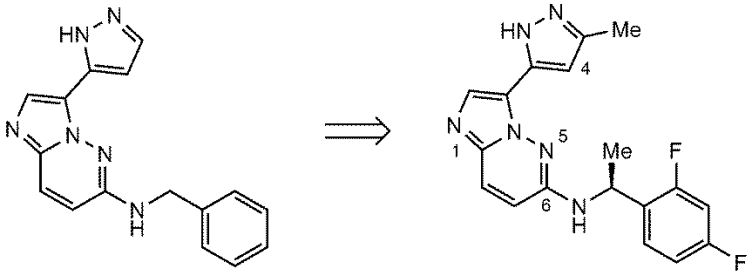

Hit Compound	1
Assays	IC_{50} (nM) [a]
ALK enzyme[b]	2.0 (1.8–2.2)

ALK cell[c]	6.0 (4.2–10)
TrkA enzyme[b]	0.10 (0.096-0.11)

[a] IC_{50} values and 95% confidence intervals (given in parentheses) were calculated by nonlinear regression analysis of percent inhibition data (n = 2). [b] ATP concentration is 1 μM. [c] Phospho-ALK levels were measured in cell assay.

Selectivity Improvement over Trks. It is well known that the Trk family is located in nerve cells and mediates the survival and differentiation of neuronal cells via interactions with various neurotrophic factors such as nerve growth factor (NGF) and brain-derived neurotrophic factor (BDNF).[18] Thus, for the tool compounds to accurately probe ALK function in the brain they should be selective over the Trk family kinases. SBDD is a frequently utilized method for the development of selective kinase inhibitors.[19] To support our SBDD efforts, we cocrystallized compound **1** with the ALK kinase domain and successfully generated a cocrystal structure of **1** in the ALK active site (Figure 2). The cocrystal structure revealed that the pyrazole ring interacted with the hinge residues Glu1197 and Met1199. The nitrogen at the 5-position of the imidazo[1,2-*b*]pyridazine core allows the pyrazole to adopt a coplanar orientation relative to the core by alleviating the steric clash with the pyrazole 4-hydrogen that would arise if a carbon were at the same position. This coplanarity well mimics the adenine structure of ATP, and it may

explain the high potency of compound **1**. Interestingly, the residue of Leu1256 formed three CH-π interactions with the imidazole ring, the pyridazine ring in the imidazo[1,2-*b*]pyridazine core, and the 2,4-difluorophenyl group, leading to robust stabilization of the L-shaped conformation of the molecule. Next, we analyzed the difference of the amino acid sequence in the ATP binding pocket between ALK and TrkA to improve selectivity over the Trks. Four amino acid residues in ALK were identified for consideration: Ala1200, His1124, Leu1196, and Leu1198. Of these, we focused on Leu1198, an amino acid in the hinge region of ALK which is a tyrosine in all the Trk family proteins. The side chains of Leu1198 and the corresponding Tyr590 in TrkA extended on the left obliquely upward from the hinge towards the P-loop adjacent to the 1-position of the imidazo[1,2-b]pyridazine core (Figure 2). The bulky Tyr residue led to a narrower binding space in the Trk family relative to ALK. Thus, we concluded that targeting this space should lead to better selectivity over Trks.[17] Conversely, we chose not to target the other three residues, His1124, Leu1196, and Ala1200: 1) His1124 could not be analyzed due to its structural disorder, 2) the modification of the methyl group on the pyrazole ring adjacent to Leu1196 resulted in a decrease of ALK inhibitory activity (data not shown), and 3) Ala1200 and the corresponding Arg592 in TrkA were considered challenging to study a specific interaction since the residues were oriented toward the outside of the ligand binding pocket.

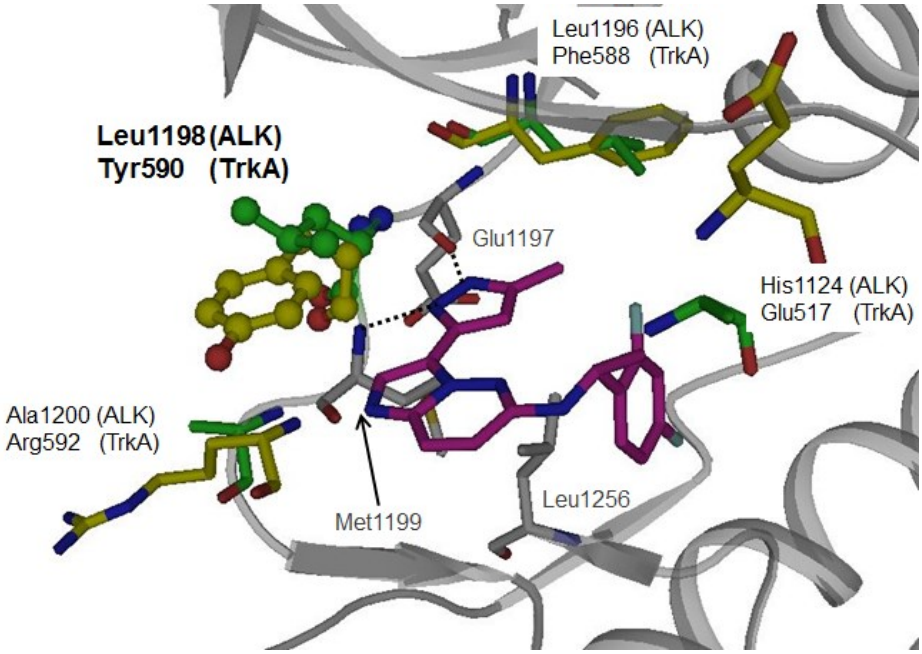

Figure 2. Cocrystal structure of compound **1** bound to the ATP binding site of human ALK protein (PDB code 6EDL). Different residues in ALK (green) and TrkA (yellow, PDB code 4F0I) around compound **1** (magenta). Glu1197 and Met1199 are hinge residues. The imidazole portion of His1124 in ALK is not shown due to poor electron density for the sidechain.

To access the Leu1198 region, the imidazo[1,2-*b*]pyridazine (which lacks an attachment point at the 1-position) was converted to 1*H*-pyrrolo[2,3-*b*]pyridine **2**, which could then be modified at the corresponding position (Figure 3A). Compound **2** demonstrated moderate ALK inhibitory activity in both enzymatic and cellular assays with IC_{50} values of 14 nM and 140 nM, respectively. We envisioned that the introduction of 3-substituent groups that would clash with the TrkA Tyr residue would facilitate improving the selectivity of compound **2** over Trks. This

assumption encouraged us to examine the introduction of sulfonyl and carbonyl moieties attached with an R^1 substitution at the 3-position (Figure 3B). For both sulfonyl and carbonyl compounds, the bulky R^1 group would be directed in such a way to avoid the repulsion with the adjacent 4-position of the 1*H*-pyrrolo[2,3-*b*]pyridine core, which would be beneficial to the acquisition of selectivity. In addition, the sulfonyl and carbonyl groups were predicted to have complementary conformational preferences with the R^1 group and the 1*H*-pyrrolo[2,3-*b*]pyridine core relatively perpendicular[20] or moderately twisted, respectively (Figure 3C).

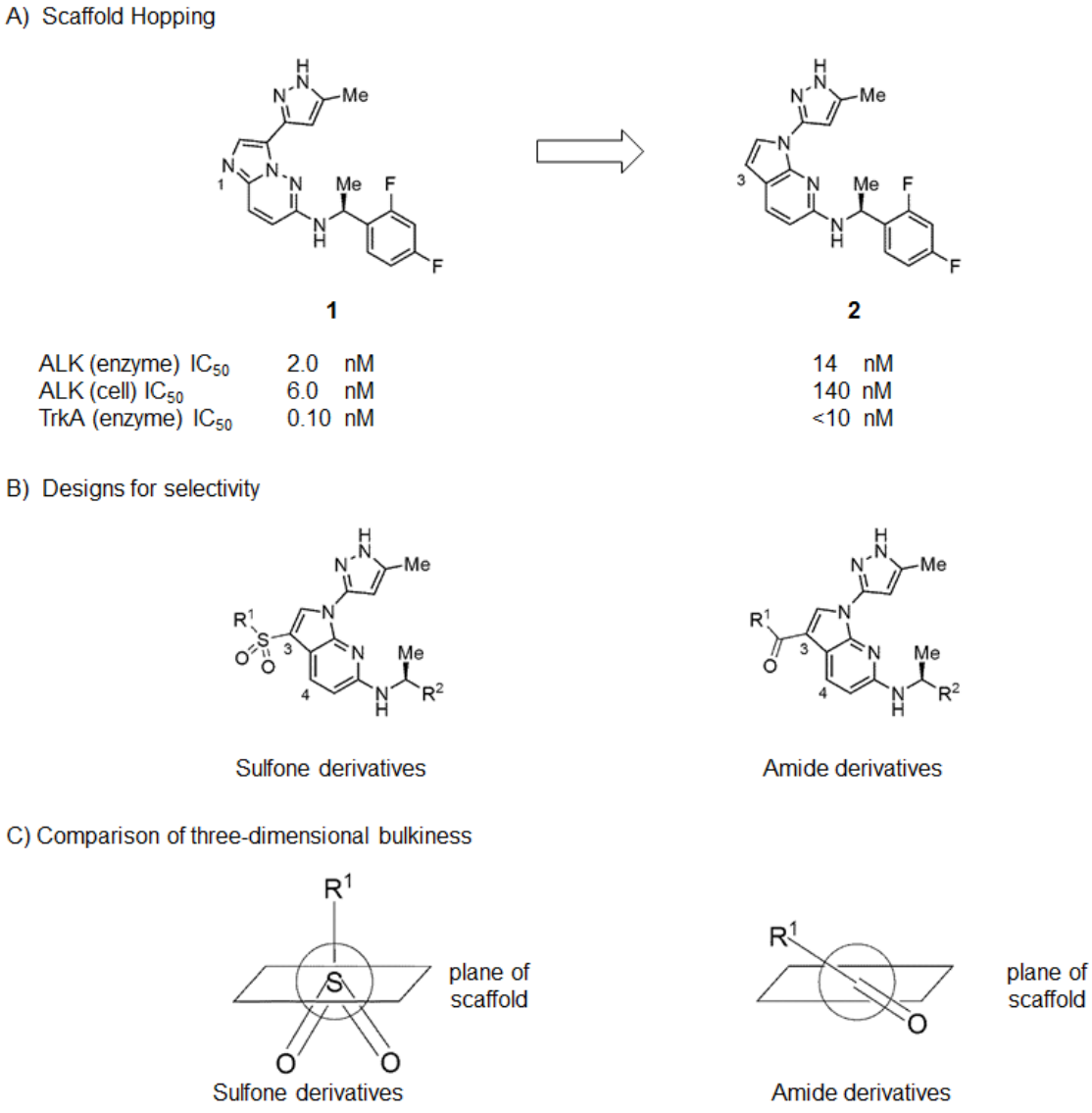

Figure 3. (A) Results of scaffold hopping. (B) Design to improve selectivity over Trks. (C) Comparison of three-dimensional bulkiness between sulfonyl and carbonyl moieties.

We assessed the hypothesis mentioned above with sulfone and amide derivatives at the 3-position and simultaneously evaluated modification of the tail benzene ring at the 6-position. Table 2 summarizes the results. As expected, methyl sulfone **3** showed increased potency for

ALK and reduced activity for TrkA when compared with those of the compound **2**. With respect to the tail benzene ring, the conversion from 2,4-difluorobenzene into 5-fluoro-2-pyridine increased the cellular potency and the ligand lipophilicity efficiency (LLE)[21] of compound **4**. Thus, we utilized the 5-fluoro-2-pyridyl group instead of the 2,4-fluorophenyl group for further optimization. An increase in the size of the R^1 group in sulfonyl derivatives was detrimental to ALK inhibitory activity based on the potencies of ethyl, isopropyl, and oxetan-3-yl compounds (**5**−**7**). However, these bulkier modifications improved the selectivity for ALK over TrkA to a greater extent. Among the sulfone derivatives tested, isopropyl compound **6** achieved the highest selectivity with 94-fold higher activity for ALK than for TrkA, though the ALK cellular inhibitory activity was only moderate (IC_{50} = 270 nM). Interestingly, the amide derivatives produced better results. Dimethyl amide **8** demonstrated equipotent ALK inhibition and decreased TrkA inhibition relative to compound **4**, leading to 67-fold ALK selectivity over TrkA. The cellular activity of compound **8** was also maintained with an IC_{50} value of 16 nM. Morpholylamide **9** exhibited substantial improvement in the selectivity (480-fold) while maintaining cellular potency (IC_{50} = 23 nM), whereas *N*-methylpiperazine **10** resulted in a drop in selectivity. However, dihydropyran **11** without sulfone or amide linkers did not improve the selectivity over TrkA. These results suggested that the sulfonyl/amide linker was the key to selectivity over TrkA.

Table 2. *In vitro* Profiles of Sulfone and Amide Derivatives at 3-Position of 1*H*-pyrrolo[2,3-*b*]pyridine.

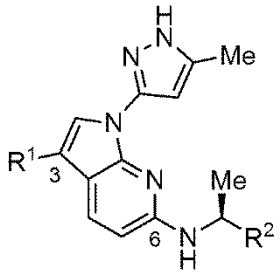

Compd	R^1	R^2	ALK IC_{50} (nM)[a]	ALK cell IC_{50} (nM)[a]	TrkA IC_{50} (nM)[a]	LLE[b]
2	H	2,4-diF-Ph	14 (9.8–19)	140 (120–160)	<10	3.4
3	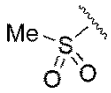	2,4-diF-Ph	1.2 (0.92–1.5)	27 (22–33)	15 (12–19)	5.6
4	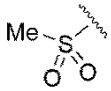	5-F-2-Py	3.3 (2.5–4.4)	13 (10–17)	45 (24–84)	6.8
5	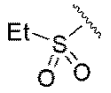	5-F-2-Py	9.6 (7.3–13)	37 (20–66)	110 (63–210)	5.8
6	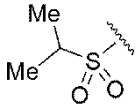	5-F-2-Py	18 (13–25)	270 (240–320)	1700 (1300–2200)	5.2
7	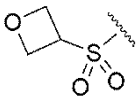	5-F-2-Py	20 (17–23)	60 (32–110)	730 (600–890)	5.7
8	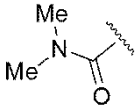	5-F-2-Py	1.8 (1.5–2.1)	16 (14–18)	120 (87–170)	7.1
9	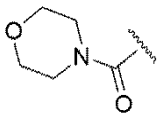	5-F-2-Py	2.5 (2.0–3.2)	23 (19–27)	1200 (1000–1500)	6.8

10	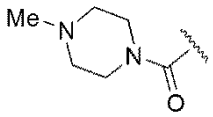	5-F-2-Py	6.1 (4.9–7.7)	37 (22–62)	250 (190–320)	6.0
11	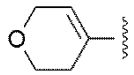	5-F-2-Py	1.9 (1.5–2.4)	9.4 (7.6–12)	2.7 (2.4–3.2)	5.9

[a] IC_{50} values and 95% confidence intervals (given in parentheses) were calculated by nonlinear regression analysis of percent inhibition data (n = 2). [b] LLE = pIC_{50} – *c*LogP.

As described above, our efforts succeeded in the identification of sulfone and amide derivatives with high ALK selectivity over TrkA. To build a rationale for this finding, cocrystallization was attempted for several of these compounds and two cocrystal structures of ALK were successfully obtained. The structures of amide **9** (PDB code 6EBW) and sulfone **7** (PDB code 6E0R) aligned with TrkA (PDB code 4F0I) are shown in Figures 4A and 4B, respectively. The binding mode of amide **9** is consistent with our design hypothesis, where the amide substituent pointed toward Leu1198 via twisting of the amide plane. The morpholine ring oriented obliquely to the pyrrolo[2,3-b]pyridine core due to intramolecular strain preventing a co-planar conformation. In the TrkA active site, compound **9** cannot accommodate this conformation because of the repulsion between the morpholine ring and Tyr590 thus dramatically reducing the TrkA inhibitory activity of compound **9**. Interestingly, as Figure 4B shows, the binding mode of compound **7** is inconsistent with our expectation that R^1 would orient towards Leu1198. The sulfonyl group of compound **7** appeared to have more freedom of rotation than the

amide group in compound **9**. Consequently, the cocrystal structure with the ALK showed the (oxetan-3-yl)sulfonyl moiety of compound **7** in the projecting away from the hinge towards the vacant solvent-exposed region and created an unfavorable contact between the sulfonyl oxygen and hinge backbone carbonyl oxygen of Met1199. This likely explains the lower ALK inhibitory activity of compound **7** relative to compound **9**. In the case of the similar compound **4**, the methylsulfonyl group is expected to adopt several conformations, some of which avoid the repulsion between the sulfonyl oxygen and the Met1199 carbonyl oxygen, thus resulting in tighter binding. As the R^1 substituent becomes bulkier (**5**–**7**), it becomes harder to access conformations that do not create a repulsive interaction. With either greater strain or greater electrostatic repulsion, with the carbonyl of Met1199, the overall binding energy becomes less favorable. Regarding the binding to TrkA, we speculate that the narrower binding space does not allow orientation of the sulfonyl group without forcing one of the sulfonyl oxygens into a repulsive interaction even when the R^1 substitution is as small as a methyl group. While these analyses provide the rationale behind the improvement of the selectivity over TrkA in the sulfonyl derivatives, complete understanding at the molecular level requires additional structural information. Toward this end, a cocrystal with TrkA is currently under investigation.

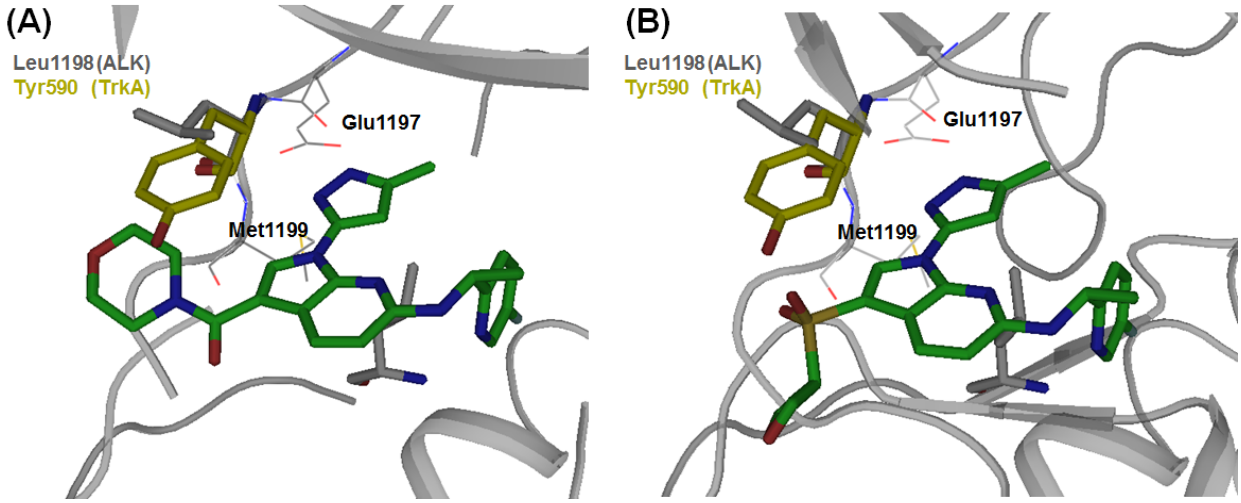

Figure 4. X-ray crystal structures of the amide compound **9** (**A**) and the sulfone compound **7** (**B**) bound to the ATP binding site of human ALK protein (gray, PDB 6EBW and 6E0R, respectively). The relative position of Tyr590, based on the PDB 4F0I crystal structure, is shown in yellow.

Avoidance of Multidrug Resistance Protein 1 (MDR1) Efflux. The blood-brain barrier tightly regulates the passage of molecules from the blood into the brain and highly expresses various efflux transporters, represented by P-glycoprotein (P-gp) which is referred to by its gene name MDR1.[22] Brain penetrant molecules need to have good membrane permeability and avoid being an MDR1 substrate. As Table 2 shows, the selectivity over TrkA was dramatically improved by the introduction of the morpholylamide group at the 3-position of the 1*H*-pyrrolo[2,3-*b*]pyridine core. However it was revealed that compound **9** demonstrated high P-gp efflux (MDR1 BA/AB ratio = 18), presumably because of its increased polarity.

One of the practical approaches to avoid being an MDR1 substrate is removing or weakening hydrogen-bond donors (HBDs) and hydrogen-bond acceptors (HBAs).[23] Using the cocrystal structures for guidance, we explored removing HBAs and HBDs that did not form essential interactions with the ALK active site. The cocrystal structure of compound **9** with ALK revealed that the benzylamine NH at the 6-position of 1*H*-pyrrolo[2,3-*b*]pyridine did not form any interactions with either structural waters or amino acid residues in the ALK protein. Therefore, we replaced the benzylamine group with a benzyl ether group to remove one of the HBDs.

Table 3. *In vitro* Profiles of Benzyl ether Derivatives at 6-Position of 1*H*-pyrrolo[2,3-*b*]pyridine.

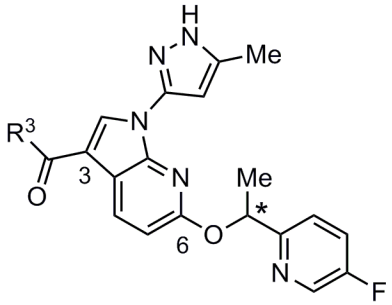

Compd	R^3	ALK IC_{50} (nM)[a]	ALK cell IC_{50} (nM)[a]	TrkA IC_{50} (nM)[a]	MDR ratio[b]
12[c]	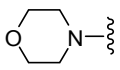	6.2 (5.2–7.4)	69 (37–130)	1400 (1000–1800)	3.1
13[d]	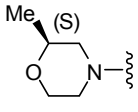	2.9 (2.5–3.4)	27 (19–39)	2600 (1600–4300)	1.0

14[d]	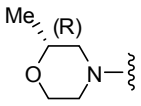	4.6 (3.5–6.1)	42 (29–61)	3400 (2200–5100)	1.3

[a] IC_{50} values and 95% confidence intervals (given in parentheses) were calculated by nonlinear regression analysis of percent inhibition data (n = 2). [b] Multidrug resistance protein 1 (MDR1) efflux ratio in P-glycoprotein (P-gp)-overexpressing cells. [c] Racemic compound. [d] Both of **13** and **14** are enantiomerically pure compounds.

Table 3 summarizes the results of this effort. As expected, benzyl ether **12** significantly improved the MDR1 efflux ratio while maintaining potent enzymatic and cellular ALK inhibitory activities. The shielding of the oxygen atom on the morpholine ring by a methyl group further improved the MDR1 efflux ratio (**13** and **14**). The (S)-isomer compound **13** demonstrated better enzymatic and cellular ALK potency than (R)-isomer compound **14**.

Determination of Eutomer and Distomer by Methoxyether Derivatives. For the determination of the eutomer and the distomer of the ether-linker derivatives, the chiral compound **15** and **16** were prepared. The compounds **13** and **14** were assumed to be eutomers because they were derivatized from the common intermediate **52a** with the eutomer **15** in Table 4. According to the benzylamine derivatives in Table 2, the absolute configuration of the eutomer of the benzyl ether derivatives was also estimated as S-form. The absolute configuration of the methyl group at the benzyl position could not be determined because the single crystallization was not achieved

despite a number of single-crystallization trials. The endeavor to determine the absolute configuration of **13** will be continued.

Table 4. Determination of Eutomer and Distomer by Methoxyether Derivatives.

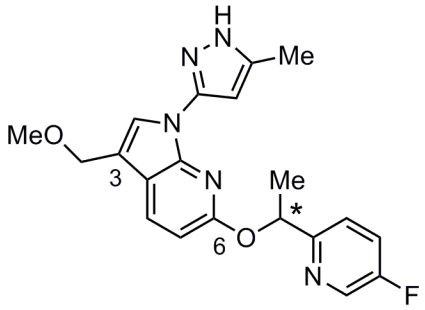

Compd	Chirality	ALK IC_{50} (nM)[a]	TrkA IC_{50} (nM)[a]
15	(S) or (R)	3.2 (2.2–4.8)	<10
16	(R) or (S)	2800 (1700–4700)	1500 (1200–1800)

[a] IC_{50} values and 95% confidence intervals (given in parentheses) were calculated by nonlinear regression analysis of percent inhibition data (n = 2).

Selectivity and Pharmacokinetic Profiles of Compound 13. With the promising *in vitro* profiles, such as the high enzymatic and cellular ALK inhibitory activity, the excellent selectivity over TrkA, and the lower MDR1 efflux ratio, compound **13** was additionally characterized in kinase selectivity assays (Table 5). Compound **13** displayed good selectivity in the enzymatic

kinase panel with almost negligible inhibition for all kinases except for focal adhesion kinase (FAK) at 100 nM. A follow-up enzymatic assay for FAK under 0.5 μM ATP concentration determined the IC_{50} value to be 25 nM, indicating 10-fold ALK selectivity over FAK. The more broad-spectrum kinase selectivity has also been examined by Kinome Scan (Supporting Information, Table S2). It was revealed that compound **13** showed good selectivity over TrkB and TrkC that play an important role in CNS. The CNS penetration of compound **13** was also evaluated in mice. As Table 6 shows, after a single intraperitoneal administration at 100mg/kg dose, brain and plasma samples were collected at 0.5 h, 1.0 h, and 2.0 h. The highest brain concentration and plasma partition coefficient (Kp) values were observed at 1.0 h after the administration. The Kp value properly reflected the MDR1 efflux ratio of compound **13**. In addition, the plasma protein binding and brain tissue binding of compound **13** depicted as an unbound fraction (fu) was measured as 0.08 and 0.017, respectively.

Table 5. Enzymatic Kinase Selectivity Profile of Compound **13**.

kinase	% inhibition[a]	kinase	% inhibition[a]	kinase	% inhibition[a]
FAK	83	MAPKAPK2	3	PI3Kα	−2
Aurora B	21	IRK	2	SRC	−2
PKA	12	PKCθ	2	p38α	-4
TrkA	9	VEGFR2	2	cMET	−5
CK1δ	6	ASK1	−1	ROCK1	−5

CDK2	5	EGFR	−1	IRAK4	−7
PLK1	5	MEK1	−1	JAK1	−8
ERK1	3	CDC7	−2	CHEK1	−9
GSK3β	3	EphA5	−2	AKT1	−11

[a] % inhibition at 100 nM.

Table 6. Mouse Pharmacokinetic Properties of **13** in Plasma and Brain[a].

Time (h)	Concentration[b] (μg/mL)		K_p [b,c]	K_{puu} [d]
	Plasma	Brain		
0.5	26.2	33.0	1.26	0.27
1.0	26.2	33.4	1.28	0.27
2.0	11.6	10.3	0.515	0.11

[a] 100 mg/kg intraperitoneal administration in mice. [b] Average of three mice. [c] Brain-to-plasma ratio. [d] calculated with fu in plasma and brain of 0.08 and 0.017, respectively.

Effect of Compound 13 on Phosphorylation Level of ALK in Mouse's Brain. After determining that compound **13** had acceptable kinase selectivity and brain penetration, it was then evaluated for *in vivo* efficacy. The pharmacodynamic effect of compound **13** was investigated by measuring the level of p-ALK in the mouse's brain via western blot at 1 h after the intraperitoneal administration. As Figure 5 shows, compound **13** decreased p-ALK levels in the hippocampus in a dose-dependent manner with a statistical significance at 30 mg/kg and higher. In addition, this compound significantly decreased the p-ALK level in the prefrontal cortex (PFC) at 100 mg/kg. These results clearly demonstrated that compound **13** inhibited ALK autophosphorylation not

only in the *in vitro* cellular system but also *in vivo* in the mouse brain, suggesting that it could be useful as a chemical probe to elucidate the brain functions mediated by ALK. The hippocampus is a brain area that is responsible for various functions including spatial memory, contextual recognition, and emotional control, while the prefrontal cortex is implicated in executive, cognitive, emotional, and motivational functions. Interestingly, some of these functions were observed to be augmented in the ALK knock-out mice as reported.[4-6] It is expected that behavioral tests with compound **13** in various animal models would contribute to understanding the role of ALK in the brain functions; hence, further investigation will be carried out.

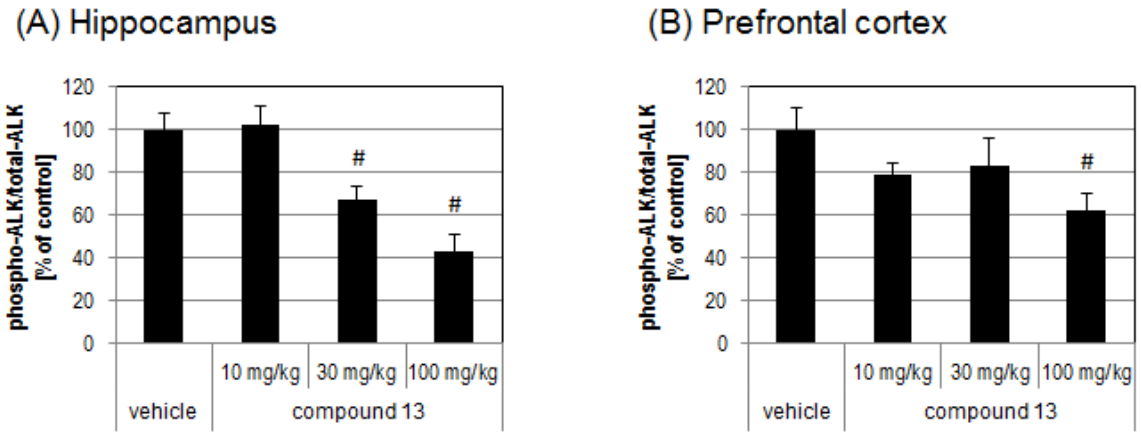

Figure 5. Decrease of phosphorylated ALK levels in mouse's (A) hippocampus and (B) prefrontal cortex after 1 h of the intraperitoneal administration of compound **13** at 10, 30, and 100 mg/mL/kg to the ICR mice. Data are presented as the mean + SEM (n = 3); p-values < 0.025 vs. vehicle by one-tailed Williams' test.

CHEMISTRY

Scheme 1 shows the synthesis of *N*-Benzyl-3-(1*H*-pyrazol-5-yl)imidazo[1,2-*b*]pyridazin-6-amine **1**. 6-Chloroimidazo[1,2-*b*]pyridazine **17** was iodized by NIS to afford 6-chloro-3-iodoimidazo[1,2-*b*]pyridazine **18**. The methylpyrazole moiety was introduced by Suzuki-coupling reaction with the THP-protected pyrazole boronic ester **22** to give the intermediate **19**. A chiral 1-(2,4-difluorophenyl)ethanamine was substituted by Buchwald-Hartwig reaction followed by the deprotection of the THP group to give the target compound **1**. The pyrazole boronic ester **22** was prepared in a two-step reaction; THP protection and regioselective borylation from the commercially available material **20**.

Scheme 1. Synthesis of *N*-Benzyl-3-(1*H*-pyrazol-5-yl)imidazo[1,2-*b*]pyridazin-6-amine **1**[a]

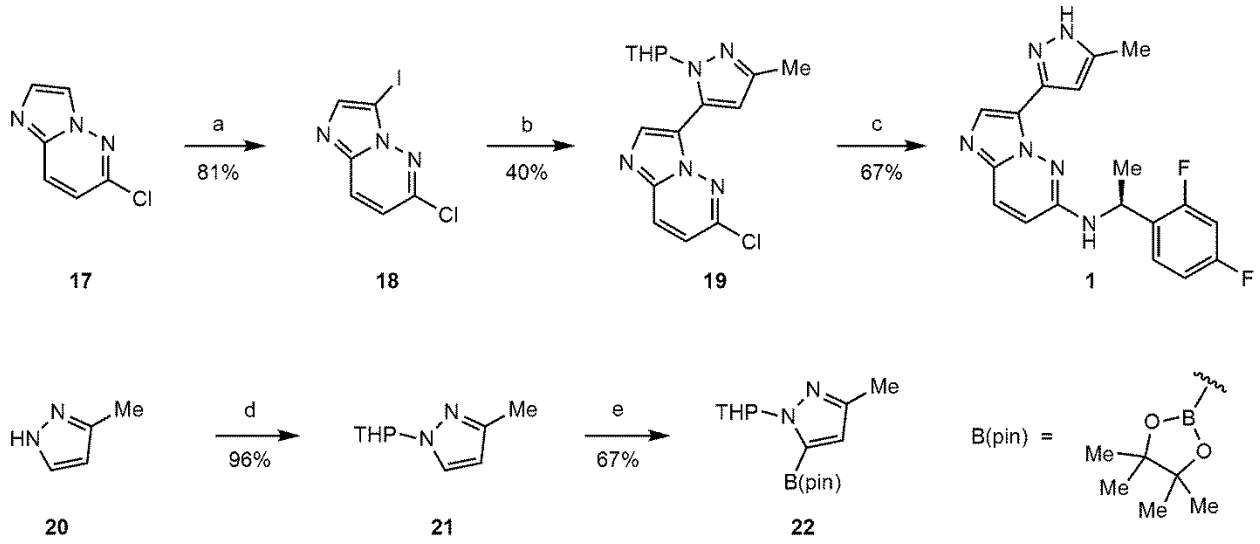

[a] Reagents and conditions: (a) NIS, DMF, 90 °C; (b) **22**, $Pd(PPh_3)_4$, Na_2CO_3, DME-H_2O, reflux; (c) $Pd_2(dba)_3$, (±)-BINAP, NaO*t*-Bu, 1-(2,4-difluorophenyl)ethanamine, toluene, reflux, then 4 N HCl/EtOAc, EtOAc-MeOH, 0 °C; (d) dihydropyrane, TFA, toluene, reflux; (e) *n*-BuLi, triisoprolyl borate, THF, -78 °C, then pinacol, acetic acid, rt.

Scheme 2 shows the syntheses of 1*H*-pyrrolo[2,3-*b*]pyridine derivatives **2** and **11**. 1*H*-pyrrolo[2,3-*b*]pyridine templates **23a**–**b** were oxidized by *m*-CPBA to afford *N*-oxides **24a**–**b** and the subsequent substitution by each chiral benzylamine **28**–**29** gave the intermediates **25a**–**b**. The methylpyrazole moiety was introduced by Ullmann coupling reaction with the THP-protected iodopyrazole **27** to give the intermediates **26a**–**26b**. The deprotection of the THP group under an acidic condition gave the target compound **2**. Preparation of the 3-substituted compound **11** was accomplished by Suzuki-reaction with boronic acid pinacol ester followed by the deprotection of the THP group. The iodopyrazole **27** was prepared by regioselective iodination from the THP protected pyrazole **21**.

Scheme 2. Synthesis of 1*H*-pyrrolo[2,3-*b*]pyridine Derivatives[a]

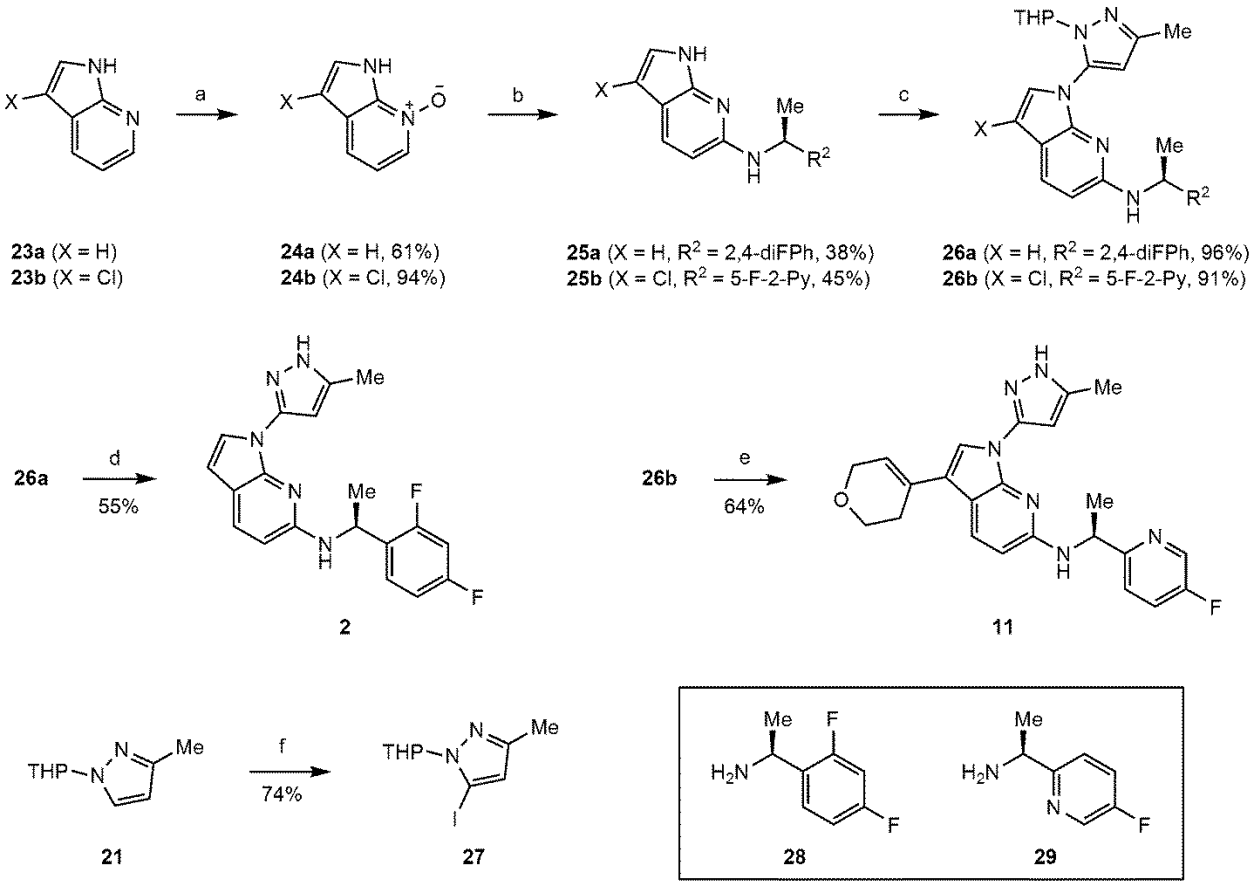

[a] Reagents and conditions: (a) *m*-CPBA, Et_2O, 0 °C; (b) *m*-CBA, Me_2SO_4, DIPEA, **28**–**29**, MeCN, 80 °C; (c) **27**, CuI, (±)-*trans*-1,2-diaminocyclohexane, Cs_2CO_3, dioxane, reflux; (d) 2 N HCl/MeOH, MeOH, 0 °C; (e) boronic acid pinacol ester, $PdCl_2(AmPhos)_2$, K_2CO_3, toluene-H_2O, 110 °C, then 4 N HCl/EOAc, EtOAc; (f) *n*-BuLi, I_2, THF, -78 °C to rt.

Scheme 3 shows the synthesis of 3-methylsulfonyl-6-amino-1*H*-pyrrolo[2,3-*b*]pyridine derivative **3**. The BOC group protected the indole NH group of a commercially available 3-iodo-1*H*-pyrrolo[2,3-*b*]pyridine **30** to enhance the reactivity of the iodine group. The 2-thiopropionate group was readily introduced at the 3-position of 1*H*-pyrrolo[2,3-*b*]pyridine by

Buchwald-Hartwig coupling reaction. The thiol group with the propionate moiety was deprotected under a basic condition and, subsequently, substituted by iodomethane. The chiral benzylamine **28** and methylpyrazole group were introduced by the same method, as shown in Scheme 2, and the following deprotection reaction of the THP group under an acid condition afforded 3-sulfonyl derivative **3**.

Scheme 3. Synthesis of 3-methylsulfonyl-6-amino-1*H*-pyrrolo[2,3-*b*]pyridine derivative **3**[a]

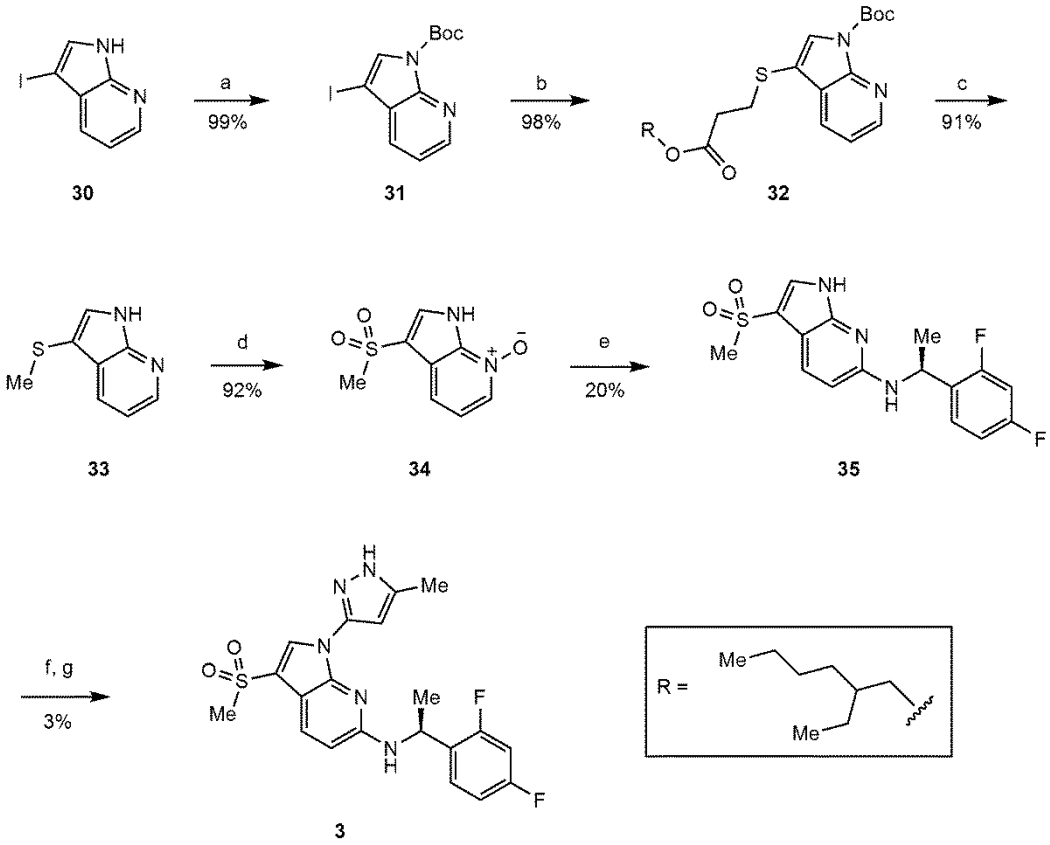

[a] Reagents and conditions: (a) Boc_2O, KO*t*-Bu, THF, rt; (b) 2-ethylhexyl 3-mercaptopropanoate, $Pd_2(dba)_3$, Xantphos, DIPEA, toluene, 70 °C; (c) MeI, KO*t*-Bu, THF, 0 °C to rt, then 2 N HCl/MeOH, MeOH, 80 °C; (d) *m*-CPBA, Et_2O, rt; (e) *m*-CBA, Me_2SO_4, **28**, DIPEA, MeCN,

80 °C; (f) **27**, CuI, (±)-trans-1,2-diaminocyclohexane, Cs_2CO_3, DME, 90 °C; (g) 4 N HCl/EtOAc, EtOAc, 0 °C.

Scheme 4 shows the syntheses of 3-sulfonyl-6-amino-1*H*-pyrrolo[2,3-*b*]pyridine derivatives **4**–**7**. A commercially available 3-iodo-1*H*-pyrrolo[2,3-*b*]pyridine **30** was oxidized into *N*-oxide **36** to enhance the reactivity of the iodine group. The 2-thiopropionate group was readily introduced at the 3-position of 1*H*-pyrrolo[2,3-*b*]pyridine by Buchwald-Hartwig coupling reaction. The chiral benzylamines **29** and methylpyrazole group were introduced by the same method, as shown in Scheme 2. The 2-thiopropionate intermediate **39** was subjected to the retro-Michael reaction by potassium *tert*-butoxide to furnish the free thiol group *in situ* which was immediately substituted with a series of alkyl halides. The subsequent oxidation reaction into a sulfonyl group by *m*-CPBA and the deprotection reaction of the THP group by acid afforded 3-sulfonyl derivatives **4**–**7**.

Scheme 4. Synthesis of 3-alkylsulfonyl-6-amino-1*H*-pyrrolo[2,3-*b*]pyridine Derivatives **4**–**7**[a]

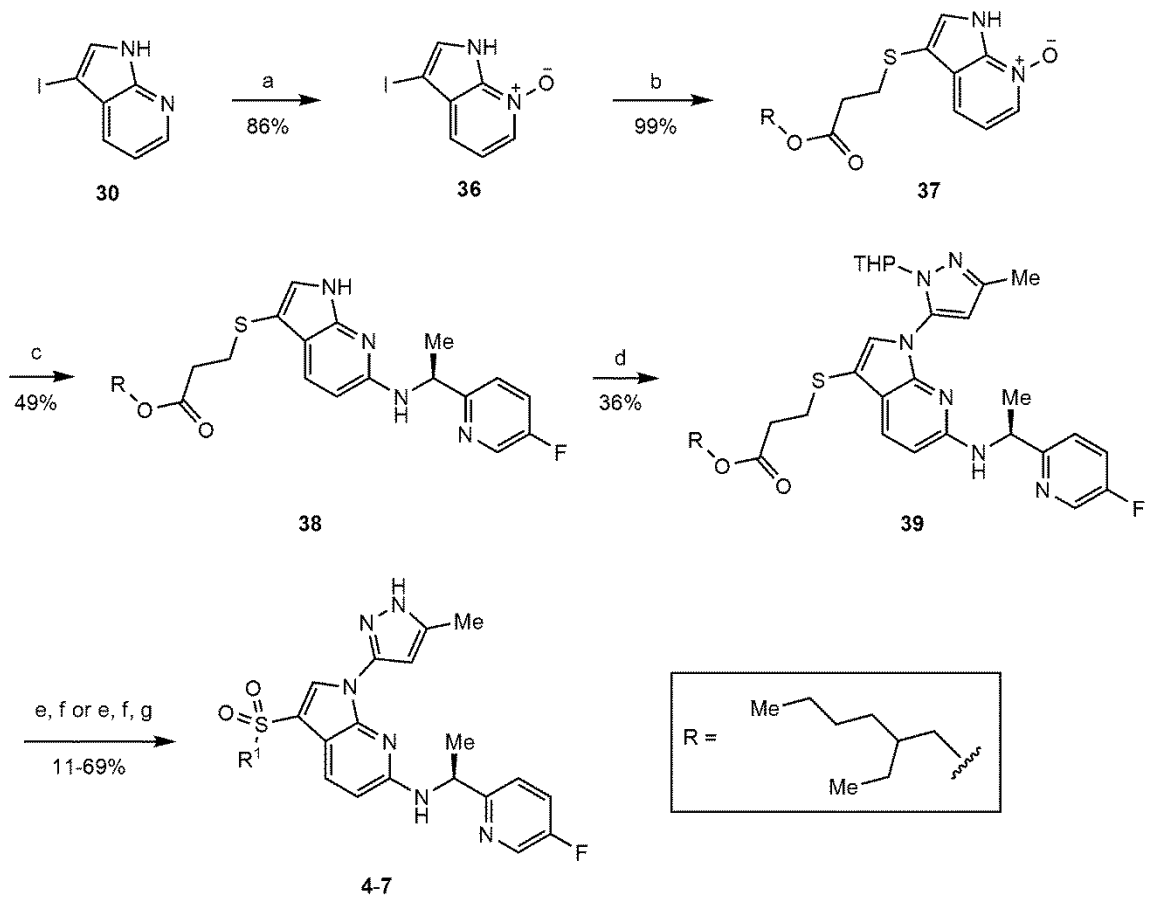

[a] Reagents and conditions: (a) *m*-CPBA, Et_2O, rt; (b) 2-ethylhexyl 3-mercaptopropanoate, $Pd_2(dba)_3$, Xantphos, DIPEA, toluene, 80 °C; (c) *m*-CBA, Me_2SO_4, **29**, DIPEA, MeCN, 80 °C; (d) **27**, CuI, (±)-trans-1,2-diaminocyclohexane, Cs_2CO_3, DME, 90 °C; (e) R^1I, KO*t*-Bu, THF, 0 °C to rt,; (f) *m*-CPBA, EtOAc, 0 °C; (g) 4 N HCl/EtOAc, EtOAc, 0 °C.

Scheme 5 shows the syntheses of 3-aminocarbonyl-6-amino-1*H*-pyrrolo[2,3-*b*]pyridine derivatives **8**–**10**. An aldehyde group was introduced at the 3-position of 1*H*-pyrrolo[2,3-*b*]pyridine **23a** utilizing hexamethylenetetramine as a carbonyl source. The subsequent reduction to alcohol which was followed by protection with the TIPS group and oxidation by *m*-CPBA provided the intermediate **41**. As Scheme 2 shows, the introduction of

(*R*)-5-fluoro-2-pyridylethanamine moiety and 2-methylpyrazole group were conducted by the same method. An aldehyde group at the 3-position was regenerated via the deprotection of the TIPS group by TBAF and the oxidation of alcohol by manganese dioxide. The aldehyde **44** was converted to the carboxylic acid by Pinnick oxidation. The subsequent amidation with the corresponding amine reagents and the deprotection of the THP group gave the amide derivatives **8**–**10**.

Scheme 5. Synthesis of 3-Aminocarobonyl-6-amino-1*H*-pyrrolo[2,3-*b*]pyridine Derivatives **8**–**10**[a]

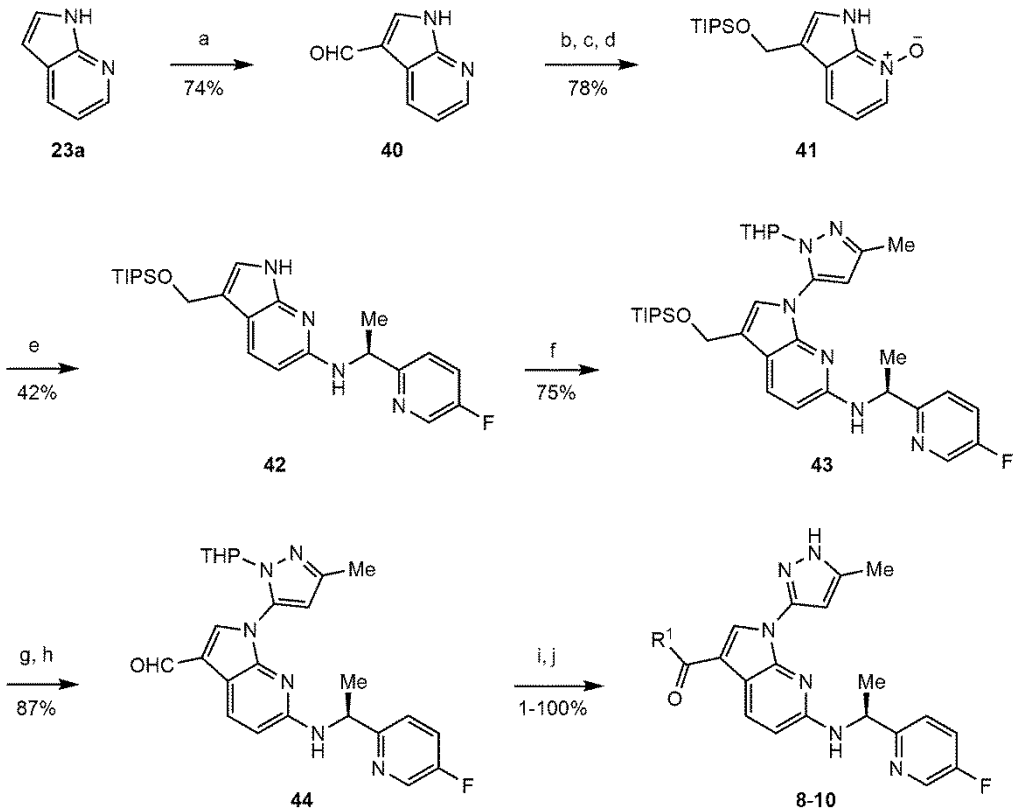

[a] Reagents and conditions: (a) hexamethylenetetramine, AcOH-H_2O, 120 °C; (b) $NaBH_4$, MeOH, 0 °C;. (c) TIPSCl, imidazole, DMF, rt; (d) *m*-CPBA, *i*-Pr_2O, rt; (e) *m*-CBA, Me_2SO_4, **29**, DIPEA, MeCN, 40 °C; (f) **27**, CuI, (±)-trans-1,2-diaminocyclohexane, K_3PO_4, DME, reflux; (g) TBAF, THF, rt; (h) MnO_2, THF, reflux; (i) $NaClO_2$, NaH_2PO_4, 2-methyl-2-butene, THF-*t*-BuOH-H_2O, rt then amine, EDC·HCl, HOBt·H_2O, TEA, THF; (j) 2 N HCl/MeOH, MeOH, 0 °C.

Scheme 6 outlines the preparation of the racemic ether-linker derivatives **12**. Utilizing the common intermediate **41** as a starting material, an acetoxy group was introduced at the 6-position under reflux in acetic anhydride with NH group of the azaindole simultaneously being acetylated. The obtained diacetyl compound was hydrolyzed by a weak basic condition to afford the intermediate **46**. The hydroxyl group at the 6-position was substituted with (±)-5-fluoro-2-pyridylethyl group using the tosylate **51** synthesized in one step from **50**. Scheme 5 shows the reactions toward the compound **12** were performed under the same conditions.

Scheme 6. Synthesis of 3-Aminocarbonyl-6-benzyloxy-1*H*-pyrrolo[2,3-*b*]pyridine **12**[a]

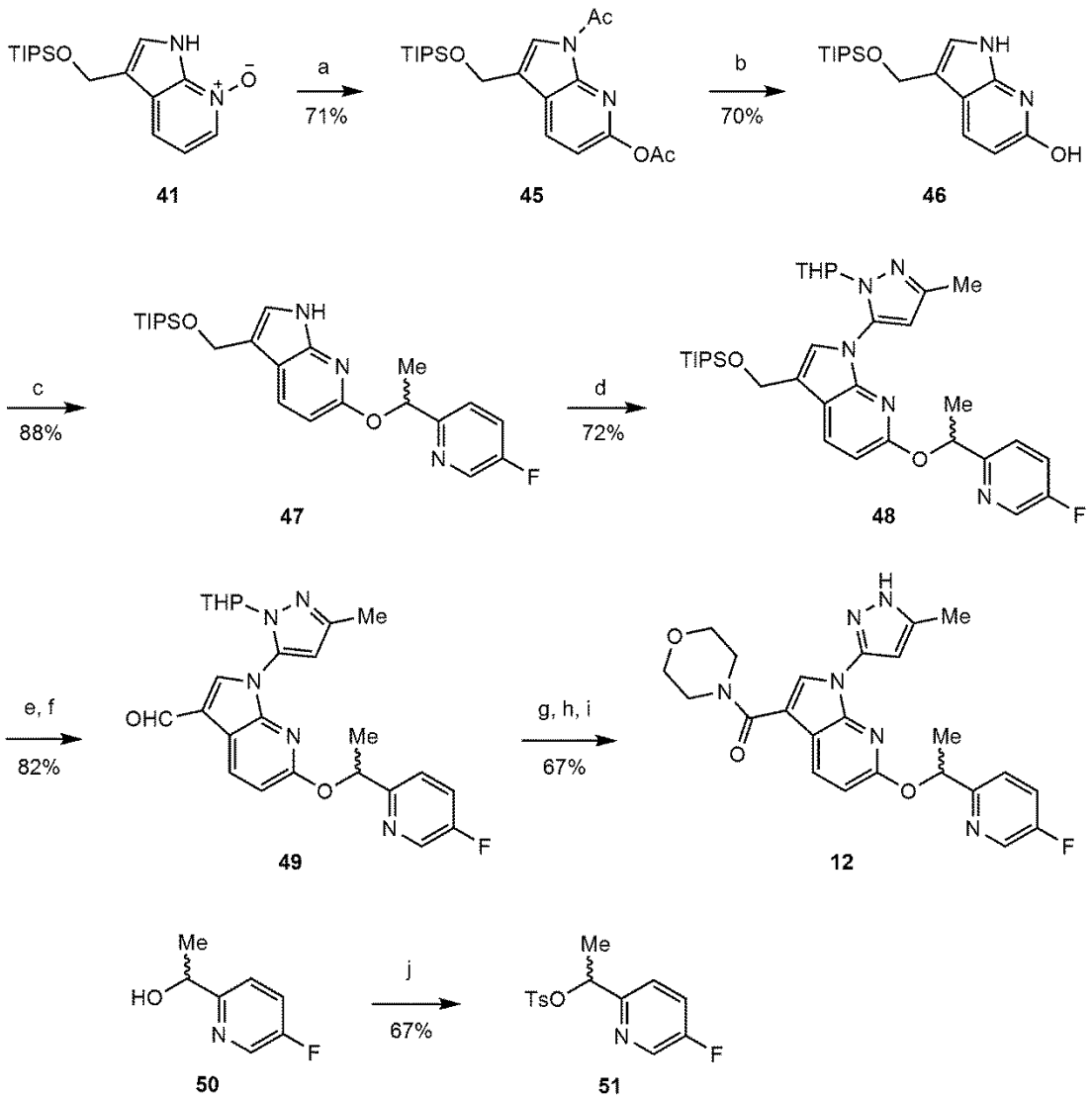

[a] Reagents and conditions: (a) Ac_2O, reflux; (b) K_2CO_3, MeOH-H_2O, rt; (c) **51**, Cs_2CO_3, DMF, rt; (d) **27**, CuI, (±)-trans-1,2-diaminocyclohexane, K_3PO_4, DME, reflux; (e) TBAF, THF, rt; (f) MnO_2, THF, reflux; (g) $NaClO_2$, NaH_2PO_4, 2-methyl-2-butene, THF-*t*-BuOH-H_2O, rt; (h) morpholine, EDC·HCl, HOBt·H_2O, TEA, THF, rt; (i) 4 N HCl/EtOAc, MeOH, 0 °C; (j) NaH, TsCl, THF, rt.

The syntheses of the chiral compounds **13** and **14** are shown in Scheme 7. Enantiomers **52a** (tR1) and **52b** (tR2) were obtained by a preparative chiral HPLC separation of racemic

compound **47** using a Chiralpak AD column. The chiral aldehyde **53** was prepared from the compounds **52a** via the introduction of methylpyrazole moiety, the deprotection of the TIPS group, and the oxidation with manganese dioxide. The chiral compounds **13** and **14** were synthesized from the aldehyde **53** through the same reactions in Scheme 5.

Scheme 7. Synthesis of Chiral 3-Amimocarbonyl-6-benzyloxy-1*H*-pyrrolo[2,3-*b*]pyridine Derivatives **13**–**14**[a]

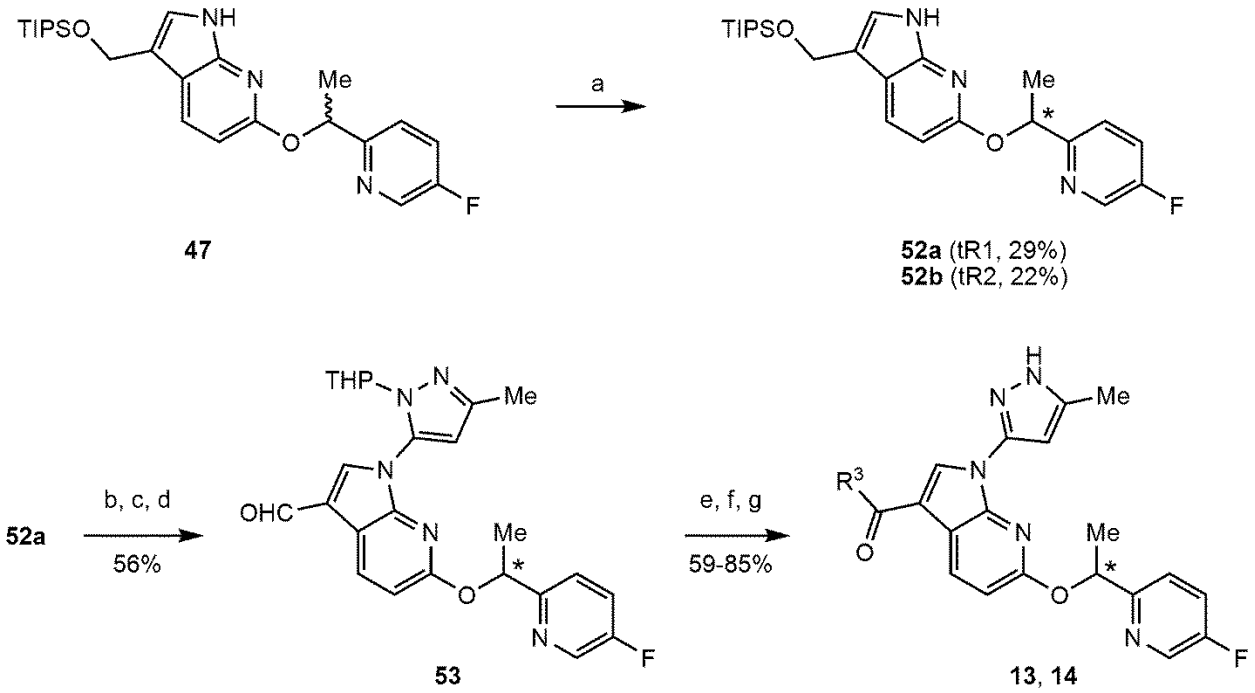

[a] Reagents and conditions: (a) Optical resolution ; (b) **27**, CuI, (±)-trans-1,2-diaminocyclohexane, K_3PO_4, DME, reflux; (c) TBAF, THF, rt; (d) MnO_2, THF, reflux; (e) $NaClO_2$, NaH_2PO_4, 2-methyl-2-butene, THF-*t*-BuOH-H_2O, rt; (f) R^3-amine, EDC·HCl, HOBt·H_2O, TEA, THF, rt.; (g) 4 N HCl/EtOAc, MeOH, 0 °C.

The chiral compound **15**–**16** were prepared by following scheme 8. After the introduction of the methylpyrazole moiety, the deproctection of THP group and the substitution of the triisopropylsilyloxy group with the methoxy group simultaneously occurred under acidic condition to afford the methoxymethyl derivatives **15**–**16**.

Scheme 8. Synthesis of Chiral 3-Methoxymethyl-6-benzyloxy-pyrrolo[3,2-*d*]pyrimidine Derivatives **15**–**16**[a]

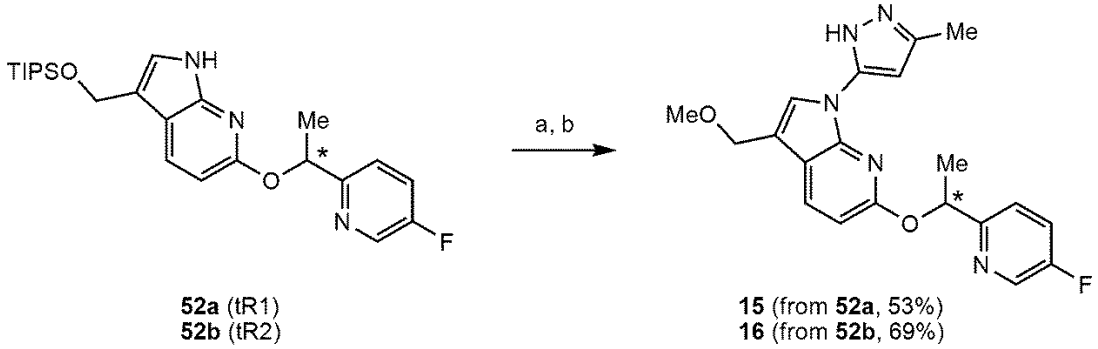

52a (tR1)
52b (tR2)

15 (from **52a**, 53%)
16 (from **52b**, 69%)

[a] Reagents and conditions: (a) **27**, CuI, (±)-*trans*-1,2-diaminocyclohexane, K_3PO_4, DME, reflux; (b) 2N HCl/MeOH, MeOH, 0 °C.

CONCLUSION

Here, we have described the discovery process of a highly selective and brain-penetrant ALK inhibitor. The process started with identification of a hit via high-throughput screening followed by slight modification that led to highly potent imidazo[1,2-*b*]pyridazine **1**. The selectivity of **1** over TrkA was low, and SBDD efforts were initiated to correct this shortfalling. Cocrystal

structure analysis of **1** suggested that the substituent at the 1-position of the imidazo[1,2-*b*]pyridazine core would improve the selectivity for ALK over Trks. The scaffold hopping from the imidazo[1,2-*b*]pyridazine into the 1*H*-pyrrolo[2,3-*b*]pyridine enabled an introduction of substituents at the corresponding position; the amide group substituent at the 3-position of the 1*H*-pyrrolo[2,3-*b*]pyridine core dramatically improved the selectivity over Trks. Further structural modification to reduce the number of the HBDs prevented compound **13** from being an MDR1 substrate, resulting in a promising brain-penetrant ALK inhibitor. The highly selective ALK inhibitor **13** exhibits good pharmacokinetic and brain penetration profiles as well as Lorlatinib, which also showed a strong cellular inhibitory activity of ALK with IC_{50} value of 1.7 nM and 38-fold selectivity over TrkB.[17] Moreover, compound **13** demonstrated a significant *in vivo* reduction of p-ALK levels in the hippocampus, following intraperitoneal administration. To the best of our knowledge, this is the first example of an ALK inhibitor that decreased the p-ALK level in the brain. The results indicated that **13** could be valuable as an *in vivo* tool to elucidate the role of ALK in the CNS disorders such as cognitive impairment, anxiety, and depression. Further research will be explored to improve the *in vivo* efficacy and kinase selectivity of the target compound.

EXPERIMENTAL SECTION

General Methods: General Chemistry Information. All solvents and reagents were obtained from commercial sources and were used as received. Yields were not optimized. All reactions were monitored by thin layer chromatography (TLC) analysis on Merck Kieselgel 60 F254 plates or Fuji Silysia NH plates, or LC−MS (liquid chromatography−mass spectrometry) analysis. LC−MS analysis was performed on a Shimadzu liquid chromatography−mass spectrometer system, operating in APCI (+ or −) or ESI (+ or −) ionization mode. Analytes were eluted using a linear gradient of 0.05% TFA containing water/acetonitrile or 5 mM ammonium acetate containing water/acetonitrile mobile phase and detected at 220 nm. Column chromatography was carried out on silica gel [(Merck Kieselgel 60, 70−230 mesh, Merck) or (Chromatorex NH-DM 1020, 100−200 mesh, Fuji Silysia Chemical, Ltd.)], or on prepacked Purif-Pack columns (SI or NH, particle size: 60 μm, Fuji Silysia Chemical, Ltd.). Analytical HPLC was performed with Corona Charged Aerosol Detector (CAD) or photo diode array detector. The column was a Capcell Pak C18AQ (50 mm × 3.0 mm i.d., Shiseido, Japan) or L-column 2 ODS (30 mm × 2.0 mm i.d., CERI, Japan) with a temperature of 50 °C and a flow rate of 0.5 mL/min. Mobile phase A and B under neutral conditions were a mixture of 50 mmol/L ammonium acetate, water, and acetonitrile (1:8:1, v/v/v) and a mixture of 50 mmol/L ammonium acetate and acetonitrile (1:9, v/v), respectively. The ratio of mobile phase B was increased linearly from 5% to 95% over 3 min, 95% over the next 1 min. Mobile phase A and B under acidic conditions were a mixture of

0.2% formic acid in 10 mmol/L ammonium formate and 0.2% formic acid in acetonitrile, respectively. The ratio of mobile phase B was increased linearly from 14% to 86% over 3 min, 86% over the next 1 min. Elemental analyses were carried out by Takeda Analytical Laboratories, and the results were within ±0.4% of theoretical values. All final test compounds were purified to >95% chemical purity as measured by analytical HPLC. Proton nuclear magnetic resonance (1H NMR) spectra were in all cases consistent with the proposed structures. 1H NMR spectra were recorded on a Varian Mercury-300 (300 MHz) or a Bruker DPX300 (300 MHz) instrument. All proton shifts are given in parts per million (ppm) downfield from tetramethysilane (δ) as the internal standard in deuterated solvent, and coupling constants (J) are in hertz (Hz). NMR data are reported as follows: chemical shift, integration, multiplicity (s, singlet; d, doublet; t, triplet; q, quartet; quint, quintet; m, multiplet; dd, doublet of doublets; td, triplet of doublets; ddd, doublet of doublet of doublets; and brs, broad singlet), and coupling constants.

(*S*)-*N*-(1-(2,4-difluorophenyl)ethyl)-3-(3-methyl-1*H*-pyrazol-5-yl)imidazo[1,2-*b*]pyridazin-6-amine (**1**). A mixture of **19** (250 mg, 0.790 mmol), (*S*)-1-(2,4-difluorophenyl)ethanamine hydrochloride (457 mg, 2.36 mmol), $Pd_2(dba)_3$ (72.0 mg, 0.080 mmol), (±)-BINAP (98.0 mg, 0.160 mmol), and sodium *tert*-butoxide (378 mg, 3.93 mmol) in toluene (15 mL) was heated under reflux with stirring under argon atmosphere for 15 h. After cooling, the mixture was partitioned between EtOAc and water. The organic layer was washed with brine, dried over

$MgSO_4$, and concentrated in vacuo. The residue was purified by column chromatography (NH-silica gel, hexane/ethyl acetate, 90:10 to 20:80) to give a coupling intermediate (275 mg), and it was dissolved in EtOAc (5 mL) and MeOH (5 mL). To the solution was added 4 N HCl/EtOAc (4 mL). After being stirred at room temperature for 4 h, the mixture was concentrated in vacuo, basified with sat. $NaHCO_3$ aq. and extracted with EtOAc. The extract was washed with brine, dried over $MgSO_4$, and concentrated in vacuo. The residue was purified by column chromatography (NH-silica gel, ethyl acetate e/methanol, 100:0 to 90:10) and successively recrystallized from EtOAc/hexane to give **1** (186 mg, 0.525 mmol, 67%) as a pale pink solid. ^{1}H NMR (300 MHz, DMSO-d_6) δ 1.50 (3H, d, J = 6.8 Hz), 2.26 (3H, s), 5.08−5.24 (1H, m), 6.39 (1H, s), 6.78 (1H, d, J = 9.1 Hz), 6.93−7.06 (1H, m), 7.19−7.33 (1H, m), 7.36−7.49 (1H, m), 7.53−7.85 (3H, m), 12.46−12.82 (1H, m). MS (ESI/APCI) m/z 355.2 [M + H]+. HPLC purity: 100%.

(*S*)-*N*-(1-(2,4-difluorophenyl)ethyl)-1-(3-methyl-1*H*-pyrazol-5-yl)-1*H*-pyrrolo[2,3-*b*]pyridin-6-amine (**2**). The compound **26a** (0.460 g, 1.05 mmol) was disolved in MeOH (15 ml). To the solution was added 2M HCl in MeOH (1.50 mL, 3.00 mmol) at 0 °C. After 1 h, sat. $NaHCO_3$ was added, extracted with EtOAc, washed with brine, dried over Na_2SO_4, filtered, concentrated in vacuo, and purified by column chromatography (NH-silica gel, hexane/ethyl acetate, 67:33 to 33:67) to yield **2** (0.203 g, 0.574 mmol, 55%) as a white solid. ^{1}H NMR (300 MHz, DMSO-d_6) δ

1.46 (3H, d, J = 6.8 Hz), 2.27 (3H, s), 5.21−5.33 (1H, m), 6.33 (1H, d, J = 3.6 Hz), 6.44 (1H, s), 6.49 (1H, d, J = 8.5 Hz), 6.91−7.01 (1H, m), 7.10−7.25 (2H, m), 7.36−7.48 (2H, m), 7.62 (1H, d, J = 8.5 Hz), 12.18 (1H, s). MS (ESI/APCI) *m/z* 354.2 $[M + H]^+$. HPLC purity: 100%.

(*S*)-*N*-(1-(2,4-difluorophenyl)ethyl)-1-(5-methyl-1*H*-pyrazol-3-yl)-3-(methylsulfonyl)-1*H*-pyrrolo[2,3-*b*]pyridin-6-amine (3). The title compound was prepared in 3.0% yield as colorless crystals from **35** using the procedure analogous to that described for the synthesis of **26a** and **2**. ^{1}H NMR (300 MHz, DMSO-d_6) δ 1.47 (3H, d, J = 6.9 Hz), 2.30 (3H, s), 3.21 (3H, s), 5.25 (1H, quin, J = 6.7 Hz), 6.40 (1H, s), 6.70 (1H, d, J = 8.7 Hz), 6.97 (1H, td, J = 8.5, 2.4 Hz), 7.17−7.29 (1H, m), 7.33−7.45 (1H, m), 7.60 (1H, d, J = 6.4 Hz), 7.86 (1H, d, J = 8.7 Hz), 7.93 (1H, s), 12.54 (1H, s). MS (ESI/APCI) *m/z* 431.9 $[M + H]^+$. HPLC purity: 100%.

***N*-((1*S*)-1-(5-Fluoropyridin-2-yl)ethyl)-1-(5-methyl-1*H*-pyrazol-3-yl)-3-(methylsulfonyl)-1*H*-pyrrolo[2,3-*b*]pyridin-6-amine** (**4**). To a solution of **39** (130 mg, 0.20 mmol) in dry THF (1 ml) was added KO*t*-Bu (29.8 mg, 0.27 mmol) at 0 °C. The reaction mixture was stirred for 1 h, and then iodomethane (0.019 ml, 0.31 mmol) was added to this mixture at room temperature. The reaction color immediately turned to colorless, and then concentrated in vacuo. The residue was dissolved in water and extracted with EtOAc twice. The combined organic layers were washed with brine, dried over Na_2SO_4 and concentrated in vacuo. The residue was purified by column chromatography (silica gel, hexane/ethyl acetate, 95:5 to 80:20) to give the sulfide intermediate

(55.1 mg) as a brown gum. To a solution of the intermediate in EtOAc (1 ml) was added *m*-CPBA (71.0 mg, 0.29 mmol) at 0 °C. After stirring at this temperature for 1 h, the reaction was quenched by sat. $Na_2S_2O_3$ aq. and then extracted with EtOAc twice. The combined organic layers were washed with brine, dried over $MgSO_4$ and concentrated in vacuo. The residue was purified by column chromatography (silica gel, hexane/ethyl acetate, 80:20 to 60:40) to give **4** (36.7 mg, 0.089 mmol, 43% in 2 steps) as a pale yellow amorphous powder. ^{1}H NMR (300 MHz, DMSO-d_6) δ 1.50 (3H, d, J = 7.0 Hz), 2.28 (3H, s), 3.21 (3H, s), 4.92−5.07 (1H, m), 6.27 (1H, s), 6.72 (1H, d, J = 8.8 Hz), 7.41 (1H, dd, J = 8.7, 4.5 Hz), 7.53−7.64 (2H, m), 7.86 (1H, d, J = 8.8 Hz), 7.93 (1H, s), 8.54 (1H, d, J = 2.9 Hz), 12.51 (1H, s). MS (ESI/APCI) *m/z* 415.1 $[M + H]^+$. HPLC purity: 97.3%.

3-(Ethylsulfonyl)-*N*-((1*S*)-1-(5-fluoropyridin-2-yl)ethyl)-1-(5-methyl-1*H*-pyrazol-3-yl)-1*H*-pyrrolo[2,3-*b*]pyridin-6-amine (5). The title compound was prepared in 36% yield as brown gum from **39** using the procedure analogous to that described for the synthesis of **4**. ^{1}H NMR (300 MHz, DMSO-d_6) δ 1.13 (3H, t, J = 7.4 Hz), 1.50 (3H, d, J = 7.1 Hz), 2.28 (3H, s), 3.25 (2H, q, J = 7.4 Hz), 4.91−5.09 (1H, m), 6.29 (1H, s), 6.72 (1H, d, J = 8.8 Hz), 7.42 (1H, dd, J = 8.7, 4.6 Hz), 7.54−7.67 (2H, m), 7.82 (1H, d, J = 8.7 Hz), 7.91 (1H, s), 8.54 (1H, d, J = 3.0 Hz), 12.52 (1H, s). MS (ESI/APCI) *m/z* 429.2 $[M + H]^+$. HPLC purity: 97.8%.

***N*-((1*S*)-1-(5-Fluoropyridin-2-yl)ethyl)-3-(isopropylsulfonyl)-1-(5-methyl-1*H*-pyrazol-3-yl)-1**

***H*-pyrrolo[2,3-*b*]pyridin-6-amine (6).** To a solution of **39** (0.278 g, 0.44 mmol) in dry THF (2.5 ml) was added KO*t*-Bu (0.059 g, 0.52 mmol) at 0 °C. The reaction mixture was stirred for 3 min, and then 2-iodopropane (0.065 ml, 0.65 mmol) was added to this mixture at room temperature. The reaction color immediately turned to orange, and then concentrated in vacuo. The residue was dissolved in water and extracted with EtOAc twice. The combined organic layers were washed with brine, dried over Na_2SO_4 and concentrated in vacuo. The residue was purified by column chromatography (silica gel, hexane/ethyl acetate, 90:10 to 70:30) to give the sulfide intermediate (0.153 g) as (a) colorless solid. To a solution of the intermediate in EtOAc (3 ml) was added *m*-CPBA (151 mg, 0.61 mmol) at 0 °C. After stirring at this temperature for 1 h, the reaction was quenched by sat. $Na_2S_2O_3$ aq. and then extracted with EtOAc twice. The combined organic layers were washed with brine, dried over $MgSO_4$ and concentrated in vacuo. The residue was purified by column chromatography (silica gel, hexane/ethyl acetate, 80:20 to 40:60) to give the sulfone intermediate (138 mg) as a colorless gum. To a solution of the sulfone intermediate (138 mg, 0.26 mmol) in MeOH (3 ml) was added 4 N HCl in EtOAc (0.50 ml, 2.00 mmol) at 0 °C. After stirring for 10 min, the reaction was neutralized by sat. $NaHCO_3$ aq. and extracted with EtOAc twice. The combined organic layers were washed with brine, dried over Na_2SO_4 and concentrated in vacuo. The residue was purified by column chromatography (silica gel, hexane/ethyl acetate, 80:20 to 60:40) to give **6** (80.0 mg, 0.181 mmol, 69%) as a colorless

amorphous powder. ^{1}H NMR (300 MHz, DMSO-d_6) δ 1.19 (6H, d, J = 6.8 Hz), 1.50 (3H, d, J = 7.0 Hz), 2.29 (3H, s), 3.24−3.39 (1H, m), 5.01 (1H, quint, J = 6.5 Hz), 6.31 (1H, s), 6.72 (1H, d, J = 8.7 Hz), 7.43 (1H, dd, J = 8.9, 4.5 Hz), 7.54−7.67 (2H, m), 7.80 (1H, d, J = 8.9 Hz), 7.88 (1H, s), 8.54 (1H, d, J = 3.0 Hz), 12.53 (1H, s). MS (ESI/APCI) *m/z* 443.2 $[M + H]^+$. HPLC purity: 100%.

***N*-((1*S*)-1-(5-fluoropyridin-2-yl)ethyl)-1-(5-methyl-1*H*-pyrazol-3-yl)-3-(oxetan-3-ylsulfonyl)-1*H*-pyrrolo[2,3-*b*]pyridin-6-amine (7).** The title compound was prepared in 11% yield as brown gum from **39** using the procedure analogous to that described for the synthesis of **4**. ^{1}H NMR (300 MHz, DMSO-d_6) δ 1.50 (3H, d, J = 7.0 Hz), 2.29 (3H, s), 4.59−4.88 (6H, m), 5.01 (1H, quint, J = 6.7 Hz), 6.27 (1H, s), 6.73 (1H, d, J = 8.7 Hz), 7.42 (1H, dd, J = 8.9, 4.5 Hz), 7.56−7.67 (2H, m), 7.83 (1H, d, J = 8.7 Hz), 8.01 (1H, s), 8.54 (1H, d, J = 3.0 Hz), 12.56 (1H, s). MS (ESI/APCI) *m/z* 457.2 $[M + H]^+$. HPLC purity: 95.7%.

6-(((1*S*)-1-(5-Fluoropyridin-2-yl)ethyl)amino)-*N*,*N*-dimethyl-1-(3-methyl-1*H*-pyrazol-5-yl)-1*H*-pyrrolo[2,3-*b*]pyridine-3-carboxamide (8). To a mixture of **44** (0.040 g, 0.090 mmol) and 2-methyl-2-butene (0.24 ml, 2.2 mmol) in THF (0.45 ml) and *t*-BuOH (0.45 ml) was added a mixture of sodium chlorite (0.048 g, 0.54 mmol) and sodium phosphate, monobasic (0.075 g, 0.62 mmol) in water (0.89 ml) at 0 °C. The mixture was stirred at room temperature for 23 h. The mixture was diluted with water and saturated brine, extracted with EtOAc, dried over Na_2SO_4,

filtered, and concentrated in vacuo. To the residue (0.060 g) were added dry THF (1.8 ml), TEA (0.056 ml, 0.40 mmol), dimethylamine hydrochloride (0.015 g, 0.18 mmol), EDC·HCl (0.034 g, 0.18 mmol), and HOBt·H_2O (0.027 g, 0.18 mmol) at room temperature. The mixture was stirred at room temperature for 22 h. The mixture was diluted with water, saturated brine, and saturated $NaHCO_3$ aq. at room temperature, extracted with EtOAc, dried over Na_2SO_4, filtered, and concentrated in vacuo. To the residue (0.071 g) were added MeOH (0.89 ml) and 2 N HCl in MeOH (0.18 ml, 0.36 mmol) at 0 °C. The mixture was stirred at 0 °C for 1.5 h, and then diluted with saturated $NaHCO_3$ aq., water, and saturated brine at 0 °C, extracted with EtOAc, dried over Na_2SO_4, filtered, concentrated in vacuo, and purified by column chromatography (NH-silica gel, hexane/ethyl acetate, 50:50 to 0:100) and preparative HPLC to yield **8** (0.024 g, 0.059 mmol, 66%) as a pale yellow amorphous solid. ^{1}H NMR (300 MHz, DMSO-d_6) δ 1.50 (3H, d, J = 7.0 Hz), 2.27 (3H, s), 3.07 (6H, s), 4.93−5.08 (1H, m), 6.27 (1H, s), 6.59 (1H, d, J = 8.7 Hz), 7.32 (1H, d, J = 6.1 Hz), 7.42 (1H, dd, J = 8.9, 4.6 Hz), 7.59 (1H, td, J = 8.9, 3.0 Hz), 7.71 (1H, s), 7.81 (1H, d, J = 8.6 Hz), 8.53 (1H, d, J = 2.8 Hz), 12.32 (1H, s). MS (ESI/APCI) *m/z* 408.2 [M + H]$^+$. HPLC purity: 98.2%.

(6-(((1*S*)-1-(5-Fluoropyridin-2-yl)ethyl)amino)-1-(3-methyl-1*H*-pyrazol-5-yl)-1*H*-pyrrolo[2,3-*b*]pyridin-3-yl)(morpholin-4-yl)methanone (9). The title compound was prepared in quantitative yield from **44** using the procedure analogous to that described for the synthesis of **8**.

^{1}H NMR (300 MHz, DMSO-d_6) δ 1.50 (3H, d, J = 7.0 Hz), 2.27 (3H, s), 3.61 (8H, s), 4.94−5.08 (1H, m), 6.27 (1H, s), 6.61 (1H, d, J = 8.7 Hz), 7.33 (1H, d, J = 6.0 Hz), 7.42 (1H, dd, J = 8.7, 4.4 Hz), 7.59 (1H, td, J = 8.8, 2.9 Hz), 7.68 (1H, s), 7.74 (1H, d, J = 8.7 Hz), 8.53 (1H, d, J = 2.9 Hz), 12.32 (1H, s). MS (ESI/APCI) *m/z* 450.1 $[M + H]^+$. HPLC purity: 98.7%.

(6-(((1*S*)-1-(5-Fluoropyridin-2-yl)ethyl)amino)-1-(3-methyl-1*H*-pyrazol-5-yl)-1*H*-pyrrolo[2,3-*b*]pyridin-3-yl)(4-methylpiperazin-1-yl)methanone (10). The title compound was prepared in 0.91% yield as a white amorphous solid from **44** using the procedure analogous to that described for the synthesis of **8**. ^{1}H NMR (300 MHz, DMSO-d_6) δ 1.50 (3H, d, J = 7.0 Hz), 2.19 (3H, s), 2.24−2.36 (7H, m), 3.55−3.65 (4H, m), 4.93−5.09 (1H, m), 6.27 (1H, s), 6.61 (1H, d, J = 8.7 Hz), 7.34 (1H, d, J = 6.2 Hz), 7.42 (1H, dd, J = 8.7, 4.3 Hz), 7.55−7.63 (1H, m), 7.65 (1H, s), 7.71 (1H, d, J = 8.7 Hz), 8.53 (1H, d, J = 2.8 Hz), 12.31 (1H, s). MS (ESI/APCI) *m/z* 463.1 $[M + H]^+$. HPLC purity: 95%.

***N*-((1*S*)-1-(5-Fluoropyridin-2-yl)ethyl)-1-(3-methyl-1*H*-pyrazol-5-yl)-3-(1-methyl-1,2,3,6-tetrahydropyran-4-yl)-1*H*-pyrrolo[2,3-*b*]pyridin-6-amine (11).** To a mixture of **26b** (7.65 g, 16.8 mmol) in toluene (60 ml)/water (6 ml) were added 2-(3,6-dihydro-2H-pyran-4-yl)-4,4,5,5-tetramethyl-1,3,2-dioxaborolane (20.0 g, 95.2 mmol), $PdCl_2(AmPhos)_2$ (1.79 g, 2.52 mmol) and potassium carbonate (13.9 g, 101 mmol) at room temperature. The mixture was stirred at 110 ^{o}C overnight under argon atmosphere. The mixture

was quenched with water, extracted with EtOAc, dried over $MgSO_4$, and concentrated in vacuo. The residue was purified by column chromatography (silica gel, hexane/ethyl acetate, 85:15 to 60:40) to give a THP protected intermediate as a yellow amorphous. The compound was diluted in MeOH (60 ml), and was added 4 N HCl in EtOAc (6.12 ml, 24.5 mmol) at 0 ^{o}C. After stirring for 10 min, the reaction was neutrallized by sat. $NaHCO_3$ aq. and extracted with EtOAc twice. The combined organic layers were washed with brine, dried over Na_2SO_4 and concentrated in vacuo. The residue was purified by column chromatography (silica gel, hexane/ethyl acetate, 90:10 to 70:30). The obtained solid was washed with hexane-EtOAc to give **11** (3.26 g, 7.79 mmol, 64%) as a colorless powder. ^{1}H NMR (300 MHz, DMSO-d_6) δ 1.50 (3H, d, J = 7.0 Hz), 2.25 (3H, s), 2.42 (2H, brs), 3.82 (2H, t, J = 5.4 Hz), 4.23 (2H, d, J = 2.3 Hz), 5.01 (1H, quint, J = 6.8 Hz), 6.18 (1H, brs), 6.26 (1H, s), 6.54 (1H, d, J = 8.7 Hz), 7.21 (1H, d, J = 6.0 Hz), 7.42 (1H, dd, J = 8.9, 4.5 Hz), 7.47 (1H, s), 7.59 (1H, td, J = 8.8, 2.9 Hz), 7.89−7.99 (1H, m), 8.53 (1H, d, J =2.8 Hz), 12.20 (1H, s). MS (ESI/APCI) *m/z* 419.2 $[M + H]^+$. HPLC purity: 100%. Anal. Calcd for $C_{23}H_{23}N_6OF$: C, 66.01; H, 5.54; N, 20.08; Found: C, 65.98; H, 5.58; N, 19.93.

(6-(1-(5-fluoropyridin-2-yl)ethoxy)-1-(3-methyl-1*H*-pyrazol-5-yl)-1*H*-pyrrolo[2,3-*b*]pyridin-3-yl)(morpholin-4-yl)methanone (12). To a mixture of **49** (0.863 g, 1.92 mmol) and 2-methyl-2-butene (5.09 ml, 48.0 mmol) in THF (dry) (9.6 ml)/*t*-BuOH (9.6 ml) was added a mixture of sodium chlorite (1.04 g, 11.5 mmol) and sodium phosphate, monobasic (1.61 g, 13.4

mmol) in water (19.2 ml) at 0 °C. The mixture was stirred at room temperature for 15 h. The mixture was diluted with water and saturated brine, extracted with EtOAc, dried over Na_2SO_4, filtered, and concentrated in vacuo to yield carboxylic acid intermediate as a yellow amorphous solid in quantitative yield. A mixture of the carboxylic acid intermediate (18.6 mg, 0.040 mmol), morpholine (6.97 mg, 0.080 mmol), HATU (30.4 mg, 0.080 mmol), and DIPEA (0.014 mL, 0.080 mmol) in DMF (1 ml) was stirred at room temperature overnight, then added 2 N HCl in MeOH (0.500 ml). The mixture was stirred at room temperature for 10 min. The reaction mixture was poured into EtOAc (3 mL) and $NaHCO_3$/water (1 mL), and stirred for 5 min. The organic layer was filtered on Top-Phase Separation Filter Tube, and the filtrate was evaporated by blowing away with the air at 60 °C. The residue was purified by preparative HPLC (YMCTriartC18, eluted with MeCN/10mM NH_4HCO_3 aq.). The desired fraction was evaporated by blowing away with the air at 60 °C to give **12** (12.1 mg, 0.0269 mmol, 67%). ^{1}H NMR (300 MHz, $CDCl_3$) δ 1.74 (3H, d, *J* = 6.6 Hz), 2.32−2.45 (3H, m), 3.64-3.86 (9H, m), 6.18 (1H, q, *J* = 6.6 Hz), 6.47 (1H, s), 6.82 (1H, d, *J* = 8.6 Hz), 7.28−7.38 (1H, m), 7.40−7.49 (1H, m), 7.97 (1H, s), 8.02 (1H, d, *J* = 8.6 Hz), 8.47 (1H, d, *J* = 2.8 Hz), 1H not observed. MS (ESI/APCI) *m/z* 451.1 $[M + H]^+$. HPLC purity: 99.2%.

(6-(1*S)-(5-fluoropyridin-2-yl)ethoxy)-1-(5-methyl-1*H*-pyrazol-3-yl)-1*H*-pyrrolo[2,3-*b*]pyridin-3-yl)((2*S*)-2-methylmorpholin-4-yl)methanone (13).** To an ice-cooled solution of **53** (1.35 g,

3.00 mmol) and 2-methyl-2-butene (7.95 ml, 75.1 mmol) in THF (15 ml) and *t*-BuOH (15 ml) was added a mixture of sodium chlorite (2.06 g, 18.0 mmol) and sodium phosphate, monobasic (2.52 g, 21.0 mmol) in water (30 ml). The mixture was stirred at room temperature for 15 h. The mixture was diluted with water and extracted with EtOAc. The extract was washed with sat. brine, dried over $MgSO_4$, and concentrated in vacuo to yield a carboxylic intermediate (1.39 g, 2.99 mmol, 99 %) as a yellow amorphous solid. To a stirred mixture of the obtained carboxylic acid (0.20 g, 0.43 mmol), (S)-2-methylmorpholine (0.052 g, 0.52 mmol), and TEA (0.18 ml, 1.3 mmol) in DMF (3.6 ml) was added HATU (0.18 g, 0.47 mmol). The reaction mixture was stirred at room temperature for 15 h, diluted with water, and extracted with EtOAc. The extract was washed with sat. brine, dried over $MgSO_4$, and concentrated in vacuo. The residue was purified to give amide intermediate (190 mg), which was dissolved in EtOAc (3 ml)/MeOH (3 ml). To the solution at 0 °C was added 4M HCl in EtOAc (0.50 ml, 2.0 mmol). After being stirred for 30 min at 0 °C, the mixture was basified with sat. $NaHCO_3$ and extracted with EtOAc. The extract was washed with sat. brine, dried over $MgSO_4$ and concentrated in vacuo. The residue was purified by column chromatography (silica gel, hexane/ethyl acetate, 90:10 to 0:100) to give **13** (170 mg, 0.37 mmol, 85%) as a pale yellow oil. ^{1}H NMR (300 MHz, $CDCl_3$) δ 1.18 (3H, d, J = 6.2 Hz), 1.74 (3H, d, J = 6.6 Hz), 2.40 (3H, s), 2.74−2.91 (1H, m), 3.12 - 3.30 (1H, m), 3.50−3.68 (2H, m), 3.86−3.98 (1H, m), 4.19−4.39 (2H, m), 6.18 (1H, q, J = 6.5 Hz), 6.47 (1H, s), 6.82 (1H, d, J = 8.5

Hz), 7.28−7.37 (1H, m), 7.39−7.49 (1H, m), 7.89−8.07 (2H, m), 8.47 (1H, d, *J* = 2.8 Hz). MS (ESI/APCI) *m/z* 465.2 [M+H]+; HPLC purity: 100%.

(6-(1*R)-(5-fluoropyridin-2-yl)ethoxy)-1-(3-methyl-1*H*-pyrazol-5-yl)-1*H*-pyrrolo[2,3-*b*]pyridin-3-yl)((2*R*)-2-methylmorpholin-4-yl)methanone (14).** To an ice-cooled solution of **53** (1.35 g, 3.00 mmol) and 2-methyl-2-butene (7.95 ml, 75.1 mmol) in THF (15 ml)/*t*-BuOH (15 ml) was added a mixture of sodium chlorite (2.06 g, 18.0 mmol) and sodium phosphate, monobasic (2.52 g, 21.0 mmol) in water (30 ml). The mixture was stirred at room temperature for 15 h. The mixture was diluted with water and extracted with EtOAc. The extract was washed with sat. brine, dried over $MgSO_4$, and concentrated in vacuo to yield a carboxylic intermediate (1.39 g, 2.99 mmol, 99 %) as a yellow amorphous solid. To a stirred mixture of the obtained carboxylic acid (0.077 g, 0.17 mmol), HOBt monohydrate (0.051 g, 0.33 mmol), (*R*)-2-methylmorpholine hydrochloride (0.025 g, 0.18 mmol), and TEA (0.092 ml, 0.66 mmol) in DMF (1.1 ml) was added EDC·HCl (0.063 g, 0.33 mmol). The reaction mixture was stirred at room temperature for 15 h, diluted with water, and extracted with EtOAc. The extract was washed with sat. brine, dried over $MgSO_4$, and concentrated in vacuo. The residue was purified by column chromatography (NH-silica gel, hexane/ethyl acetate, 95:5 to 0:100) to give the intermediary amide, which was dissolved in EtOAc (3 ml) and MeOH (3 ml). To the solution at 0 °C was added 4M HCl in EtOAc (0.50 ml, 2.0 mmol). After being stirred for 30 min at 0 °C, the mixture was basified with

sat. $NaHCO_3$ and extracted with EtOAc. The extract was washed with sat. brine, dried over $MgSO_4$ and concentrated in vacuo. The residue was purified by column chromatography (silica gel, hexane/ethyl acetate, 50:50 to 0:100) to give **14** (45 mg, 0.097 mmol, 59%) as a pale yellow solid. ^{1}H NMR (300 MHz, $CDCl_3$) δ 1.18 (3H, d, *J* = 6.2 Hz), 1.74 (3H, d, *J* = 6.6 Hz), 2.40 (3H, s), 2.76−2.90 (1H, m), 3.13−3.29 (1H, m), 3.52−3.67 (2H, m), 3.86−3.97 (1H, m), 4.18−4.39 (2H, m), 6.18 (1H, q, *J* = 6.6 Hz), 6.47 (1H, s), 6.82 (1 H, d, *J* = 8.7 Hz), 7.29−7.38 (1H, m), 7.41−7.48 (1H, m), 7.95 (1H, s), 8.01 (1H, d, *J* = 8.5 Hz), 8.47 (1H, d, *J* = 2.8 Hz). MS (ESI/APCI) *m/z* 465.1 [M+H]+; HPLC purity: 100%.

6-(1*S)-(5-fluoropyridin-2-yl)ethoxy)-3-(methoxymethyl)-1-(3-methyl-1*H*-pyrazol-5-yl)-1*H*-pyrrolo[2,3-*b*]pyridine (15).** The title compound was prepared in 53% yield as colorless oil from **52a** using the procedure analogous to that described for the synthesis of **26a** and **2**. ^{1}H NMR (300 MHz, $CDCl_3$) δ 1.73 (3H, d, *J* = 6.7 Hz), 2.37 (3H, s), 3.35 (3H, s), 4.58 (2H, s), 6.18 (1H, q, *J* = 6.7 Hz), 6.35 (1H, s), 6.73 (1H, d, *J* = 8.5 Hz), 7.28−7.38 (1H, m), 7.41−7.49 (1H, m), 7.52 (1H, s), 7.91 (1H, d, *J* = 8.5 Hz), 8.50 (1H, d, *J* = 2.8 Hz). MS (ESI/APCI) *m/z* 382.1 [M+H]+. HPLC purity: 100%.

6-(1*R)-(5-fluoropyridin-2-yl)ethoxy)-3-(methoxymethyl)-1-(3-methyl-1*H*-pyrazol-5-yl)-1*H*-pyrrolo[2,3-*b*]pyridine (16).** The title compound was prepared in 69% yield as colorless oil from **52b** using the procedure analogous to that described for the synthesis of **26a** and **2**. ^{1}H NMR (300

MHz, $CDCl_3$) δ 1.73 (3H, d, *J* = 6.6 Hz), 2.37 (3H, s), 3.35 (3H, s), 4.58 (2H, s), 6.18 (1H, q, *J* = 6.8 Hz), 6.35 (1H, s), 6.73 (1H, d, *J* = 8.5 Hz), 7.29−7.38 (1H, m), 7.41−7.49 (1H, m), 7.52 (1H, s), 7.91 (1H, d, *J* = 8.5 Hz), 8.50 (1H, d, *J* = 3.0 Hz). MS (ESI/APCI) *m/z* 382.1 [M+H]+. HPLC purity: 100%.

6-Chloro-3-iodoimidazo[1,2-*b*]pyridazine (**18**). A mixture of 6-chloroimidazo[1,2-b]pyridazine **17** (10.0 g, 65.1 mmol) and NIS (16.1 g, 71.6 mmol) in DMF (150 mL) was heated at 90 °C for 15 h. After cooling, the mixture was poured into water and stirred for 1 h. The resulting precipitate was collected by filtration and dried to give **18** (14.7 g, 52.6 mmol, 81%) as a brown solid. ^{1}H NMR (300 MHz, DMSO-d_6) δ 7.42 (1H, d, *J* = 9.4 Hz), 7.97 (1H, s), 8.22 (1H, d, *J* = 9.4 Hz).

6-Chloro-3-(3-methyl-1-(tetrahydro-2*H*-pyran-2-yl)-1*H*-pyrazol-5-yl)imidazo[1,2-*b*]pyridazine (**19**). A mixture of 6-chloro-3-iodoimidazo[1,2-b]pyridazine **18** (2.00 g, 7.16 mmol), 3-methyl-1-(tetrahydro-2H-pyran-2-yl)-5-(4,4,5,5-tetramethyl-1,3,2-dioxaborolan-2-yl)-1H-pyrazole **22** (4.18 g, 14.3 mmol), $Pd(PPh_3)_4$ (0.827 g, 0.720 mmol), and aqueous 2 N Na_2CO_3 (15 mL) in DME (60 mL) was heated at reflux under argon atmosphere for 15 h. After cooling, the mixture was partitioned between EtOAc and water. The organic layer was washed with brine, dried over $MgSO_4$, and concentrated in vacuo. The residue was purified by column chromatography (silica gel, hexane/ethyl acetate, 90:10 to 20:80) to give **19** (910 mg, 2.86 mmol,

40%) as a pale yellow solid. ^{1}H NMR (300 MHz, $CDCl_3$) δ 1.51−1.87 (3H, m), 1.92−2.16 (2H, m), 2.39 (3H, s), 2.50−2.71 (1H, m), 3.59−3.75 (1H, m), 4.06−4.19 (1H, m), 5.23 (1H, dd, *J* = 10.2, 2.6 Hz), 6.69 (1H, s), 7.15 (1H, d, *J* = 9.4 Hz), 7.99 (1H, d, *J* = 9.4 Hz), 8.02 (1H, s). MS (ESI/APCI) m/z 318.1 [M + H]+.

3-Methyl-1-(tetrahydro-2*H*-pyran-2-yl)-1*H*-pyrazole (21). To a mixture of 3-methyl-1*H*-pyrazole **20** (25.0 g, 304 mmol) in toluene (152 ml) were added 3,4-dihydro-2*H*-pyrane (30.6 ml, 335 mmol) and TFA (1.17 ml, 15.2 mmol) at room temperature. The mixture was stirred under reflux for 1 day. The mixture was diluted with brine and $NaHCO_3$ aq. at room temperature, extracted with EtOAc, dried over $MgSO_4$, filtered, concentrated in vacuo and purified by column chromatography (silica gel, hexane/ethyl acetate, 100:0 to 50:50) to yield **21** (48.5 g, 292 mmol, 96%) as a yellow oil. ^{1}H NMR (300 MHz, DMSO-d_6) δ 1.40−1.73 (3H, m), 1.78−2.11 (3H, m), 2.15 (3H, s), 3.52−3.69 (1H, m), 3.80−3.96 (1H, m), 5.26 (1H, dd, *J* = 10.4, 2.4 Hz), 6.06 (1H, d, *J* = 2.3 Hz), 7.70 (1H, d, *J* = 2.3 Hz).

3-Methyl-1-(tetrahydro-2*H*-pyran-2-yl)-5-(4,4,5,5-tetramethyl-1,3,2-dioxaborolan-2-yl)-1*H*-pyrazole (**22**). To a solution of **21** (23.0 g, 138 mmol) in THF (dry) (173 ml) was added *n*-BuLi (91 ml, 145 mmol) dropwise at -78 °C. The reaction mixture was stirred at the same temperature for 2 h. To this solution was added triisopropyl borate (35.1 ml, 152 mmol) dropwise at -78 °C. The reaction mixture was gradually warmed to room temperature and stirred for 2 h. To this

mixture was added pinacol (18.0 g, 152 mmol) and acetic acid (16.0 ml, 277 mmol) at the same temperature. The mixture was stirred overnight and then concentrated in vacuo. The residue was diluted with water and extracted with EtOAc twice. The combined organic layers were washed with brine, dried over $MgSO_4$ and concentrated in vacuo. The residue was purified by column chromatography (silica gel, hexane/ethyl acetate, 100:0 to 85:15) to give **22** (26.9 g, 92.0 mmol, 67%) as a yellow oil. ^{1}H NMR (300 MHz, DMSO-d_6) 1.28 (12H, *d*, *J* = 3.9 Hz), 1.41−1.74 (3H, m), 1.84 (1H, dd, *J* = 12.7, 2.4 Hz), 1.91−2.04 (1H, m), 2.16 (3H, s), 2.18−2.33 (1H, m), 3.45−3.59 (1H, m), 3.81−3.96 (1H, m), 5.61 (1H, dd, *J* = 10.1, 2.4 Hz), 6.42 (1H, s). MS (ESI/APCI) m/z 293.3 [M + H]+.

1*H*-Pyrrolo[2,3-*b*]pyridine 7-oxide (**24a**). To a solution of 1H-pyrrolo[2,3-b]pyridine **23a** (10.0 g, 84.7 mmol) in EtOAc (500 mL) was added portionwise *m*-CPBA (85% purity, 37.8 g, 93.2 mmol) at room temperature. After addition, the resulting mixture was stirred at 20−30 °C for 12 h. This reaction was carried out twice in paralell. The mixture was filtered and the solid was washed with EtOAc (200 mL) and dried under reduced pressure to afford **24a** *m*-CBA adduct (15.0 g, 51.7 mmol, 61%) as an off-white solid. ^{1}H NMR (400 MHz, DMSO-d_6) δ 6.56 (1H, d, *J* = 3.2 Hz), 7.06 (1H, dd, *J* = 8.0, 6.4 Hz), 7.45 (1H, d, *J* = 3.2 Hz), 7.51 (1H, t, *J* = 8.0 Hz), 7.60−7.70 (2H, m), 7.85−7.92 (2H, m), 8.16 (1H, d, *J* = 6.4 Hz), 12.55 (1H, brs), 13.56 (1H, brs).

3-Chloro-1*H*-pyrrolo[2,3-*b*]pyridine 7-oxide (**24b**). To a mixture of **23b** (4.53 g, 29.7 mmol) in

Et_2O (297 ml) was portionwise added *m*-CPBA (10.3 g, 44.5 mmol) at room temperature. The mixture was stirred at room temperature for 1 day. The precipitates were collected by filtration, washed with cold Et_2O and dried in vacuo to yield **24b** (4.72 g, 28.0 mmol, 94%) as a yellow solid. ^{1}H NMR (300 MHz, DMSO-d_6) δ 7.17 (1H, dd, J = 8.1, 6.2 Hz), 7.59 (1H, d, J = 8.3 Hz), 7.70 (1H, s), 8.23 (1H, d, J = 6.0 Hz), 12.86 (1H, brs). MS (ESI/APCI) m/z 169.0 $[M + H]^+$.

(*S*)-*N*-(1-(2,4-difluorophenyl)ethyl)-1*H*-pyrrolo[2,3-*b*]pyridin-6-amine (**25a**). To a mixture of **24a** *m*-CBA adduct (0.85 g, 2.92 mmol) in CH_3CN (14.62 ml) were added dimethyl sulfate (0.304 ml, 3.22 mmol) at room temperature. The mixture was heated to 80 °C overnight under argon atmosphere. To the mixture was added DIPEA (2.043 ml, 11.70 mmol) and (*R*)-1-(2,4-difluorophenyl)ethanamine **28** (0.689 g, 4.39 mmol), and the mixture was stirred at 80 °C for overnight under argon atmosphere. The mixture was diluted with water, extracted with EtOAc twice, dried over Na_2SO_4, filtered, concentrated in vacuo. The residue was purified by column chromatography (silica gel, hexane/ethyl acetate, 90:10 to 70:30) to give **25a** (0.300 g, 1.098 mmol, 38%) as a brown gum. ^{1}H NMR (300 MHz, $CDCl_3$) δ 1.54 (3H, d, J = 6.8 Hz), 4.78 (1H, d, J = 5.7 Hz), 5.08−5.20 (1H, m), 6.17 (1H, d, J = 8.3 Hz), 6.29 (1H, dd, J = 3.4, 1.9 Hz), 6.68−6.82 (2H, m), 6.90 (1H, dd, J = 3.4, 2.3 Hz), 7.26−7.37 (1H, m), 7.62 (1H, d, J = 8.3 Hz), 9.16 (1H, brs). MS (ESI/APCI) m/z 274.1 [M + H]+.

3-Chloro-*N*-((1*S*)-1-(5-fluoropyridin-2-yl)ethyl)-1*H*-pyrrolo[2,3-*b*]pyridin-6-amine (25b). To

a mixture of **24b** (6.00 g, 35.6 mmol) in CH_3CN (300 ml) were added *m*-CBA (4.46 g, 28.5 mmol) and dimethyl sulfate (3.70 ml, 39.2 mmol) at room temperature. The mixture was heated to 80 °C overnight under nitrogen atmosphere. To the mixture was added (*S*)-1-(5-fluoropyridin-2-yl)ethanamine **29** (7.48 g, 53.4 mmol) and DIPEA (24.9 ml, 142 mmol), and the mixture was stirred at 80 °C for 3 days under nitrogen atmosphere. The mixture was diluted with $NaHCO_3$ aq. at room temperature, extracted with EtOAc twice, dried over $MgSO_4$, filtered, concentrated in vacuo. The residue was purified by column chromatography (silica gel, hexane/ethyl acetate, 90:10 to 70:30) to give **25b** (4.65 g, 16.0 mmol, 45%) as brown gum. ^{1}H NMR (300 MHz, DMSO-d_6) δ 1.47 (3H, d, J = 7.0 Hz), 5.14 (1H, quint, J = 7.2 Hz), 6.49 (1H, d, J = 8.6 Hz), 7.00 (1H, d, J = 2.6 Hz), 7.06 (1H, d, J = 7.7 Hz), 7.42 (1H, dd, J = 8.7, 4.6 Hz), 7.51 (1H, dd, J = 8.6, 0.4 Hz), 7.61 (1H, td, J = 8.8, 3.0 Hz), 8.49 (1H, d, J = 2.9 Hz), 11.14 (1H, brs). MS (ESI/APCI) *m/z* 291.1 $[M + H]^+$.

***N*-((*S*)-1-(2,4-difluorophenyl)ethyl)-1-(3-methyl-1-(tetrahydro-2*H*-pyran-2-yl)-1*H*-pyrazol-5-yl)-1*H*-pyrrolo[2,3-*b*]pyridin-6-amine** (**26a**). To a mixture of **25a** (0.30 g, 1.10 mmol) in dioxane (1.10 ml) were added **27** (0.802 g, 2.74 mmol), copper(I) iodide (0.063 g, 0.330 mmol), (±)-*trans*-1,2-diaminocyclohexane (0.277 ml, 2.31 mmol) and K_3PO_4 (0.816 g, 3.84 mmol) at room temperature. The mixture was heated to 120 °C for 16 h under argon atmosphere. The mixture was diluted with brine and $NaHCO_3$ aq. at room temperature, extracted with EtOAc,

dried over Na_2SO_4, filtered, concentrated in vacuo and purified by column chromatography (silica gel, hexane/ethyl acetate, 80:20 to 67:33) to yield **26a** (0.460 g, 1.051 mmol, 96%) as a white powder. MS (ESI/APCI) m/z 438.2 [M + H]+.

3-Chloro-*N*-((1*S*)-1-(5-fluoropyridin-2-yl)ethyl)-1-(3-methyl-1-(tetrahydro-2*H*-pyran-2-yl)-1*H*-pyrazol-5-yl)-1*H*-pyrrolo[2,3-*b*]pyridin-6-amine (26b). The title compound was prepared in 91% yield as a pale yellow from **25b** and **27** using the procedure analogous to that described for the synthesis of **26a**. ^{1}H NMR (300 MHz, DMSO-d_6) δ 1.27−1.57 (6H, m), 1.60−1.98 (2H, m), 2.03−2.36 (4H, m), 3.09−3.23 (1H, m), 3.66−3.88 (1H, m), 4.71−5.13 (2H, m), 5.76−6.11 (1H, m), 6.59 (1H, dd, J = 8.6, 1.5 Hz), 7.19−7.45 (3H, m), 7.49−7.66 (2H, m), 8.45 (1H, dd, J = 7.6, 2.9 Hz). MS (ESI/APCI) *m/z* 455.2 $[M + H]^+$.

5-Iodo-3-methyl-1-(tetrahydro-2*H*-pyran-2-yl)-1*H*-pyrazole (27). To a mixture of **21** (50.0 g, 301 mmol) in dry THF (301 ml) was added *n*-BuLi in hexane (193 ml, 308 mmol) dropwise at -78 °C under nitrogen atmosphere. The mixture was stirred at -78 °C for 20 min. To the mixture was dropwise added iodine (80.0 g, 316 mmol) in dry THF (301 ml) at -78 °C. The mixture was gradually warmed to room temperature and stirred at room temperature overnight. The reaction mixture was quenched at room temperature by saturated $Na_2S_2O_3$ aq., diluted with brine and $NaHCO_3$ aq., extracted with EtOAc, dried over $MgSO_4$, filtered, concentrated in vacuo, and purified by column chromatography (silica gel, hexane/ethyl acetate, 100:0 to 80:20) to yield **27**

(65.0 g, 222 mmol, 74%) as a pale yellow powder. ^{1}H NMR (300 MHz, DMSO-d_6) δ 1.43−1.57 (2H, m), 1.57−1.76 (1H, m), 1.81 (1H, dq, J = 13.2, 3.1 Hz), 1.90−2.04 (1H, m), 2.09−2.18 (3H, m), 2.18−2.35 (1H, m), 3.49−3.67 (1H, m), 3.90 (1H, dd, J = 10.9, 1.8 Hz), 5.27 (1H, dd, J = 10.0, 2.5 Hz), 6.33 (1H, s). MS (ESI/APCI) *m/z* 209.0 $[M + H]^+$.

***tert*-Butyl 3-iodo-1*H*-pyrrolo[2,3-*b*]pyridine-1-carboxylate (31).** To a solution of **30** (5.65 g, 23.1 mmol) in THF (dry) (150 ml) was added KO*t*-Bu (3.89 g, 34.7 mmol) and BOC_2O (8.06 ml, 34.7 mmol) at room temperature. The reaction mixture became slurry and was stirred overnight. The mixture was partitioned between EtOAc and water. The separated organic layer was washed with brine, dried over Na_2SO_4 and concentrated in vacuo. The residue was purified by column chromatography (silica gel, hexane/ethyl acetate, 99:1 to 90:10) to give **31** (7.90 g, 23.0 mmol, 99%) as a colorless oil. ^{1}H NMR (300 MHz, DMSO-d_6) δ 1.61 (9H, s), 7.39 (1H, dd, J = 7.9, 4.8 Hz), 7.79 (1H, dd, J = 7.9, 1.6 Hz), 8.02 (1H, s), 8.44 (1H, dd, J = 4.8, 1.6 Hz). MS (ESI/APCI) *m/z* 289.0 $[M + H]^+$.

***tert*-Butyl**

3-((3-((2-ethylhexyl)oxy)-3-oxopropyl)thio)-1*H*-pyrrolo[2,3-*b*]pyridine-1-carboxylate (32). A mixture of **31** (7.65 g, 22.2 mmol), 2-ethylhexyl 3-mercaptopropanoate (5.54 ml, 24.5 mmol), $Pd_2(dba)_3$ (0.407 g, 0.440 mmol), Xantophos (0.514 g, 0.890 mmol) and DIPEA (5.82 ml, 33.3 mmol) in toluene was stirred at 70 ^{o}C under Ar for 3 h. The reaction mixture was directly purified

by column chromatography (silica gel, eluted with 2% - 10% EtOAc in hexane) to give **32** (9.50 g, 21.9 mmol, 98%) as a yellow oil. ^{1}H NMR (300 MHz, DMSO-d_6) δ 0.79−0.89 (6H, m), 1.18−1.34 (8 H, m), 1.37−1.55 (1 H, m), 1.58−1.66 (9H, m), 2.57 (2H, t, J = 6.8 Hz), 3.02 (2H, t, J = 6.8 Hz), 3.90 (2H, d, J = 5.8 Hz), 7.37 (1H, dd, J = 7.9, 4.8 Hz), 7.86 (1H, s), 8.05 (1H, dd, J = 7.9, 1.7 Hz), 8.46 (1H, dd, J = 4.7, 1.6 Hz). MS (ESI/APCI) *m/z* 435.0 $[M + H]^+$.

3-(Methylthio)-1H-pyrrolo[2,3-b]pyridine (33). To a solution of **32** (1.74 g, 4.00 mmol) in THF (dry) (8 ml) was added KO*t*-Bu (539 mg, 4.80 mmol) at 0 ^{o}C. The reaction mixture was stirred for 1 h and then iodomethane (0.374 ml, 6.00 mmol) was added to this mixture at 0 ^{o}C. The reaction was stirred for 3 h, and then concentrated in vacuo. The residue was dissolved in MeOH (10 mL) and 2 N HCl in MeOH (5.00 ml, 10.0 mmol) was added to this mixture. The mixture was stirred at 80 ^{o}C for 30 min and then concentrated in vacuo. The residue was dissolved in water, neutrallized by sat.$NaHCO_3$ aq. and extracted with EtOAc twice. The combined organic layers were washed with brine, dried over Na_2SO_4 and concentrated in vacuo. The residue was purified by column chromatography (silica gel, hexane/ethyl acetate, 95:5 to 60:40) to give **33** (596 mg, 3.63 mmol, 91%) as a brown solid. ^{1}H NMR (300 MHz, DMSO-d_6) δ 2.33 (3H, s), 7.14 (1H, dd, J = 7.8, 4.7 Hz), 7.61 (1H, d, J = 2.6 Hz), 7.99 (1H, dd, J = 7.8, 0.9 Hz), 8.26 (1H, dd, J = 4.7, 1.6 Hz), 11.87 (1H, brs). MS (ESI/APCI) *m/z* 165.2 $[M + H]^+$.

3-(Methylsulfonyl)-1*H*-pyrrolo[2,3-*b*]pyridine 7-oxide (34). To a solution of **33** (0.596 g, 3.63

mmol) in EtOAc (18 ml) was added *m*-CPBA (3.13 g, 12.7 mmol) at room temperature. After stirring for 2 h, the precipitate was collected by filtration, washed with hexane-EtOAc (1:1) and dried in vacuo to give **34** (0.705 g, 3.32 mmol, 92%) as a colorless solid. ^{1}H NMR (300 MHz, DMSO-d_6) δ 3.26 (3H, s), 7.29 (1H, dd, J = 8.1, 6.2 Hz), 7.82 (1H, dd, J = 8.1, 0.8 Hz), 8.11 (1H, s), 8.32 (1H, dd, J = 6.2, 0.6 Hz), 13.66 (1H, s). MS (ESI/APCI) *m/z* 213.1 $[M + H]^+$.

(*S*)-*N*-(1-(2,4-Difluorophenyl)ethyl)-3-(methylsulfonyl)-1*H*-pyrrolo[2,3-*b*]pyridin-6-amine (35). The title compound was prepared in 20% yield as brown gum from **34** and **28** using the procedure analogous to that described for the synthesis of **25b**. ^{1}H NMR (300 MHz, DMSO-d_6) δ 1.44 (3H, d, J = 6.9 Hz), 3.11 (3H, s), 5.32 (1H, quin, J = 7.2 Hz), 6.58 (1H, d, J = 8.7 Hz), 7.13−7.21 (1H, m), 7.24 (1H, d, J = 7.7 Hz), 7.36−7.67 (3H, m), 7.78 (1H, d, J = 8.7 Hz), 11.99 (1H, brs). MS (ESI/APCI) *m/z* 352.1 $[M + H]^+$.

3-Iodo-1*H*-pyrrolo[2,3-*b*]pyridine 7-oxide (36). To a mixture of **30** (11.1 g, 45.4 mmol) in Et_2O (400 ml) was added *m*-CPBA (11.3 g, 49.1 mmol) portionwise at room temperature. The mixture was stirred at room temperature for 5 h. The precipitates were collected by filtration, washed with cold Et_2O and dried in vacuo to yield **36** (10.2 g, 39.2 mmol, 86%) as a light brown solid. ^{1}H NMR (300 MHz, DMSO-d_6) δ 7.17 (1H, dd, J = 8.1, 6.1 Hz), 7.36 (1H, dd, J = 8.0, 0.8 Hz), 7.69 (1H, s), 8.21 (1H, dd, J = 6.1, 0.5 Hz), 12.91 (1H, brs). MS (ESI/APCI) *m/z* 261.1 $[M + H]^+$.

2-Ethylhexyl 3-((7-oxido-1*H*-pyrrolo[2,3-*b*]pyridin-3-yl)sulfanyl)propanoate (37). The title

compound was prepared in 99% yield as brown gum from **36** using the procedure analogous to that described for the synthesis of **32**. ^{1}H NMR (300 MHz, DMSO-d_6) δ 0.79−0.90 (6H, m), 1.19−1.34 (8H, m), 1.41−1.55 (1H, m), 2.45−2.56 (2H, m), 2.89 (2H, t, J = 6.8 Hz), 3.79−3.97 (2H, m), 7.16 (1H, dd, J = 8.0, 6.2 Hz), 7.60−7.74 (2H, m), 8.20 (1H, d, J = 5.7 Hz), 12.87 (1H, brs). MS (ESI/APCI) *m/z* 351.2 $[M + H]^+$.

2-Ethylhexyl

3-((6-(((1*S*)-1-(5-fluoropyridin-2-yl)ethyl)amino)-1*H*-pyrrolo[2,3-*b*]pyridin-3-yl)sulfanyl)propanoate (**38**). The title compound was prepared in 49% yield as brown gum from **37** and **29** using the procedure analogous to that described for the synthesis of **25b**. ^{1}H NMR (300 MHz, DMSO-d_6) δ 0.78−0.90 (6H, m), 1.20−1.34 (8H, m), 1.41−1.57 (4H, m), 2.41−2.49 (2H, m), 2.70−2.82 (2H, m), 3.85−3.95 (2H, m), 5.13 (1H, quint, J = 7.1 Hz), 6.47 (1H, d, J = 8.6 Hz), 6.97 (1H, d, J = 7.7 Hz), 7.01 (1H, d, J = 2.5 Hz), 7.44 (1H, dd, J = 8.8, 4.5 Hz), 7.55−7.67 (2H, m), 8.49 (1H, d, J = 2.9 Hz), 11.23 (1H, d, J = 2.0 Hz). MS (ESI/APCI) *m/z* 473.2 $[M + H]^+$.

2-Ethylhexyl

3-((6-(((1*S*)-1-(5-fluoropyridin-2-yl)ethyl)amino)-1-(3-methyl-1-(tetrahydro-2*H*-pyran-2-yl)-1*H*-pyrazol-5-yl)-1*H*-pyrrolo[2,3-*b*]pyridin-3-yl)sulfanyl)propanoate (**39**). The title compound was prepared in 36% yield as brown gum from **38** using the procedure analogous to that described for the synthesis of **26a**. ^{1}H NMR (300 MHz, DMSO-d_6) δ 0.73−0.88 (6 H, m),

1.10−1.57 (16H, m), 1.61−1.90 (1H, m), 1.99−2.18 (1H, m), 2.19−2.26 (3H, m), 2.52−2.57 (2H, m), 2.89 (2H, t, J = 6.8 Hz), 3.10−3.25 (1H, m), 3.63−3.98 (3H, m), 4.64−5.10 (2H, m), 5.69−6.16 (1H, m), 6.46−6.61 (1H, m), 7.08−7.20 (1H, m), 7.22−7.38 (2H, m), 7.56 (1H, td, J = 8.8, 2.9 Hz), 7.67 (1H, d, J = 8.6 Hz), 8.45 (1H, d, J = 2.8 Hz). MS (ESI/APCI) *m/z* 637.3 $[M + H]^+$.

1*H*-Pyrrolo[2,3-*b*]pyridine-3-carbaldehyde (40). To a mixture of hexamethylenetetramine (77.0 g, 550 mmol) and **23a** (50.0 g, 423 mmol) in water (340 ml) was added acetic acid (170 ml) at room temperature. The mixture was heated to 120 °C for 2 h. The mixture was diluted with water at room temperature and cooled to 0 °C. The precipitates were collected by filtration, washed with water, and dried to yield **40** (45.9 g, 314 mmol, 74%) as a white solid. ^{1}H NMR (300 MHz, DMSO-d_6) δ 7.19−7.31 (1H, m), 8.32−8.41 (2H, m), 8.45 (1H, s), 9.90 (1H, s), 12.68 (1H, brs). MS (ESI/APCI) *m/z* 146.9 $[M + H]^+$.

3-(((Triisopropylsilyl)oxy)methyl)-1*H*-pyrrolo[2,3-*b*]pyridine 7-oxide (41). To a mixture of **40** (52.6 g, 360 mmol) in MeOH (1440 ml) was added $NaBH_4$ (13.6 g, 360 mmol) at 0 °C. The mixture was stirred at 0 °C for 1 h. The mixture was concentrated in vacuo and diluted with water. The precipitates were collected by filtration, washed with water, and dried in vacuo to afford an alcohol intermediate (48.5 g) as a white solid. To a mixture of the alcohol intermediate (48.5 g, 327 mmol) in dry DMF (327 ml) were added imidazole (26.7 g, 393 mmol) and TIPSCl (73.5 ml,

344 mmol) at 0 °C. The mixture was stirred at room temperature for 14 h. To the mixture were added imidazole (1.11 g, 16.4 mmol) and TIPSCl (3.50 ml, 16.4 mmol) at room temperature. The mixture was stirred at room temperature for 6 h. The mixture was diluted with water and cooled to 0 °C. The precipitates were collected by filtration, washed with water, dissolved in EtOAc, dried over $MgSO_4$, filtered, and concentrated in vacuo to a TIPS-protected compound as a yellow solid. To a mixture of the TIPS-protected compound (100 g, 327 mmol) in *i*-Pr_2O (818 ml) was added *m*-CPBA (83.0 g, 360 mmol) at 0 °C. The mixture was stirred at room temperature for 6.5 h. To the mixture was added *m*-CPBA (3.76 g, 16.4 mmol) at room temperature. The mixture was stirred at room temperature for 17 h and cooled to 0 °C. The precipitates were collected by filtration and dried in vacuo to yield **41** (90.0 g, 282 mmol, 78% in 3 steps) as a pale yellow solid. ^{1}H NMR (300 MHz, DMSO-d_6) δ 0.94−1.24 (21H, m), 4.91 (2H, s), 7.08 (1H, dd, J = 8.0, 6.2 Hz), 7.36 (1H, d, J = 2.0 Hz), 7.64 (1H, d, J = 7.5 Hz), 8.13 (1H, d, J = 5.7 Hz), 12.29 (1H, brs). MS (ESI/APCI) *m/z* 321.0 $[M + H]^+$.

***N*-((1*S*)-1-(5-Fluoropyridin-2-yl)ethyl)-3-(((triisopropylsilyl)oxy)methyl)-1*H*-pyrrolo[2,3-*b*]pyridin-6-amine (42).** The title compound was prepared in 42% yield as brown gum from **40** and **29** using the procedure analogous to that described for the synthesis of **25b**. ^{1}H NMR (300 MHz, DMSO-d_6) δ 0.94−1.22 (21H, m), 1.46 (3H, d, J = 7.0 Hz), 4.78 (2H, s), 5.13 (1H, quint, J = 7.0 Hz), 6.37 (1H, d, J = 8.5 Hz), 6.73−6.82 (2H, m), 7.43 (1H, dd, J = 8.7, 4.6 Hz), 7.54−7.65 (2H,

m), 8.48 (1H, d, *J* = 2.9 Hz), 10.70 (1H, s). MS (ESI/APCI) *m/z* 443.3 $[M + H]^+$.

***N*-((1*S*)-1-(5-Fluoropyridin-2-yl)ethyl)-1-(3-methyl-1-(tetrahydro-2*H*-pyran-2-yl)-1*H*-pyrazol-5-yl)-3-(((triisopropylsilyl)oxy)methyl)-1*H*-pyrrolo[2,3-*b*]pyridin-6-amine (43).** The title compound was prepared in 75% yield as a yellow form from **42** using the procedure analogous to that described for the synthesis of **26a**. ^{1}H NMR (300 MHz, DMSO-d_6) δ 0.95−1.59 (56H, m), 1.66−2.01 (3H, m), 2.03−2.35 (7H, m), 3.10−3.23 (1H, m), 3.24−3.41 (1H, m), 3.69−3.91 (2H, m), 4.73−5.08 (8H, m), 5.63 (1H, s), 6.01 (1H, s), 6.48 (2H, dd, *J* = 8.6, 5.3 Hz), 6.94 (1H, s), 6.97 (1H, s), 7.12 (2H, dd, *J* = 12.1, 7.1 Hz), 7.26−7.39 (2H, m), 7.57 (2H, td, *J* = 8.8, 2.9 Hz), 7.67 (2H, dd, *J* = 8.5, 1.8 Hz), 8.46 (2H, d, *J* = 2.9 Hz).

6-(((1*S*)-1-(5-Fluoropyridin-2-yl)ethyl)amino)-1-(3-methyl-1-(tetrahydro-2*H*-pyran-2-yl)-1*H*-pyrazol-5-yl)-1*H*-pyrrolo[2,3-*b*]pyridine-3-carbaldehyde (44). To a mixture of **43** (1.00 g, 1.65 mmol) in dry THF (16.5 ml) was added 1M TBAF in THF (1.81 ml, 1.81 mmol) at 0 °C. The mixture was stirred at room temperature for 2 h. The mixture was diluted with water and saturated brine at 0 °C, extracted with EtOAc, dried over Na_2SO_4, filtered, concentrated in vacuo, and purified by column chromatography (silica gel, hexane/ethyl acetate, 60:40 to 0:100) to yield an alcohol intermediate as a pale yellow amorphous solid. To a mixture of the alcohol intermediate (0.619 g, 1.37 mmol) in dry THF (13.7 ml) was added MnO_2 (0.703 g, 6.87 mmol) at room temperature. The mixture was heated to reflux for 5.5 h. To the mixture was added MnO_2

(0.422 g, 4.12 mmol) at room temperature. The mixture was heated to reflux for 3.5 h. The mixture was filtered through a pad of celite. The filtrate was concentrated in vacuo to yield **44** (0.568 g, 1.27 mmol, 87% in 2 steps) as a brown amorphous solid. ^{1}H NMR (300 MHz, DMSO-d_6) δ 1.13−1.54 (12H, m), 1.64−2.30 (12H, m), 3.09−3.23 (1H, m, J = 7.0 Hz), 3.25−3.34 (1H, m), 3.64−3.73 (1H, m), 3.74−3.84 (1H, m), 4.77 (1H, d, J = 6.6 Hz), 4.84−5.02 (2H, m), 5.08 (1H, d, J = 7.6 Hz), 5.95 (1H, s), 6.23 (1H, s), 6.64 (2H, d, J = 8.6 Hz), 7.25 (1H, dd, J = 8.9, 4.7 Hz), 7.32 (1H, dd, J = 8.7, 4.5 Hz), 7.45 (2H, d, J = 7.3 Hz), 7.49−7.62 (2H, m), 7.98−8.10 (4H, m), 8.45 (2H, dd, J = 8.6, 3.0 Hz), 9.84 (2H, d, J = 2.7 Hz). MS (ESI/APCI) *m/z* 449.2 $[M + H]^+$.

1-Acetyl-3-(((triisopropylsilyl)oxy)methyl)-1*H*-pyrrolo[2,3-*b*]pyridin-6-yl acetate (45). A mixture of **41** (26.9 g, 83.8 mmol) in acetic acid anhydride (84 ml) was heated to reflux for 100 min. The mixture was concentrated in vacuo and purified by column chromatography (silica gel, hexane/ethyl acetate, 100: 0 to 70:30) to yield **45** (24.0 g, 59.2 mmol, 71%) as a colorless oil. ^{1}H NMR (300 MHz, DMSO-d_6) δ 0.99−1.24 (21H, m), 2.35 (3H, s), 2.87 (3H, s), 4.96 (2H, d, J = 1.1 Hz), 7.16 (1H, d, J = 8.3 Hz), 7.90 (1H, s), 8.19 (1H, d, J = 8.3 Hz). MS (ESI/APCI) *m/z* 405.1 $[M + H]^+$.

3-(((Triisopropylsilyl)oxy)methyl)-1*H*-pyrrolo[2,3-*b*]pyridin-6-ol (46). To a mixture of **45** (34.3 g, 84.7 mmol) in MeOH (85 ml) and water (85 ml) was added K_2CO_3 (23.4 g, 169 mmol) at

room temperature. The mixture was stirred at room temperature for 1.5 h. The mixture was concentrated in vacuo and diluted with water. The precipitates were collected by filtration, washed with water, and dried to yield **46** (19.0 g, 59.3 mmol, 70%) as a pale red solid after trituration with *i*-Pr_2O/hexane. ^{1}H NMR (300 MHz, DMSO-d_6) δ 0.88−1.31 (21H, m), 4.83 (2H, s), 6.31 (1H, d, *J* = 8.5 Hz), 6.97 (1H, s), 7.75 (1H, d, *J* = 8.5 Hz), 10.38 (1H, brs), 10.92 (1H, brs). MS (ESI/APCI) *m/z* 321.0 $[M + H]^+$.

6-(1-(5-Fluoropyridin-2-yl)ethoxy)-3-(((triisopropylsilyl)oxy)methyl)-1*H*-pyrrolo[2,3-*b*]pyridine (47). To a mixture of **46** (4.48 g, 14.0 mmol) in dry DMF (46.6 ml) were added **51** (4.54 g, 15.4 mmol) and Cs_2CO_3 (5.01 g, 15.4 mmol) at room temperature. The mixture was stirred at room temperature for 24 h. The mixture was diluted with water and saturated brine at room temperature, extracted with EtOAc, dried over $MgSO_4$, filtered, concentrated in vacuo, and purified by column chromatography (silica gel, hexane/ethyl acetate, 100: 0 to 50:50) to yield **47** (5.46 g, 12.3 mmol, 88%) as a yellow oil. ^{1}H NMR (300 MHz, DMSO-d_6) δ 0.95−1.20 (21H, m), 1.61 (3H, d, *J* = 6.7 Hz), 4.85 (2H, s), 6.19 (1H, q, *J* = 6.7 Hz), 6.62 (1H, d, *J* = 8.5 Hz), 7.06 (1H, d, *J* = 2.0 Hz), 7.49 (1H, dd, *J* = 8.7, 4.5 Hz), 7.67 (1H, td, *J* = 8.8, 3.0 Hz), 7.88 (1H, d, *J* = 8.4 Hz), 8.53 (1H, d, *J* = 3.0 Hz), 11.22 (1H, s). MS (ESI/APCI) *m/z* 444.1 $[M + H]^+$.

6-(1-(5-Fluoropyridin-2-yl)ethoxy)-1-(3-methyl-1-(tetrahydro-2*H*-pyran-2-yl)-1*H*-pyrazol-5-yl)-3-(((triisopropylsilyl)oxy)methyl)-1*H*-pyrrolo[2,3-*b*]pyridine (48). The title compound was

prepared in 72% yield as a pale yellow oil from **47** using the procedure analogous to that described for the synthesis of **26a**. ^{1}H NMR (300 MHz, DMSO-d_6) δ 0.78−1.61 (56H, m), 1.70−2.34 (10H, m), 3.12−3.42 (2H, m), 3.69−3.91 (2H, m), 4.75 (1H, dd, J = 10.0, 2.4 Hz), 4.93 (4H, s), 5.00 (1H, d, J = 7.8 Hz), 5.74 (1H, s), 5.87−6.05 (2H, m), 6.12 (1H, s), 6.78 (2H, d, J = 8.5 Hz), 7.20−7.26 (2H, m), 7.32−7.44 (2H, m), 7.56−7.68 (2H, m), 7.96−8.05 (2H, m), 8.49 (2H, d, J = 2.7 Hz). MS (ESI/APCI) *m/z* 608.2 $[M + H]^+$.

6-(1-(5-Fluoropyridin-2-yl)ethoxy)-1-(3-methyl-1-(tetrahydro-2*H*-pyran-2-yl)-1*H*-pyrazol-5-yl)-1*H*-pyrrolo[2,3-*b*]pyridine-3-carbaldehyde (49). The title compound was prepared in 82% yield in 2 steps as an orange amorphous solid from **48** using the procedure analogous to that described for the synthesis of **44**. ^{1}H NMR (300 MHz, DMSO-d_6) δ 1.12−1.62 (12H, m), 1.71−2.34 (12H, m), 3.20 (1H, d, J = 9.3 Hz), 3.26−3.39 (1H, m), 3.63−3.79 (2H, m), 4.76 (1H, d, J = 6.8 Hz), 5.02−5.16 (1H, m), 5.86−6.04 (2H, m), 6.06 (1H, s), 6.31 (1H, s), 6.91−6.99 (2H, m), 7.31−7.41 (2H, m), 7.61 (2H, td, J = 8.8, 3.0 Hz), 8.30 (1H, s), 8.33 (1H, s), 8.36−8.43 (2H, m), 8.46−8.52 (2H, m), 9.89−10.03 (2H, m). MS (ESI/APCI) *m/z* 450.2 $[M + H]^+$.

1-(5-Fluoropyridin-2-yl)ethyl 4-methylbenzenesulfonate (51). To a mixture of **50** (5.69 g, 40.3 mmol) in dry THF (34.1 ml) was added NaH (60% in oil) (1.93 g, 48.3 mmol) at room temperature in a water bath. The mixture was stirred at room temperature for 1 h under nitrogen atmosphere. To the mixture was added a mixture of *p*-toluenesulfonyl chloride (8.45 g, 44.3

mmol) in dry THF (11.4 ml) at room temperature in a water bath. The mixture was stirred at room temperature for 17 h under nitrogen atmosphere. The mixture was diluted with water at room temperature, extracted with EtOAc, dried over Na_2SO_4, filtered, concentrated in vacuo, and purified by column chromatography (silica gel, hexane/ethyl acetate, 100:0 to 50:50) to yield **51** (8.00 g, 27.1 mmol, 67%) as a purple oil. ^{1}H NMR (300 MHz, DMSO-d_6) δ 1.50 (3H, d, J = 6.6 Hz), 2.39 (3H, s), 5.62 (1H, q, J = 6.5 Hz), 7.35−7.46 (3H, m), 7.62−7.77 (3H, m), 8.48 (1H, d, J = 2.9 Hz). MS (ESI/APCI) *m/z* 295.9 $[M + H]^+$.

Optical Resolution of 47. The compound **47** (1.24 g, 2.84 mmol) was separated by preparative HPLC (CHIRALPAK AD, 50mmID × 500mmL, mobile phase: hexane/2-propanol 950/50, 80 mL/min, UV220 nm) to afford **52a** (0.191 g, 29%) as a white solid and **52b** (0.135 g, 22%) as a white solid. **52a**: t_R = 5.94 min (CHIRALPAK AD, 4.6 mmID × 250 mmL, mobile phase: hexane/2-propanol, 1.0 mL/min, UV220 nm); >99.9% ee. **52b**: t_R = 10.0 min (CHIRALPAK AD, 4.6 mmID × 250 mmL, mobile phase: hexane/2-propanol 950/50, 1.0 mL/min, UV220 nm); 99.9% ee. Optical rotation was not determined.

6-((1*S)-1-(5-Fluoropyridin-2-yl)ethoxy)-1-(3-methyl-1-(tetrahydro-2*H*-pyran-2-yl)-1*H*-pyrazol-5-yl)-1*H*-pyrrolo[2,3-*b*]pyridine-3-carbaldehyde (53).** The title compound was prepared in 56% yield in 3 steps as an orange amorphous solid from **52a** using the procedure analogous to that described for the synthesis of **48** and **49**. ^{1}H NMR (300 MHz, DMSO-d_6) δ 1.12−1.62 (12H,

m), 1.71−2.34 (12H, m), 3.20 (1H, d, J = 9.3 Hz), 3.26−3.39 (1H, m), 3.63−3.79 (2H, m), 4.76 (1H, d, J = 6.8 Hz), 5.02−5.16 (1H, m), 5.86−6.04 (2H, m), 6.06 (1H, s), 6.31 (1H, s), 6.91−6.99 (2H, m), 7.31−7.41 (2H, m), 7.61 (2H, td, J = 8.8, 3.0 Hz), 8.30 (1H, s), 8.33 (1H, s), 8.36−8.43 (2H, m), 8.46−8.52 (2H, m), 9.89−10.03 (2H, m). MS (ESI/APCI) *m/z* 450.2 $[M + H]^+$.

Transcellular Transport Study Using Transporter-Expression System. Human MDR1-expressing LLC-PK1 cells were cultured with minor modification as reported previously.[24] The transcellular transport study was performed as reported previously.[25] In brief, the cells were grown for 7 days in HTS Transwell 96-well permeable support (pore size 0.4 μm, 0.143 cm2 surface area) with polyethylene terephthalate membrane (Corning Life Sciences, Lowell, MA, USA) at a density of 1.125 × 105 cells/well. The cells were preincubated with M199 at 37 °C for 30 min. Subsequently, transcellular transport was initiated by the addition of M199 either to apical compartments (75 μL) or to the basolateral compartments (250 μL) containing 10 μM digoxin, 200 μM lucifer yellow as a marker for the tightness of monolayer, and 10 μM test compounds and terminated by the removal of each assay plate after 2 h. The aliquots (25 μL) in the opposite compartments were mixed with MeCN containing alprenolol and diclofenac as an internal standard and then centrifuged. The supernatants were diluted with 10 mM ammonium formate/formic acid (500:1, v/v) and measured in a LC/MS/MS analysis (API4000, AB SCIEX, Foster City, CA, USA). The apparent permeability (Papp) of test

compounds in the receiver wells was determined and the efflux ratio (ER) for MDR1 membrane permeability test was calculated using the following equation: ER = Papp, BtoA/Papp, AtoB where Papp, AtoB is the apical-to-basal passive permeability-surface area product and Papp, BtoA is the basal-to-apical passive permeability-surface area product.

Kinase Panel Protocol, Activity-based kinase profiling was performed by either radioactivity assays using [γ-33P] ATP or Alphascreen assays (PerkinElmer) with anti-phosphotyrosine antibody.[26] The kinase profiling was performed by KINOME*scan*™ Profiling Service of DiscoverX corporation.[27] Compound **13** was screened at 0.3 μM, and assay results are described as % Ctrl.

In Vitro Inhibitory Activity against ALK, FAK, and TrkA kinase.

Protein Preparation. The expression plasmid for FAK kinase domain (residues 411−686, Genebank Accession No. NM_005607) was constructed in a pFastBacHTb vector (Thermo Fisher Scientific, Waltham, MA). The expression plasmid for human ALK kinase domain (residues 1058−1620, Genebank Accession No. NM_004304) was constructed in a pFastBacGST vector (Thermo Fisher Scientific). Recombinant proteins of FAK and ALK were prepared using a baculovirus expression system. GST-tagged TrkA kinase domain (residues 436−790, Genebank Accession No. NM_001012331.1) was purchased from Carna Biosciences (Kobe, Japan).

In vitro kinase assays. For both ALK and FAK enzyme assays, HTRF® detection system was

utilized. The kinase buffer consisted of 50 mM Tris-HCl (pH 7.5), 5 mM $MgCl_2$, 5 mM $MnCl_2$, 2 mM DTT, 0.01% Tween20, and 0.01% BSA. Optimal concentrations of ATP and biotin-poly-GT for ALK enzyme assay were 1 μM and 2.5 μg/mL, respectively. For FAK enzyme assay, optimal concentrations of ATP and biotin-poly-GT were 0.5 μM and 5 μg/mL, respectively. After 10 min pre-incubation of the enzyme, poly-(GT)-biotin, and test compounds, the kinase reaction was started by adding ATP and incubated for 60 min. The reaction was terminated by adding detection mixture contained crypate labeled PT66 (Cisbio, Codolet, France) and streptavidin-Xlent! (Cisbio) dissolved in detection buffer (Cisbio). After incubation at room temperature for 60 min, the plates were read with an EnVision 2102 Multilabel Reader (PerkinElmer, Waltham, MA). Assays for TrkA enzyme was performed using the AlphaScreen® assay system (PerkinElmer). The kinase buffer consisted of 50 mM Tris-HCl (pH 7.5), 5 mM $MgCl_2$, 5 mM $MnCl_2$, 2 mM DTT, and 0.01% Tween20. After pre-incubation of the enzyme, poly-(GT)-biotin, and compounds for 5 min at room temperature, the kinase reaction was initiated by the addition of final 1 μM ATP. After 60 min incubation, the reaction was terminated by adding AlphaScreen® Phosphotyrosine (P-Tyr-100) acceptor & Streptavidin donor beads (PerkinElmer) in 62.5 mM HEPES (pH 7.5) with 250 mM NaCl, 0.1% BSA, and 100 mM EDTA. The assay plates were incubated at room temperature in the dark for more than 12 h and then read with an EnVision 2102 Multilabel Reader. Percentage inhibition was calculated from the signal intensity of either HTRF® or

AlphaScreen® assay by using the following formula; % inhibition = 100 - (A - X) x 100 / (A - B)

A: total reaction, B: without enzyme, X: Test compound.

IC_{50} values and 95% confidence intervals (CI) were estimated using a four-parameter logistic curve using XLfit software (IDBS, London, UK).

Cell-based ALK autophosphorylation assay. The full-length of cDNA encoding human ALK (NM_004304) construct was amplified by PCR and cloned into the pcDNA3.3 vector (Thermo Fisher Scientific). Human embryonic kidney 293 (HEK293) cell line was cultured with Dulbecco's modified Eagle's medium ((Thermo Fisher Scientific)) containing 10% FBS, 100 U/ml penicillin-G and 100 μg/ml streptomycin sulfate ((Thermo Fisher Scientific)). For evaluation of compound inhibitory activity in cells, the suspended HEK293 cells were transfected with expression plasmids encoding ALK full length construct using the Fugene HD reagent (Roche Diagnostics, Basel, Switzerland) according to the manufacturer's instructions. The cell suspension was seeded into 96-well culture plates at 3.0 x 10^4 cells/well using DMEM supplemented with 10% fetal bovine serum (FBS), and incubated two overnights in a 5% CO_2 atmosphere at 37°C. After two overnights incubation, cells were treated with various concentrations of test compounds for 60 min in 10% FBS containing DMEM. The cells then were lysed by adding cell lysis buffer (Cell Signaling Technology, Danvers, MA). Quantification of phopho-ALK (Tyr1604) was performed by using Phospho-ALK (Tyr1604) Sandwich ELISA Kit

(Cell Signaling Technology) according to manufacture instruction. Percentage inhibition was calculated from the signal intensity of by using the following formula; % inhibition = 100 - (A - X) x 100 / (A - B)

A: compound non-treatment, B: positive control (10 μM NVP-TAE684) treatment, X: Test compound.

IC_{50} values and 95% confidence intervals (CI) were estimated in the same way as in vitro kinase assays.

Determination of an unbound fraction in plasma (fu,p). Plasma used in the study was derived from male ICR mice. The plasma protein binding of each compound was determined by the equilibrium dialysis method with HTDialysisTM Teflon dialysis chambers and cellulose membranes (MWCO 6-8 kDa). Plasma was mixed with the compound solution for a final concentration of 1 μmol/L. Dialysis was conducted against phosphate buffered saline (PBS) in 8% CO_2 at 37 ℃ for 20 h. The concentrations of compounds in both plasma and PBS sides were determined by liquid chromatography/tandem mass spectrometry (LC-MS/MS). The unbound fraction in plasma (fu,p) was calculated as the ratio of the peak area of compounds from PBS side to those from plasma side of the dialysis apparatus. Brain used in the study was derived from male ICR mice.

Determination of an unbound fraction in brain (fu,b). The brain tissue binding of each

compound was determined by the equilibrium dialysis method with HTDialysisTM Teflon dialysis chambers and cellulose membranes (MWCO 6-8 kDa). Brain homogenate was mixed with the compound solution for a final concentration of 1 μmol/L. Dialysis was conducted against phosphate buffered saline (PBS) at 37 °C for 16-20 h. The concentrations of compounds in both brain and PBS sides were determined by liquid chromatography/tandem mass spectrometry (LC-MS/MS). The unbound fraction in brain tissue (fu,b) was calculated as the ratio of the peak area of compounds from PBS side to those from brain tissue side of the dialysis apparatus.

Animal Experiments. The care and use of the animals and the experimental protocols were approved by the Experimental Animal Care and Use Committee of Takeda Pharmaceutical Company Limited. Animals were kept under standard laboratory conditions (12:12 h light/dark cycle) with food and water available *ad libitum*.

Brain and Plasma Concentration in Mice. Compound **13** was intraperitoneally administered to Jcl ICR mice (male, non-fasted, 6-week old) at 100mg/kg. Blood and brain samples were collected at 0.5 h, 1 h, and 2 h after intraperitoneal administration. The blood samples were centrifuged to obtain the plasma fraction. The brain samples were homogenized in saline to obtain the brain homogenate. The plasma and brain homogenate samples were deproteinized with acetonitrile containing an internal standard. After centrifugation, the supernatants were diluted with the mobile phase (10 mM ammonium formate/MeCN/formic acid = 70/30/0.2 (v/v)) and

centrifuged again. The compound concentrations in the supernatant were measured by LC/MS/MS with an API5000 triple quadrupole mass spectrometer (AB Sciex).

Measurement of Phosphorylated ALK Levels in the Mouse Brain.

Sampling of rodent brain tissues. Compound **13** was suspended in 0.5% (w/v) methylcellulose in saline. 6-week-old male mice (ICR, CLEA Japan, Tokyo, Japan) were humanly sacrificed 1 hour after the intraperitoneal administration of compound **13**. Their tissues were dissected, frozen on dry ice and stored at -80 °C until use. For western blot analyses, tissues were homogenized in the lysis buffer (50 mM Tris–HCl, 5 mM Na_2EDTA, 1 mM EGTA, 100 mM NaCl, 1% NP-40, and 2.5% sodium deoxycholate, pH 7.5) supplemented with protease inhibitors (1.37 mg/l pepstatin A, 25 KIU/ml aprotinin, 1 nM microcystin LR, 1 nM MG115, 40 nM leupeptin and 100 nM 4-(2-aminoethyl)benzenesulfonyl fluoride HCl) and phosphatase inhibitors (30 mM NaF, sodium diphosphate, 2 nM sodium orthovanadate). The homogenates were centrifuged at 15,000 g for 20 min and the supernatants were collected. Protein concentration in the supernatants was determined with BCA Protein Assay Kit (Thermo Fisher Scientific). The diluted supernatants were incubated at 98 °C for 5 min after addition of SDS-PAGE sample buffer.

Western blot analysis. Each sample was subjected to electrophoresis with 5% polyacrylamide gradient gels (DRC CO., Ltd., Tokyo, Japan), followed by transferring to PVDF membranes (Bio-Rad Laboratories Inc., Hercules, CA). After blocking with PVDF Blocking Reagent for Can

Get Signal (TOYOBO Co., Ltd., Osaka, Japan) for 1 h, the membranes were probed with one of the following primary antibodies: anti-ALK antibody (ALT1-3A2), anti-phospho-ALK antibody (#Ab73996, Abcam, Cambridge, UK). The membranes were then labeled with horseradish peroxidase-conjugated anti-mouse IgG antibodies (Kirkegaard & Perry Laboratories, Inc., Gaithersburg, MD) or anti-rabbit IgG HRP-linked Antibody (Cell Signaling Technology). This was followed by visualization using the ECL Prime Western Blotting Detection Reagent (GE Healthcare, Chicago, IL) and LAS4000 imaging system (GE Healthcare). The density of each band was measured by ImageQuant TL software (GE Healthcare). The statistical significance was determined with a one –tailed Williams' test using Takeda's SAS-PCP software.

Generation of ALK specific monoclonal antibody. ALK-specific mouse monoclonal antibody (ALT1-3A2) was generated by immunizing ALK-knock out mice with recombinant human ALK kinase domain. ALK-knock out mouse was purchased from Taconic Biosciences, Inc. (New York, NY). The lymph node cells from immunized mice were fused with P3X63Ag8U.1 mouse myeloma cells to obtain hybridoma, and the culture supernatants were screened by ELISA using GST-fused mouse ALK (accession number: NM_007439, residues 1062−1621)-coated plates followed by western blotting. The purified antibody showing antigen-specific single band in western blotting was selected for further study.

Molecular biology, protein purification and crystallization of human ALK .

A clone corresponding to the kinase catalytic domain region of human ALK kinase residues 1090 to 1406 and put into pFastBacHTb vector (Thermo Fisher Inc.). It contained an N-terminal 6X Histidine tag with a cleavable TEV protease site and polyhedron replication origin site. It was subcultured in Bacculovirus insect cell strain SF9 (Spodoptera frugiperda, Thermo Fisher Inc.) for large scale expression and purification. Cells were lysed by sonication followed by centrifucation at 14,000 rpm for 1 h. The supernatant was loaded on a Nickel charged NTA column and purified by linear gradient of increasing Nickel sulfate (20mM - 200mM). The eluate was checked for purity and treated with TEV protease. The final step was size exclusion chromatography on a superdex 75 column. After confirmation of the purity of the fractions and their monodispersity, protein was concentrated to 25 mg/ml in buffer containing 20 mM Tris pH 8.0, 150 mM NaCl, 0.5 mM EDTA, 1 mM Benzamidine and 0.25 mM TCEP and used for structural studies. Initial screening in Hampton PEG Ion screen yielded several hits both with apo protein as well as in the presence of 1 mM concentration of compounds. Best diffracting crystals appeared when optimized under the following condition 19 - 25% PEG 3350, 2.0% Tacsimate pH 7.0 and a 7:3 or 8:2 ratio of Tris Chloride: Tris sodium (100mM final concentration). Crystals were harvested after cryo protection with either 15% Ethylene glycol or 15% glycerol for 15 min.

Crystal structure determination.

Data was collected at beamline 5.0.3 of the Advanced Light Source at Berkeley, USA and

beamline X6A of the National Synchrotron Light Source at Brookhaven, USA. Structure was solved by molecular replacement using MOLREP[28] a part of the CCP4 package.[29] The structure of ALK kinase (PDBId 3L9P) was used as the starting model. This was followed by iterative rounds of manual model building in Coot[30] and restrained refinement using Refmac5[31] and Phenix.Refine[32]. The ligand atoms and water molecules were fit manually after interpreting the difference map and accounting for the protein atoms.

SUPPORTING INFORMATION

Enzymatic kinase selectivity profile

Determination of eutomer and distomer

Data collections and refinement statistics of crystallography

Synthesis of chiral 3-methoxymethyl derivatives

Molecular-formula strings (CSV)

HPLC analysis data of a key target compound (**13**)

PDB ID CODES

The PDB entry codes for the crystal structures reported in this work are as follows:

1, 6EDL; **7**, 6E0R; **9**, 6EBW

Authors will release the atomic coordinates and experimental data upon article publication.

AUTHOR INFORMATION

Corresponding Author

*E-mail: ikuo.fujimori@takeda.com

Notes

The authors declare no competing financial interest.

ACKNOWLEDGEMENTS

We are grateful to Mika Inoue, Tomohiro Ookawa, and Yuta Tanaka for the synthetic supports, and Isamu Tsuji for producing ALK specific antibodies. We thank the staff of the Berkeley Center for Structural Biology, which operates Advanced Light Source beamline 5.0.3. The Berkeley Center for Structural Biology is supported in part by the National Institutes of Health and National Institute of General Medical Sciences. The Advanced Light Source is supported by the Director, Office of Science, Office of Basic Energy Sciences of the US Department of Energy under contract number DE-AC02-05CH11231. This research used beamline X6A of the National Synchrotron Light Source, a U.S. Department of Energy (DOE) Office of Science User Facility operated for the DOE Office of Science by Brookhaven National Laboratory under Contract No. DE-AC02-98CH10886.

ABBREVIATIONS USED

Ac, acetyl; AmPhos, bis(di-*t*-butyl(4-dimethylaminophenyl)phosphine); ALK, anaplastic lymphoma kinase; BDNF, brain-derived neurotrophic factor; BINAP, (2,2'-

bis(diphenylphosphino)-1,1'-binaphthyl); BOC, *t*-butoxycarbonyl; BSA, bovine serum albumin; CNS, central nervous system; dba, tris(dibenzylidene)acetone; DIPEA, *N*,*N*-diisopropylethylamine; DME, 1,2-dimethoxyethane; DMF, *N*,*N*-dimethylformamide; DMSO, dimethyl sulfoxide; dppf, [1,1'-bis(diphenylphosphino)ferrocene]; EDC, 1-ethyl-3-(3-dimethylaminopropyl)carbodiimide; EML-4, echinoderm microtubule-associated protein-like 4; FAK, focal adhesion kinase; HBA, hydrogen bond acceptor; HBD, hydrogen bond donor; HOBt, 1-hydroxybenzotriazole; HPLC, high performance liquid chromatography; IR, insulin receptor; KO, knock-out; LLE , ligand lipophilicity efficiency; MDR1, multidrug resistance protein 1; *m*-CBA, *meta*-chlorobenzoic acid; *m*-CPBA, *meta*-chloroperbenzoic acid; NGF, nerve growth factor; NIS, *N*-iodosuccinimide; NSCLC, non-small cell lung cancer; p-ALK, phosphorylated-ALK; PDB, protein data bank; PFC, prefrontal cortex; P-gp, P-glycoprotein; RTK, receptor tyrosine kinases; SAR, structure–activity relationship; SBDD, structure-based drug design; TBAF, tetrabutyammonium fluoride; TEA, triethylamine; TFA, trifluoroacetic acid; THF, tetrahydrofuran; THP, tetrahydropyranyl; TIPSCl, triisopropylsilyl chlrodie; Ts, tosyl;

REFERENCES

(1) Dengjel, J.; Kratchmarova, I.; Blagoev, B., Receptor tyrosine kinase signaling: a view from Quantitative Proteomics. *Mol Biosyst* **2009**, *5* (10), 1112–1121.

(2) Pawson, T., Regulation and targets of receptor tyrosine kinases. *Eur J Cancer* **2002**, *38 Suppl 5*, S3–10.

(3) Wiedlocha, A.; Falnes, P. O.; Rapak, A.; Munoz, R.; Klingenberg, O.; Olsnes, S., Stimulation of proliferation of a human osteosarcoma cell line by exogenous acidic fibroblast growth factor requires both activation of receptor tyrosine kinase and growth factor internalization. *Mol Cell Biol* **1996**, *16* (1), 270–280.

(4) Bilsland, J. G.; Wheeldon, A.; Mead, A.; Znamenskiy, P.; Almond, S.; Waters, K. A.; Thakur, M.; Beaumont, V.; Bonnert, T. P.; Heavens, R.; Whiting, P.; McAllister, G.; Munoz-Sanjuan, I., Behavioral and neurochemical alterations in mice deficient in anaplastic lymphoma kinase suggest therapeutic potential for psychiatric indications. *Neuropsychopharmacology* **2008**, *33* (3), 685–700.

(5) Iwahara, T.; Fujimoto, J.; Wen, D.; Cupples, R.; Bucay, N.; Arakawa, T.; Mori, S.; Ratzkin, B.; Yamamoto, T., Molecular characterization of ALK, a receptor tyrosine kinase expressed specifically in the nervous system. *Oncogene* **1997**, *14* (4), 439–449.

(6) Weiss, J. B.; Xue, C.; Benice, T.; Xue, L.; Morris, S. W.; Raber, J., Anaplastic lymphoma kinase and leukocyte tyrosine kinase: functions and genetic interactions in learning, memory and adult neurogenesis. *Pharmacol Biochem Behav* **2012**, *100* (3), 566–574.

(7) Morris, S. W.; Kirstein, M. N.; Valentine, M. B.; Dittmer, K. G.; Shapiro, D. N.; Saltman, D.

L.; Look, A. T., Fusion of a kinase gene, ALK, to a nucleolar protein gene, NPM, in non-Hodgkin's lymphoma. *Science* **1994**, *263* (5151), 1281–1284.

(8) Soda, M.; Choi, Y. L.; Enomoto, M.; Takada, S.; Yamashita, Y.; Ishikawa, S.; Fujiwara, S.; Watanabe, H.; Kurashina, K.; Hatanaka, H.; Bando, M.; Ohno, S.; Ishikawa, Y.; Aburatani, H.; Niki, T.; Sohara, Y.; Sugiyama, Y.; Mano, H., Identification of the transforming EML4-ALK fusion gene in non-small-cell lung cancer. *Nature* **2007**, *448* (7153), 561–566.

(9) Slupianek, A.; Skorski, T., NPM/ALK downregulates p27Kip1 in a PI-3K-dependent manner. *Exp Hematol* **2004**, *32* (12), 1265–1271.

(10) Armstrong, F.; Duplantier, M. M.; Trempat, P.; Hieblot, C.; Lamant, L.; Espinos, E.; Racaud-Sultan, C.; Allouche, M.; Campo, E.; Delsol, G.; Touriol, C., Differential effects of X-ALK fusion proteins on proliferation, transformation, and invasion properties of NIH3T3 cells. *Oncogene* **2004**, *23* (36), 6071–6082.

(11) Christensen, J. G.; Zou, H. Y.; Arango, M. E.; Li, Q.; Lee, J. H.; McDonnell, S. R.; Yamazaki, S.; Alton, G. R.; Mroczkowski, B.; Los, G., Cytoreductive antitumor activity of PF-2341066, a novel inhibitor of anaplastic lymphoma kinase and c-Met, in experimental models of anaplastic large-cell lymphoma. *Mol Cancer Ther* **2007**, *6* (12 Pt 1), 3314–3322.

(12) Zou, H. Y.; Li, Q.; Lee, J. H.; Arango, M. E.; McDonnell, S. R.; Yamazaki, S.; Koudriakova, T. B.; Alton, G.; Cui, J. J.; Kung, P. P.; Nambu, M. D.; Los, G.; Bender, S. L.; Mroczkowski, B.;

Christensen, J. G., An orally available small-molecule inhibitor of c-Met, PF-2341066, exhibits cytoreductive antitumor efficacy through antiproliferative and antiangiogenic mechanisms. *Cancer Res* **2007**, *67* (9), 4408–4017.

(13) Cui, J. J.; Tran-Dube, M.; Shen, H.; Nambu, M.; Kung, P. P.; Pairish, M.; Jia, L.; Meng, J.; Funk, L.; Botrous, I.; McTigue, M.; Grodsky, N.; Ryan, K.; Padrique, E.; Alton, G.; Timofeevski, S.; Yamazaki, S.; Li, Q.; Zou, H.; Christensen, J.; Mroczkowski, B.; Bender, S.; Kania, R. S.; Edwards, M. P., Structure based drug design of crizotinib (PF-02341066), a potent and selective dual inhibitor of mesenchymal-epithelial transition factor (c-MET) kinase and anaplastic lymphoma kinase (ALK). *J Med Chem* **2011**, *54* (18), 6342–6363.

(14) Marsilje, T. H.; Pei, W.; Chen, B.; Lu, W.; Uno, T.; Jin, Y.; Jiang, T.; Kim, S.; Li, N.; Warmuth, M.; Sarkisova, Y.; Sun, F.; Steffy, A.; Pferdekamper, A. C.; Li, A. G.; Joseph, S. B.; Kim, Y.; Liu, B.; Tuntland, T.; Cui, X.; Gray, N. S.; Steensma, R.; Wan, Y.; Jiang, J.; Chopiuk, G.; Li, J.; Gordon, W. P.; Richmond, W.; Johnson, K.; Chang, J.; Groessl, T.; He, Y. Q.; Phimister, A.; Aycinena, A.; Lee, C. C.; Bursulaya, B.; Karanewsky, D. S.; Seidel, H. M.; Harris, J. L.; Michellys, P. Y., Synthesis, structure-activity relationships, and in vivo efficacy of the novel potent and selective anaplastic lymphoma kinase (ALK) inhibitor 5-chloro-N2-(2-isopropoxy-5-methyl-4-(piperidin-4-yl)phenyl)-N4-(2-(isopropylsulf onyl)phenyl)pyrimidine-2,4-diamine (LDK378) currently in phase 1 and phase 2 clinical trials. *J*

Med Chem **2013**, *56* (14), 5675–5690.

(15) Huang, W. S.; Liu, S.; Zou, D.; Thomas, M.; Wang, Y.; Zhou, T.; Romero, J.; Kohlmann, A.; Li, F.; Qi, J.; Cai, L.; Dwight, T. A.; Xu, Y.; Xu, R.; Dodd, R.; Toms, A.; Parillon, L.; Lu, X.; Anjum, R.; Zhang, S.; Wang, F.; Keats, J.; Wardwell, S. D.; Ning, Y.; Xu, Q.; Moran, L. E.; Mohemmad, Q. K.; Jang, H. G.; Clackson, T.; Narasimhan, N. I.; Rivera, V. M.; Zhu, X.; Dalgarno, D.; Shakespeare, W. C., Discovery of Brigatinib (AP26113), a phosphine oxide-containing, potent, orally active inhibitor of anaplastic lymphoma kinase. *J Med Chem* **2016**, *59* (10), 4948–4964.

(16) Kinoshita, K.; Asoh, K.; Furuichi, N.; Ito, T.; Kawada, H.; Hara, S.; Ohwada, J.; Miyagi, T.; Kobayashi, T.; Takanashi, K.; Tsukaguchi, T.; Sakamoto, H.; Tsukuda, T.; Oikawa, N., Design and synthesis of a highly selective, orally active and potent anaplastic lymphoma kinase inhibitor (CH5424802). *Bioorg Med Chem* **2012**, *20* (3), 1271–1280.

(17) Johnson, T. W.; Richardson, P. F.; Bailey, S.; Brooun, A.; Burke, B. J.; Collins, M. R.; Cui, J. J.; Deal, J. G.; Deng, Y. L.; Dinh, D.; Engstrom, L. D.; He, M.; Hoffman, J.; Hoffman, R. L.; Huang, Q.; Kania, R. S.; Kath, J. C.; Lam, H.; Lam, J. L.; Le, P. T.; Lingardo, L.; Liu, W.; McTigue, M.; Palmer, C. L.; Sach, N. W.; Smeal, T.; Smith, G. L.; Stewart, A. E.; Timofeevski, S.; Zhu, H.; Zhu, J.; Zou, H. Y.; Edwards, M. P., Discovery of (10R)-7-amino-12-fluoro-2,10,16-trimethyl-15-oxo-10,15,16,17-tetrahydro-2H-8,4-(m

etheno)pyrazolo[4,3-h][2,5,11]-benzoxadiazacyclotetradecine-3-carbonitrile (PF-06463922), a macrocyclic inhibitor of anaplastic lymphoma kinase (ALK) and c-ros oncogene 1 (ROS1) with preclinical brain exposure and broad-spectrum potency against ALK-resistant mutations. *J Med Chem* **2014**, *57* (11), 4720–4744.

(18) Bartkowska, K.; Paquin, A.; Gauthier, A. S.; Kaplan, D. R.; Miller, F. D., Trk signaling regulates neural precursor cell proliferation and differentiation during cortical development. *Development* **2007**, *134* (24), 4369–4380.

(19) Norman, R. A.; Toader, D.; Ferguson, A. D., Structural approaches to obtain kinase selectivity. *Trends Pharmacol Sci* **2012**, *33* (5), 273–278.

(20) Mohraz, M.; Jian‐qi, W.; Heilbronner, E.; Solladiéa‐Cavallo, A.; Matloubi‐Moghadam, F.; Some comments on the conformations of methyl phenyl sulfides, sulfoxides and sulfones. *Helvetica Chimica Acta*, **1981**, *64*, 97–112.

(21) Edwards, M. P.; Price, D. A., Role of physicochemical properties and ligand lipophilicity efficiency in addressing drug safety risks. *Annu. Rep. Med. Chem.* **2010**, *45*, 381.

(22) Schinkel, A. H.; Wagenaar, E.; Mol, C. A.; van Deemter, L., P-glycoprotein in the blood-brain barrier of mice influences the brain penetration and pharmacological activity of many drugs. *J Clin Invest* **1996**, *97* (11), 2517–2524.

(23) Desai, P. V.; Raub, T. J.; Blanco, M. J., How hydrogen bonds impact P-glycoprotein

transport and permeability. *Bioorg Med Chem Lett* **2012,** *22* (21), 6540–6548.

(24) Sugimoto, H.; Hirabayashi, H.; Kimura, Y.; Furuta, A.; Amano, N.; Moriwaki, T. Quantitative investigation of the impact of P-glycoprotein inhibition on drug transport across blood-brain barrier in rats. *Drug Metab. Dispos.* **2011**, *39*, 8–14.

(25) Takeuchi, T.; Yoshitomi, S.; Higuchi, T.; Ikemoto, K.; Niwa, S.; Ebihara, T.; Katoh, M.; Yokoi, T.; Asahi, S., Establishment and characterization of the transformants stably-expressing MDR1 derived from various animal species in LLC-PK1. *Pharm. Res.* **2006**, *23*, 1460–1472.

(26) Kawakita, Y.; Banno, H.; Ohashi, T.; Tamura, T.; Yusa, T.; Nakayama, A.; Miki, H.; Iwata, H.; Kamiguchi, H.; Tanaka, T.; Habuka, N.; Sogabe, S.; Ohta, Y.; Ishikawa, T., Design and synthesis of pyrrolo[3,2-*d*]pyrimidine human epidermal growth factor receptor 2 (HER2)/epidermal growth factor receptor (EGFR) dual inhibitors: exploration of novel back-pocket binders. *J Med Chem* **2012**, *55* (8), 3975–3991.

(27) Fabian, M. A.; Biggs, W. H. 3rd; Treiber, D. K.; Atteridge, C. E.; Azimioara, M. D.; Benedetti, M. G.; Carter, T. A.; Ciceri, P.; Edeen, P. T.; Floyd, M.; Ford, J. M.; Galvin, M.; Gerlach, J. L.; Grotzfeld, R. M.; Herrgard, S.; Insko, D. E.; Insko, M. A.; Lai, A. G.; Lélias, J. M.; Mehta, S. A.; Milanov, Z. V.; Velasco, A. M.; Wodicka, L. M.; Patel, H. K.; Zarrinkar, P. P.; Lockhart, D. J., A small molecule-kinase interaction map for clinical kinase inhibitors. *Nat. Biotechnol.* **2005**, 23, 329–336.

(28) Vagin, A.; Teplyakov, A., Molecular replacement with MOLREP. *Acta Crystallogr D Biol Crystallogr* **2010**, *66* (Pt 1), 22-25.

(29) Winn, M. D.; Ballard, C. C.; Cowtan, K. D.; Dodson, E. J.; Emsley, P.; Evans, P. R.; Keegan, R. M.; Krissinel, E. B.; Leslie, A. G. W.; McCoy, A.; McNicholas, S. J.; Murshudov, G. N.; Pannu, N. S.; Potterton, E. A.; Powell, H. R.; Read, R. J.; Vagin, A.; Wilson, K. S., Overview of the CCP4 suite and current developments. *Acta Crystallogr D Biol Crystallogr* **2011,** *67* (Pt 4), 235-242.

(30) Emsley, P.; Lohkamp, B.; Scott, W. G,; Cowtan, K., Features and development of Coot. *Acta Crystallogr D Biol Crystallogr* **2010**, *66* (Pt 4), 486-501.

(31) Murshudov, G. N.; Vagin, A. A.; Dodson, E. J., Refinement of macromolecular structures by the maximum-likelihood method. *Acta Crystallogr D Biol Crystallogr* **1997**, *53* (Pt 3), 240-255.

(32) Afonine P. V.; Grosse-Kunstleve, R. W.; Echols, N.; Headd, J. J.; Moriarty, N. W.; Mustyakimov, M.; Terwilliger, T. C.; Urzhumtsev, A.; Zwart, P. H.; Adams, P. D., Towards automated crystallographic structure refinement with phenix.refine. *Acta Crystallogr D Biol Crystallogr* **2012,** *68* (Pt 4), 352-367.

Table of Contents Graphic

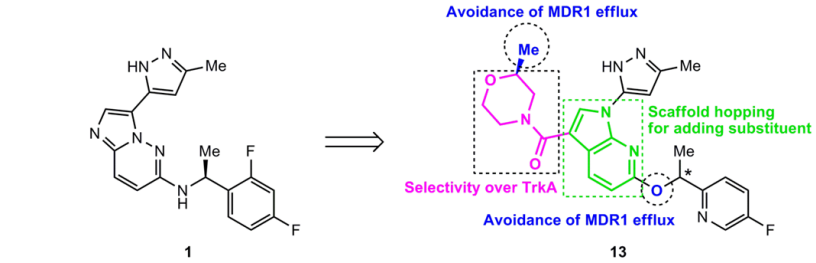

1

ALK (enzyme) IC_{50}	2.0 nM
ALK (cell) IC_{50}	6.0 nM
TrkA (enzyme) IC_{50}	0.10 nM

13

ALK (enzyme) IC_{50}	2.9 nM
ALK (cell) IC_{50}	27 nM
TrkA (enzyme) IC_{50}	2600 nM
MDR1 efflux ratio	1.0
Kp	1.3

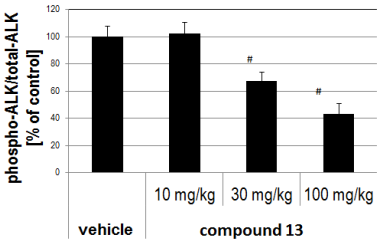

Compound 13 inhibited ALK phosphorylation in mouse brain hippocampus.

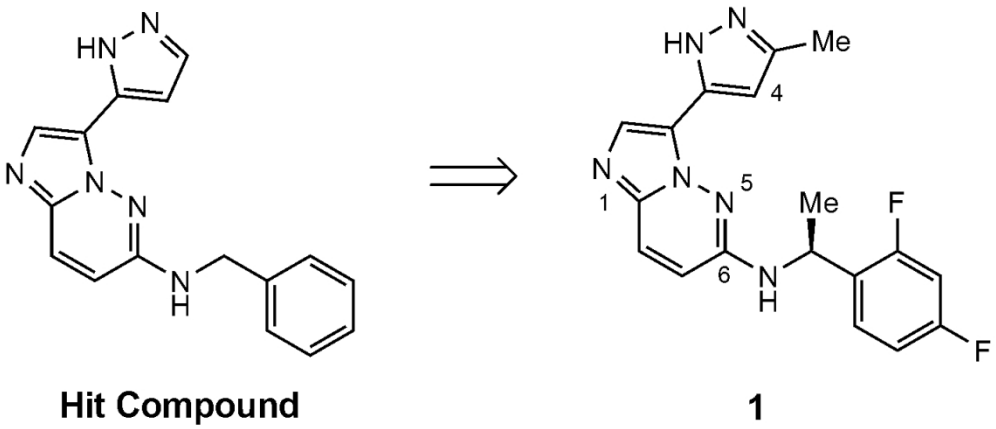

Table 1. *In vitro* Profiles of Compound **1** Derived from Hit Compound

120x52mm (300 x 300 DPI)

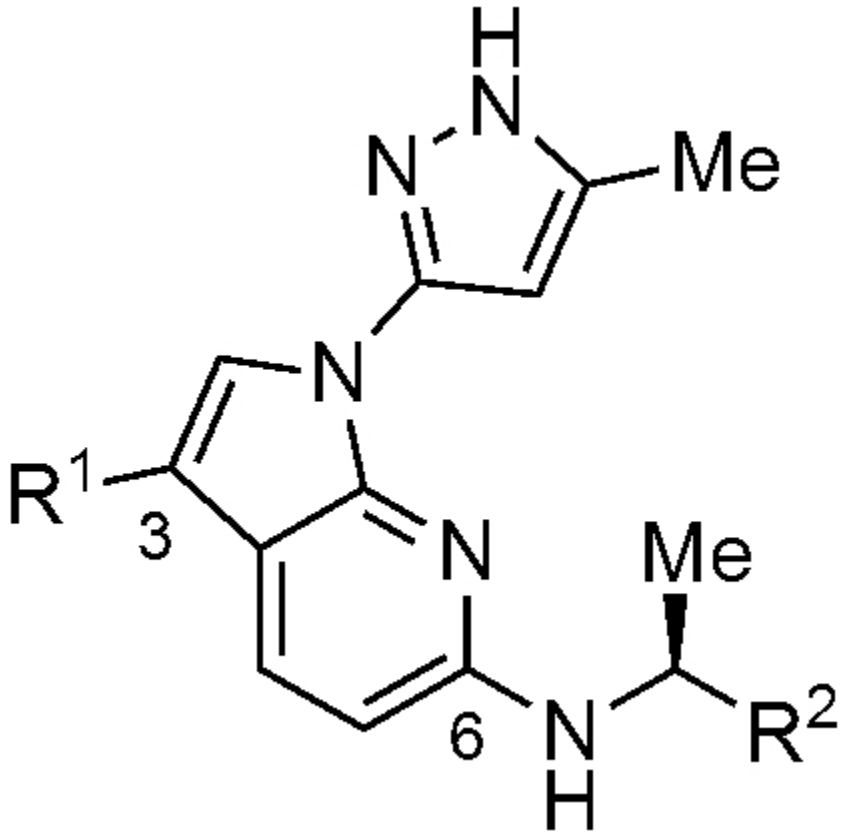

Table 2. *In vitro* Profiles of Sulfone and Amide Derivatives at 3-Position of 1*H*-pyrrolo[2,3-*b*]pyridine.

36x36mm (300 x 300 DPI)

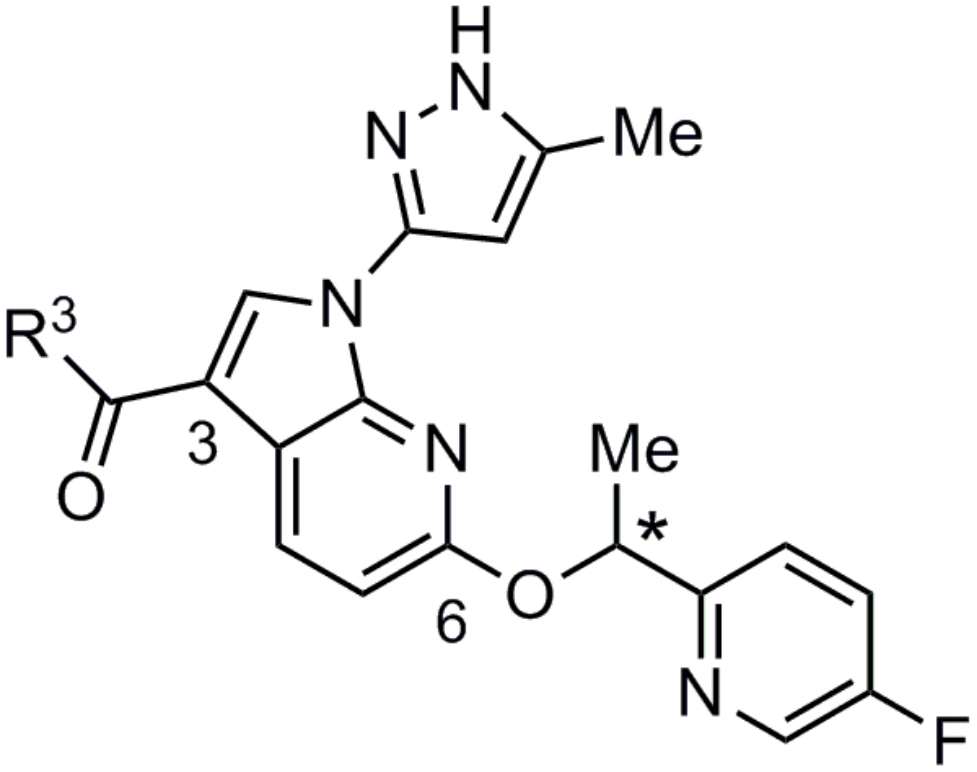

Table 3. In vitro Profiles of Benzyl ether Derivatives at 6-Position of 1*H*-pyrrolo[2,3-*b*]pyridine.

51x41mm (300 x 300 DPI)

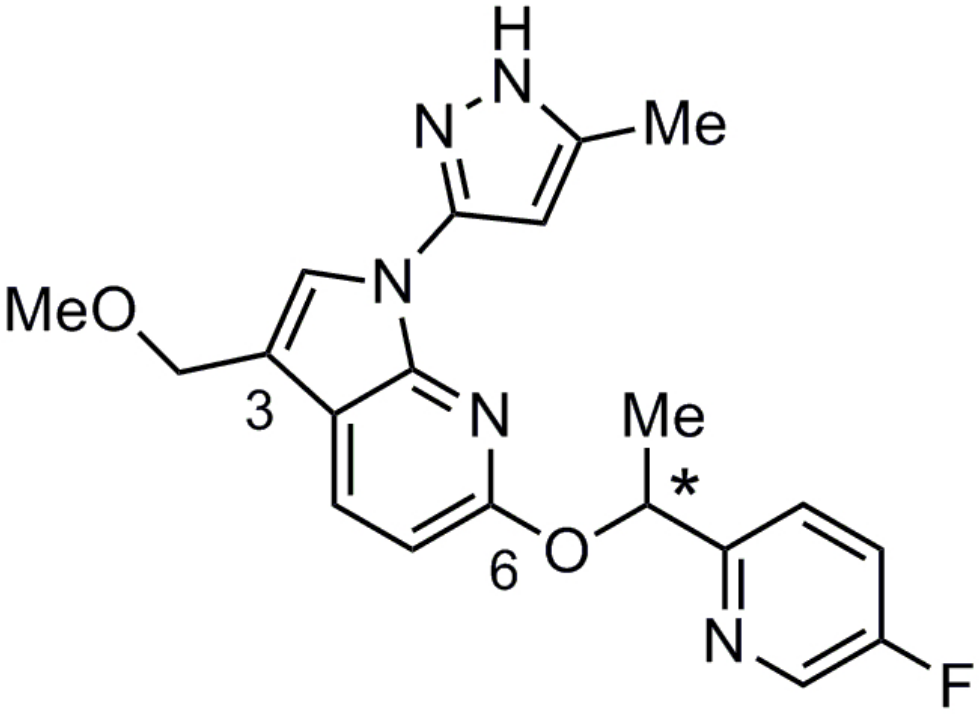

Table 4. Determination of Eutomer and Distomer by Methoxyether Derivatives.

56x40mm (300 x 300 DPI)

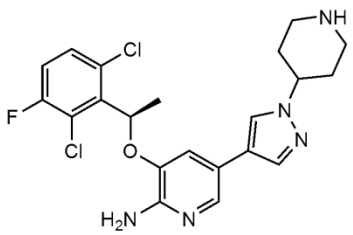

Crizotinib

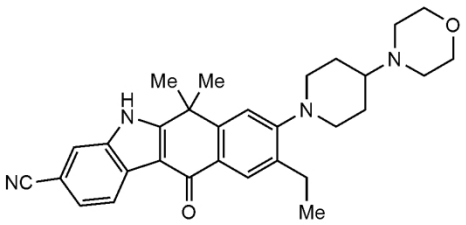

Alectinib

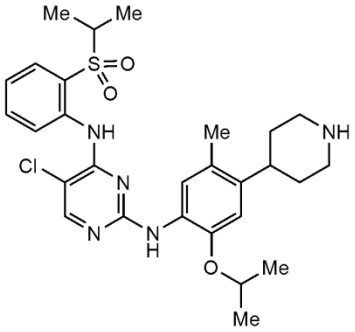

Ceritinib

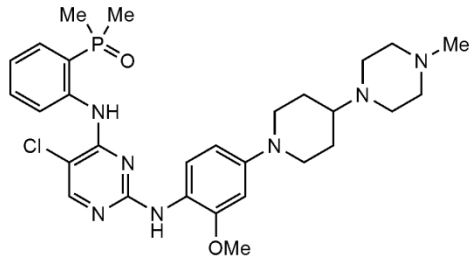

Brigatinib

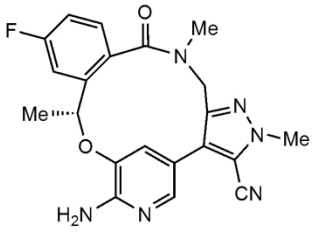

Lorlatinib

Figure 1. Structures of some reported ALK inhibitors.

176x187mm (300 x 300 DPI)

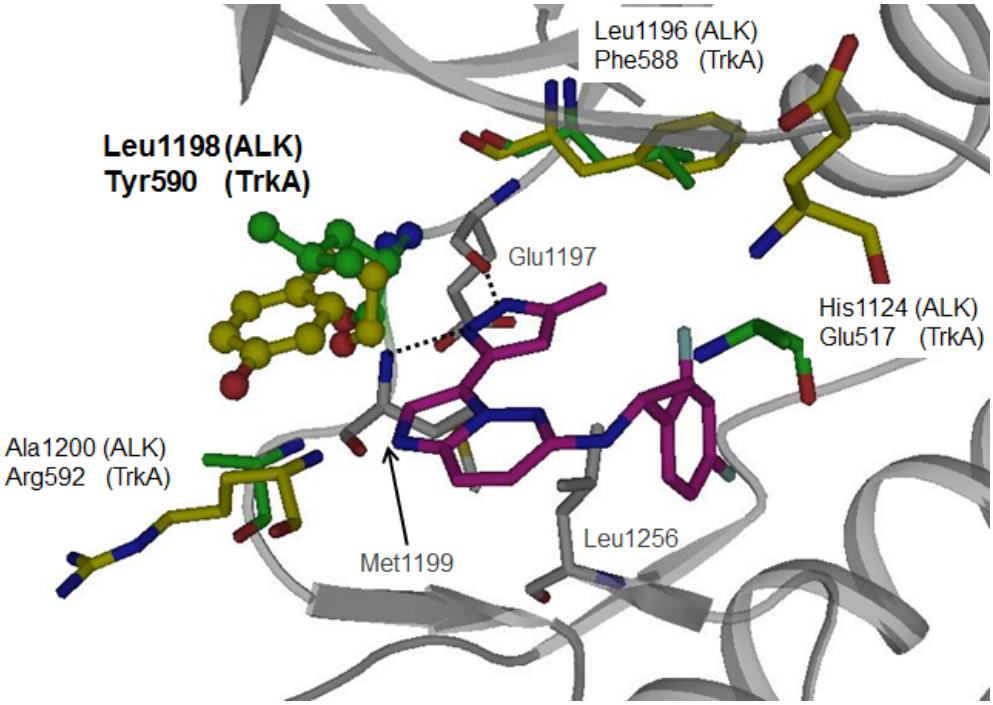

Figure 2. Cocrystal structure of compound **1** bound to human ALK protein (PDB code 6EDL). Different residues in ALK (green) and TrkA (yellow, PDB code 4F0I) around compound **1** (magenta). The imidazole portion of His1124 is not shown due to poor electron density for the sidechain.

171x119mm (96 x 96 DPI)

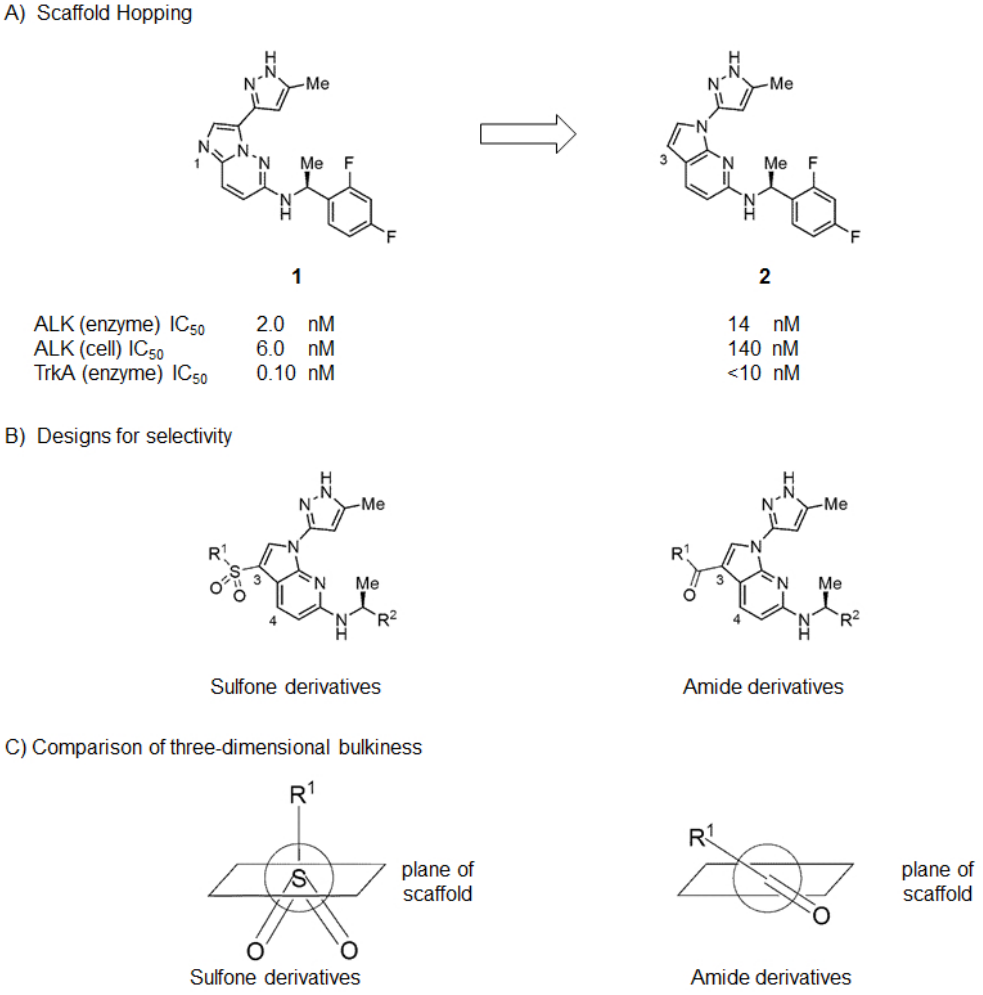

Figure 3. (A) Results of scaffold hopping. (B) Design to improve selectivity over Trks. (C) Comparison of three-dimensional bulkiness between sulfonyl and carbonyl moieties.

205x207mm (96 x 96 DPI)

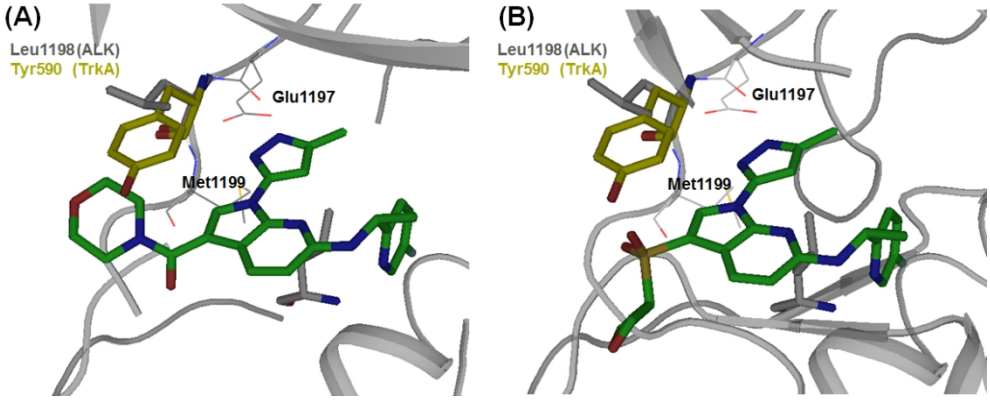

Figure 4. X-ray crystal structures of the amide compound **9** (**A**) and the sulfone compound **7** (**B**) bound in the ALK ATP binding site (gray, PDB 6EBW and 6E0R, respectively). The relative position of Tyr590, based on the PDB 4F0I crystal structure, is shown in yellow.

312x126mm (96 x 96 DPI)

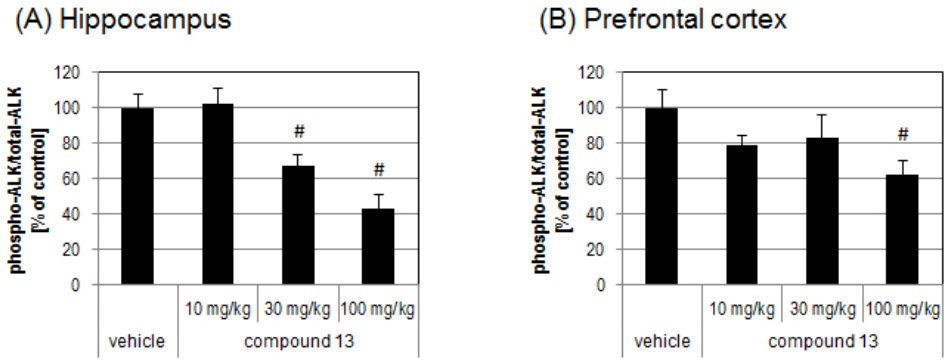

Figure 5. Decrease of phosphorylated ALK levels in mouse's (A) hippocampus and (B) prefrontal cortex after 1 h of the intraperitoneal administration of compound **13** at 10, 30, and 100 mg/mL/kg to the ICR mice. Data are presented as the mean + SEM (n = 3); p-values < 0.025 vs. vehicle by one-tailed Williams' test.

178x68mm (96 x 96 DPI)

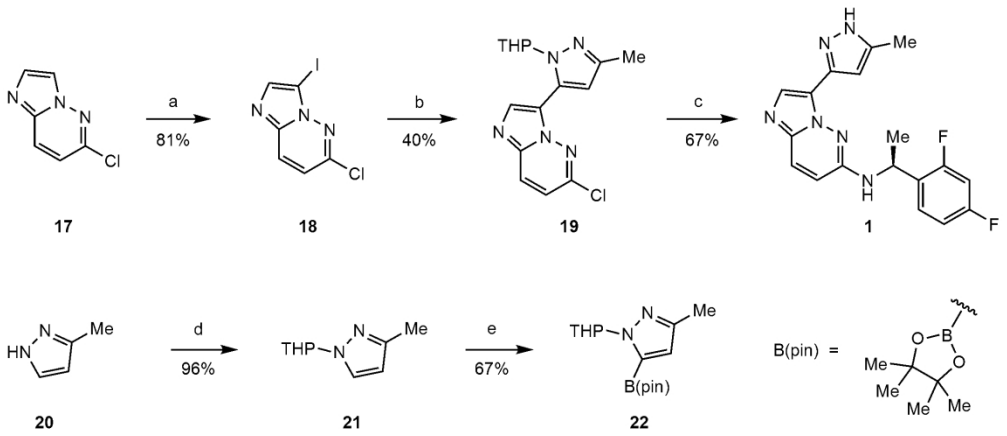

Scheme 1. Synthesis of *N*-Benzyl-3-(1*H*-pyrazol-5-yl)imidazo[1,2-*b*]pyridazin-6-amine **1**[a]

204x88mm (300 x 300 DPI)

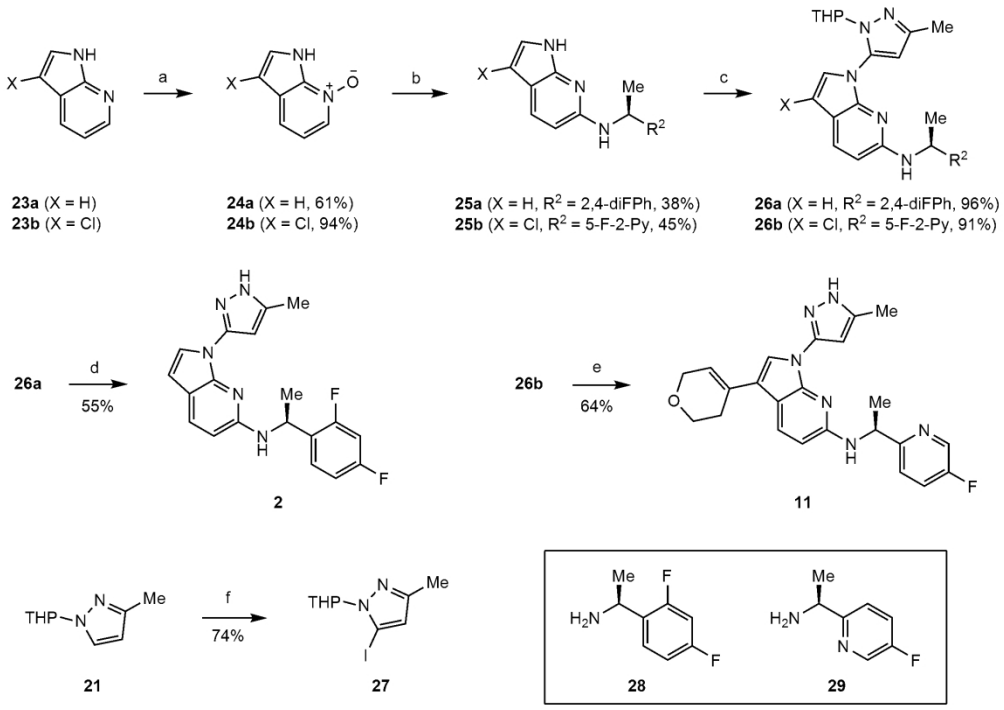

Scheme 2. Synthesis of 1*H*-pyrrolo[2,3-*b*]pyridine Derivatives[a]

213x150mm (300 x 300 DPI)

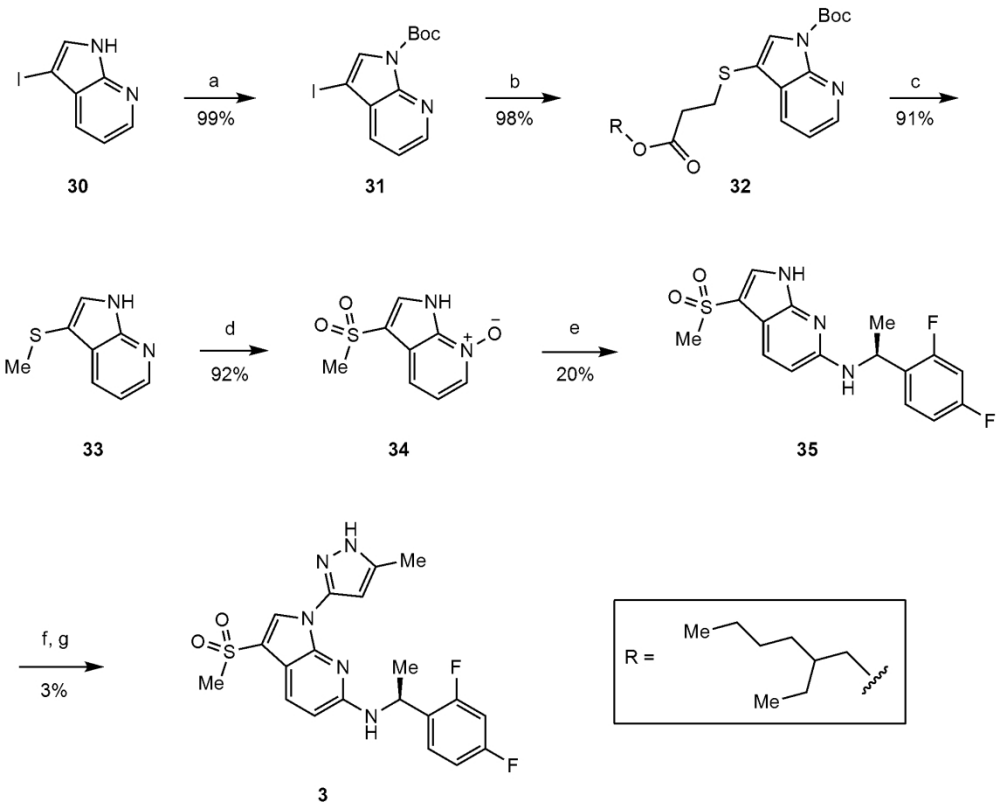

Scheme 3. Synthesis of 3-sulfonyl-6-amino-1*H*-pyrrolo[2,3-*b*]pyridine derivative **3**[a]

182x147mm (300 x 300 DPI)

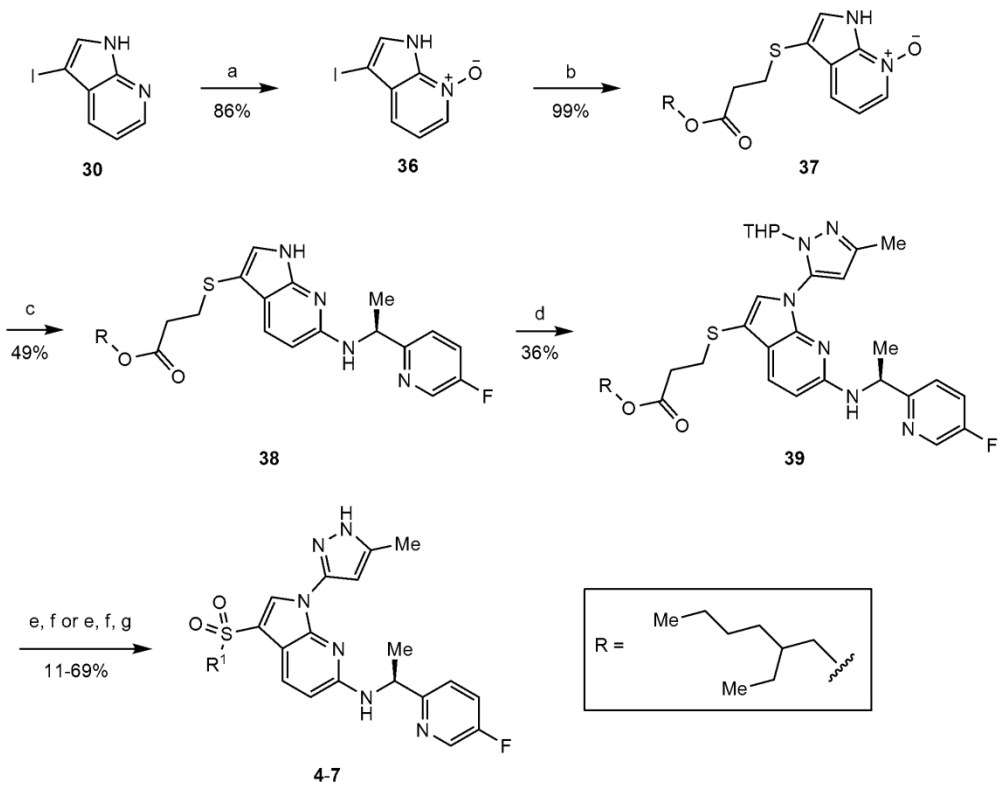

Scheme 4. Synthesis of 3-Sulfonyl-6-amino-1*H*-pyrrolo[2,3-*b*]pyridine Derivatives **4**–**7**[a]

185x145mm (300 x 300 DPI)

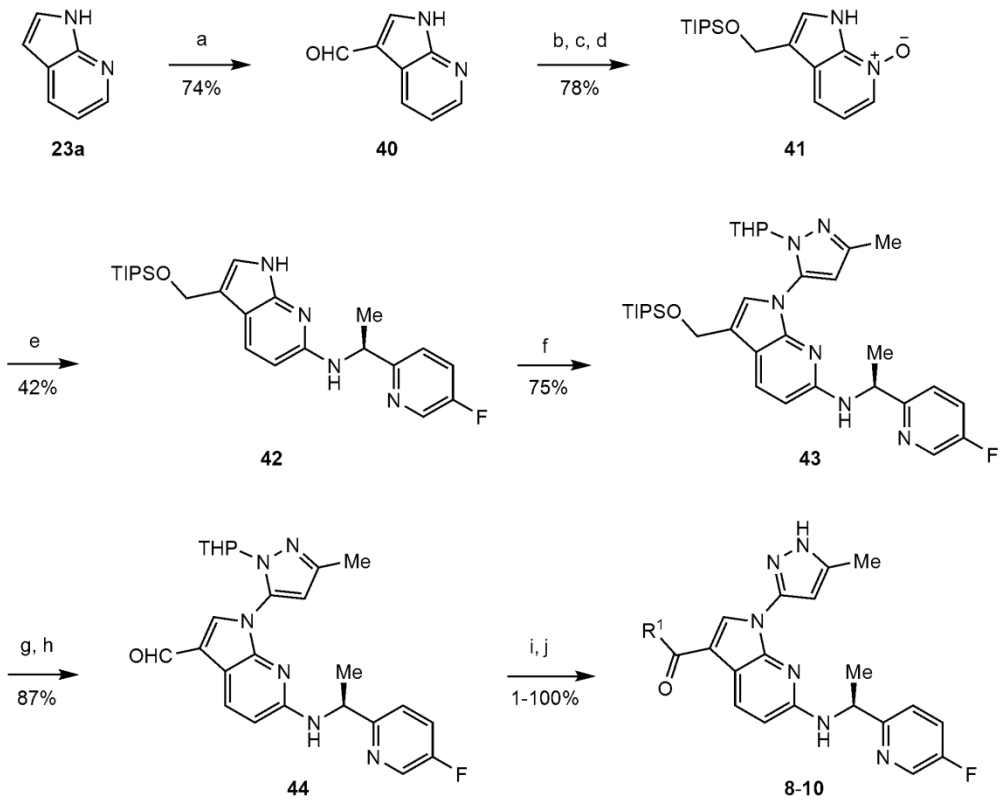

Scheme 5. Synthesis of 3-Aminocarobonyl-6-amino-1*H*-pyrrolo[2,3-*b*]pyridine Derivatives **8**–**10**[a]

175x139mm (300 x 300 DPI)

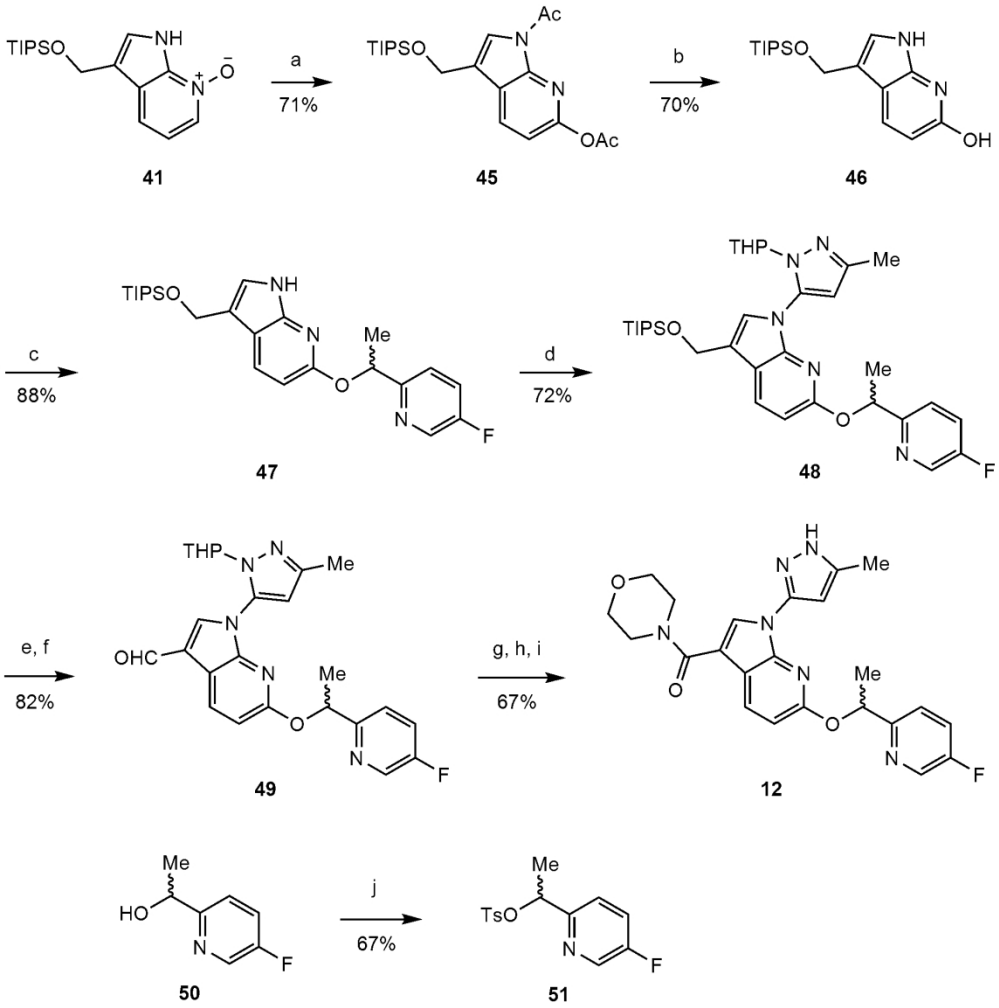

Scheme 6. Synthesis of 3-Aminocarbonyl-6-benzyloxy-1*H*-pyrrolo[2,3-*b*]pyridine **12**[a]

176x178mm (300 x 300 DPI)

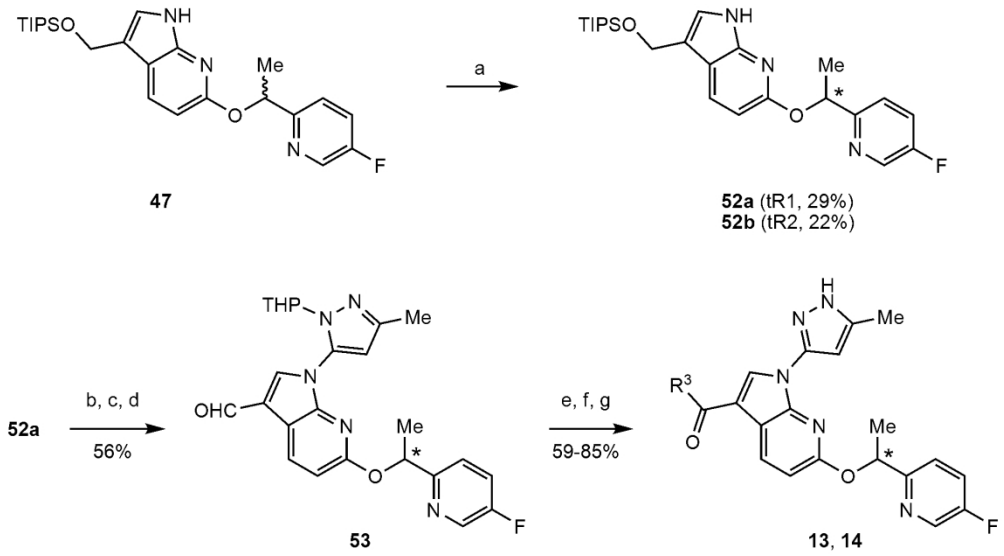

Scheme 7. Synthesis of Chiral 3-Amimocarbonyl-6-benzyloxy-1*H*-pyrrolo[2,3-*b*]pyridine Derivatives **13**–**14**[a]

178x98mm (300 x 300 DPI)

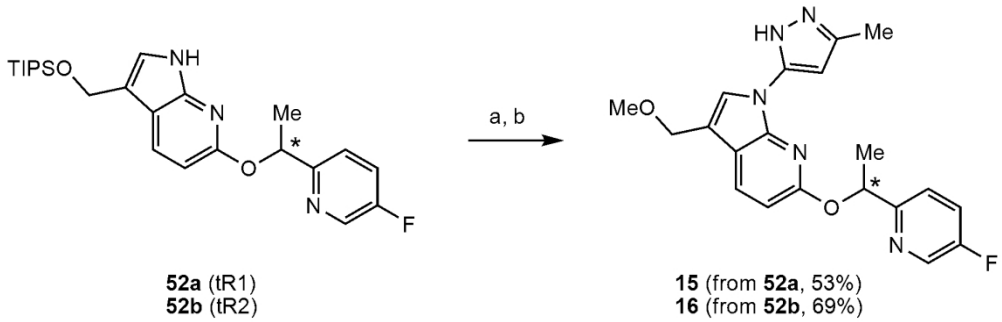

52a (tR1)
52b (tR2)

15 (from **52a**, 53%)
16 (from **52b**, 69%)

Scheme 8. Synthesis of Chiral 3-Methoxymethyl-6-benzyloxy-pyrrolo[3,2-*d*]pyrimidine Derivatives **15**–**16**[a]

161x51mm (300 x 300 DPI)

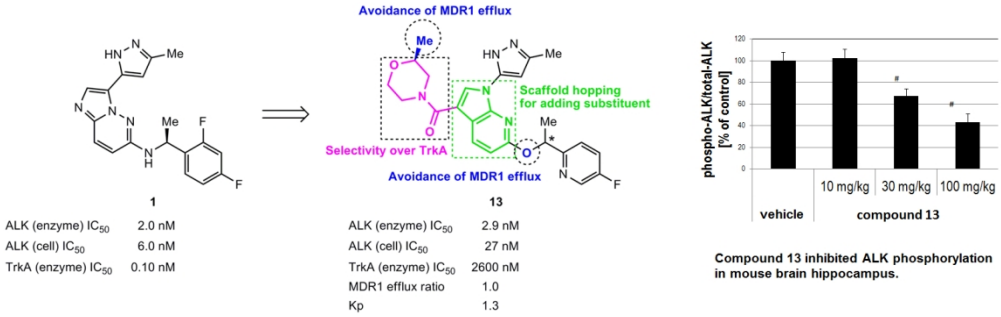

Table of Contents Graphic

434x135mm (96 x 96 DPI)